5-2018

Quantifying the Potential of Climate Mitigation and Adaptation in the United States Agricultural System with Model-data Integration

Peng Zhu
Purdue University

QUANTIFYING THE POTENTIAL OF CLIMATE MITIGATION AND ADAPTATION IN THE UNITED STATES AGRICULTURAL SYSTEM WITH MODEL-DATA INTEGRATION
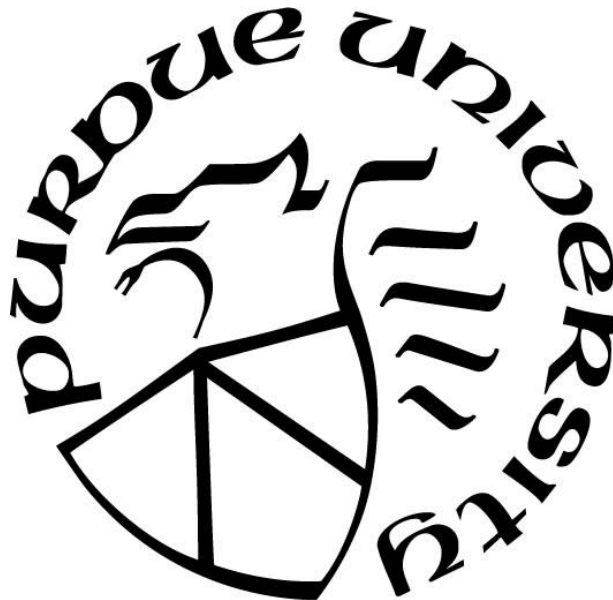
by

Peng Zhu

A Dissertation

Submitted to the Faculty of Purdue University
In Partial Fulfillment of the Requirements for the degree of

Doctor of Philosophy

Department of Earth, Atmospheric, & Planetary Sciences

West Lafayette, Indiana

May 2018

THE PURDUE UNIVERSITY GRADUATE SCHOOL
STATEMENT OF COMMITTEE APPROVAL

Dr. Qianlai Zhuang, Chair

    School of Science

Dr. Lisa Welp

    School of Science

Dr. Yutian Wu

    School of Science

Dr Tonglin Zhang

    School of Science

Approved by:

    Dr. Indrajeet Chaubey

        Head of the Graduate Program

ACKNOWLEDGMENTS

It would not have been possible to write this doctoral thesis without the help and support of the kind people around me, to only some of whom it is possible to give particular mention here.

Above all, I would like to express my sincere appreciation and thanks to my major advisor Professor Qianlai Zhuang. This thesis would not have been possible without his help, support, encouragement and patience, not to mention his advice and unsurpassed knowledge and vision of biogeochemical cycles and modeling, which have been invaluable to both an academic and a personal development. Four years ago when he recruited me who had only marginal experience in ecosystem studies for the PhD program, I already made up my mind to strive hard and live up to his expectations. For all of these, I am extremely grateful.

I would like to thank my committee members: Profs. Lisa Welp, Yutian Wu and Tonglin Zhang. Their diverse research backgrounds help me a lot on such an interdisciplinary research project. Specifically, Dr. Welp is a biogeochemist. I have always enjoyed her questions during our meetings and they are very thought-provoking. Dr. Wu's strength in climate dynamics has broadened my horizon in climate change research and her suggestions are always very helpful. Dr. Zhang's expertise lies in statistical analysis. His advices helped me a lot when I was faced with problems related with statistical methods or interpretation. I was deeply impressed by their great erudition and rigorous academic thinking. Their helps are irreplaceable for me to successfully finish this dissertation.

I am also thankful to the support of my fellow lab folks, colleagues and friends during my time at Purdue. This stimulating and welcoming academic and social environment left me with so many joyful moments and made the painstaking journey memorable.

Last, but by no means least, I want to express special thanks to my parents. Words cannot express how grateful I am to your support, trust and sacrifices that you have made on my behalf.

TABLE OF CONTENTS

LIST OF TABLES

LIST OF FIGURES

ABSTRACT

Author: Zhu, Peng. PhD
Institution: Purdue University
Degree Received: May 2018
Title: Quantifying the Potential of Climate Mitigation and Adaptation in the United States
    Agricultural System with Model-data Integration.
Committee Chair: Qianlai Zhuang

Agriculture is an important sector of U.S. economy. Faced with increasing global food demand driven by population boom, it is necessary to sustain the increasing food production. However, agricultural system is inherently sensitive to climate change and multiple lines of evidence across different spatial scales implied that the future warming will decrease global food production. In this context, this thesis focused on US cropland to investigate its potential in climate mitigation and adaptation by synthesizing the multiple crop models, long term satellite data, official survey data and field experiment. The fundamental questions addressed by this dissertation are: (1) how will the Climate Mitigation Potential (CMP) be varied when considering both biophysical and biogeochemical effects of biofuel crops expansion with different levels of management practices? (2) how will the effectiveness of adopting longer maturity maize cultivars be changed when implemented under future warmer climate? (3) how does heat stress influence maize grain yield across different maize growth stages?

In the first study, we used site-level observations of carbon, water, and energy fluxes of biofuel crops to parameterize and evaluate the Community Land Model and estimate CO_2 fluxes, surface energy balance, soil carbon dynamics of corn, Switchgrass and Miscanthus ecosystems across the conterminous United States considering different agricultural management practices and land-use scenarios. We found that, using carbon as currency, the CMP of energy crops over croplands and marginal lands is significantly changed from -1.9, 49.1 and 69.3 gC/m^2 per year considering only biogeochemical effects to 20.5, 78.5 and 96.2 gC/m^2 per year considering both biophysical and biogeochemical effects for corn, Switchgrass and Miscanthus, respectively. The CMP of biophysical effects is dominated by latent heat fluxes. When fertilization and irrigation is applied, the CMP over croplands and marginal lands reaches 79.6, 98.3 and 118.8 gC/m^2 per year, respectively. We further found that the CMP over marginal lands is lower than that over

croplands. This study highlights that biophysical effects induced from altering surface energy and water balance should be considered to adequately quantify CMP of bioenergy crops at regional scales.

In the second study, we argued that shift towards varieties with prolonged grain filling period (GFP) had a much greater contribution to the recent yield trends than previously thought. By using long term satellite data from 2000 to 2015, we identified an average lengthening of GFP of 0.37 days per year over the region, which probably results from variety renewal. An empirical statistical model demonstrated that longer GFP contributed roughly one-quarter (23%) of the yield increase trend by promoting kernel dry matter accumulation, yet less yield benefit was identified in hotter counties. Both official survey data and crop model simulations estimated a similar contribution of GFP trend to yield. If growing degree days that determines the GFP continues to prolong at the current rate for the next 50 years, yield reduction will be lessened with 25% and 18% longer GFP under Representative Concentration Pathway 2.6 (RCP 2.6) and RCP 6.0, respectively. However, this level of progress is insufficient to compensate yield losses in future climates, because drought and heat stress during the GFP will become more prevalent. Our study highlights devising multiple effective adaptation strategies is necessary to withstand the upcoming challenges in food security.

For the last study, we integrated crop models, satellite data, statistical data and field experiment data to investigate how increasing temperature influences maize yield through various processes across the US Midwest. Observational data suggests there is a nonlinear increasing temperature sensitivity of maize yield as temperature goes up, which is predominantly determined by sensitivity of harvest index, while the response of biomass growth rate and growing season length is relatively small. Although model ensemble exhibited a similar pattern of temperature sensitivity, the negative impact of warming on harvest index is underestimated. Further analysis shows that the enhanced temperature sensitivity of harvest index mainly results from a higher sensitivity of yield to temperature stress during grain filling period, which accounts for approximate 61% yield reduction. Future warming might influence yield directly through frequent heat stress or indirectly through water stress. Analysis of observational data suggests that high temperature stress is more influential than water stress, especially with warmer climate,

while model ensemble shows an opposite result. This discrepancy implies that the yield benefit of increasing atmospheric CO_2 might have been overestimated in crop models while direct temperature stress during grain formation is underestimated, because water conservation effect of increasing CO_2 brings more yield benefit under water stress conditions but shows limited benefit under heat stress. Our results suggest that, although maize yield has increased significantly in the US, limited progresses have achieved when confronted with heat stress during grain formation, highlighting more efforts are required for future climate adaptation during maize grain formation.

CHAPTER 1.   INTRODUCTION

1.1   Research background

World population is predicted to increase from 6.9 billion people today to 9.1 billion in 2050. In addition, economic development, especially in the developing countries, translates into an increased demand for food and diversified diets. Global food production has to be doubled by 2050 to meet the demand (Tilman et al., 2011), which means more land clearing and water consumption to support the increasing agricultural production. Thus, sustainable use of soil, water and land resources is critical for global food security.

Meanwhile, agricultural practices such as land clearing, soil tillage, fertilization and associated energy use for irrigation, harvesting and transport has contributed about 20% of the global annual emission of carbon dioxide (IPCC, 2012; Lal, 2002). Considering agricultural system is inherently sensitive to climatic warming, cutting down the emission from agricultural sector has important implications for stabilizing global warming and sustaining global crop production.

Although farming practices contribute to greenhouse gas emissions, it has been proved that improved soil management can substantially reduce these emissions and even remove CO_2 from the atmosphere through plants photosynthesis activity, as carbon in soil organic matter. In addition to reducing greenhouse gas emissions and storing more carbon into soil, improved soil management practices is also beneficial for soil nitrogen cycle, which might be able to enhance soil fertility and productivity and reduce soil erosion (Smith, 2012). The improved soil management practices includes like: no tillage (Ogle et al., 2005), more residue retention (Wilhelm et al., 2004) and cover crops during fallow periods (Burney et al., 2010).

In addition, shifting from fossil fuel energy to biofuel energy has been widely considered as one of the major renewable and sustainable energy sources to increase energy security and contribute to mitigating climate change at the same time (Field et al., 2008; Beringer et al., 2011). To provide energy security, bioenergy from crop-based biofuels is currently the most popular biomass feedstock for replacing fossil fuels and its demand is expected to continuingly increase

to meet the mandate targets for biofuel production (US Congress, 2007). However, traditional crop-based biofuels have many unintended consequences for feedstock availability, food security, environmental sustainability and societal welfare. Converting lands occupied by natural ecosystems to managed ecosystems for biofuel production will contaminate water quality with agricultural pollutants, threatening food supplies through competition for land (Clifton et al., 2007; Field et al., 2008; Gibbs et al., 2008).

Recently, perennial grasses such as Switchgrass and Miscanthus have been favored as a better alternative because they are easy to be established and have higher productivity with lower soil moisture request, they also accumulate and store carbon into the soil, enhancing soil organic matter storage (Anderson-Teixeira et al., 2009; Qin et al 2012; Clifton et al., 2007; Valentine et al., 2012). Meanwhile, these grasses could provide abundant biomass but require relatively less nutrient than conventional food crops (Lewandowski et al., 2003; Heaton et al., 2004; Clifton et al., 2007; Stewart et al., 2009; Zeri et al., 2013). Therefore they can grow on degraded agricultural land, i.e. marginal land, including idle or fallow cropland, abandoned or degraded cropland, and abandoned pastureland, where most food crops may not survive due to poor soil or climate conditions (Bandaru et al., 2013; Cai et al., 2010; Gopalakrishnan et al., 2012), which could avoid competing with food crops for land.

In addition to cutting down the greenhouse gas emissions from agricultural system through improved management practices and conversion to biofuel energy, adapting to future warmer climate is also necessary to sustain crop yield increase. As the world's largest producer of maize, the US cropping system has seen a steady increase in maize yield since the 1950s through improvements in agronomic practices, genetic technology and favorable growing conditions despite interannual yield variability related to hot and dry summers (USDA, 2015; Badu-Apraku et al., 1983; Cheikh and Jones, 1994; Çaki, 2004; Porter and Semenov, 2005). Several possible mechanisms have been investigated in order to understand this increasing trend in yields, including: expansion of more heat tolerant cultivars (Driedonks et al., 2016), delayed foliar senescence or stay-green traits (Thomas and Ougham, 2014), new cultivars adapted to higher sowing density (Duvick, 2005; Tollenaar and Wu, 1999), development of pest resistant maize cultivars through genetically engineering (NRC 2010), enhanced water use efficiency under

rising atmospheric CO_2 (Lobell and Field, 2008; Jin et al., 2017), and increase in accumulated solar radiation during the post-flowering phase (Tollenaar et al., 2017). A drought sensitivity analysis over the US Midwest based on field maize yield data showed, however, higher sowing density brought about side effect that field maize yield sensitivity to water stress became increased (Lobell, et al., 2014). In this context, it is necessary to understand the response of maize yield in farmers' fields to climate variation over time and thereby allowing more effective adaptation to the future climate change.

Satellite remote sensing observations such as the vegetation index derived from moderate-resolution imaging spectroradiometer (MODIS) reflectance data provide the opportunity to characterize the regional-scale spatiotemporal patterns of field crop growth status information, in particular phenological transition dates (Sakamoto et al., 2010). In this thesis, 8-day Wide Dynamic Range Vegetation Index (WDRVI) derived from MODIS reflectance data from 2000 to 2015 was used to map trends in maize phenology in Illinois, Indiana, Iowa, Nebraska across the US Midwest, which collectively account for half of the total US maize production. To extract maize phenology, shape model fitting has been shown as an effective approach and was validated at both site and state level (Sakamoto et al., 2010; Sakamoto et al., 2014; Zeng et al., 2016). On the other hand, threshold based methods can be used to extract the starting and ending of growing season more flexibly. Thus, we developed and implemented a hybrid method combining SMF and threshold-based analysis to generate 8 million samples of maize phenological date from MODIS WDRVI data at 250×250 m spatial resolution from 2000 to 2015.

To gain insight on how possible adaptation strategies work in future warmer climate, crop models is an important tool to provide predictive power for future crop yield at large scale. As crop models generally represent our understanding of response of crop plants growth to climatic variation and soil nutrient and hydrological conditions, agronomic management practices, while they normally suffer the great uncertainty induced by model structure and related parameters. It is also criticized that some basic knowledge might have not been updated for decades. Specifically, the parameters related with the crop varieties might be not able to reflect the recent progress in breeding techniques. Thus, when using these models to reproduce historic or predict future crop yield, there are often considerable mismatch between simulation and field

observations. Model ensemble is often supposed to be an effective way to narrow down the mismatch. Thus, multiple ensemble mean of global gridded crop model simulation outputs were used in this study, which results from the joint effort of Agricultural Model Intercomparison and Improvement Project (Rosenzweig et al., 2013) and Inter-Sectoral Impact Model Intercomparison Project 1 (Warszawski et al., 2014) for assessing the impact of climate change on global main crop production.

To better understand how specific management practices will change maize yield under future climate, agricultural system modeling platform APSIM version 7.7 is used here to simulate the benefit of GFP extension under future climate. It can simulate a number of crops in field under various climatic, soil physical and management conditions, and therefore is used widely to address a range of research questions related to agricultural systems (Holzworth et al., 2014). In particular, maize is simulated by the APSIM-Maize module. The APSIM-Maize module is inherited from the CERESMaize, with some modifications on the stress representation during grain set and grain filling, biomass accumulation and phenological development (Hammer et al., 2010). This flexible process-based model allows us to investigate the effectiveness of agronomic practices derived from the satellite observational data analysis like the cultivar shift indicated by higher thermal time requirement during grain fillling.

1.2 Research objectives

Agricultural system could be a substantial carbon source but the improved management might reverse it and make it become a carbon sink, in this thesis we used model-data integration to understand how climate change effect will be mitigated and adapted in the US agricultural system. The primary objective of this study is to understand the potential of climate mitigation and adaptation through improved various human intervention. The intervention here includes expansion of biofuel crops, improved farming practices and advancement in crop breeding technology. At the same time, multiple lines of evidence have consistently suggested the reduction in global crop productivity under warmer climate. However, there are still limited knowledge about which crop growth process is negatively or positively impacted by an increase

in temperature, between biomass growth rate, growing season length and grain formation, which is critical to develop targeted crop adaptation strategy for future warming.

Therefore, this thesis research begins with a model simulation with different scenarios of land conversion and management practices combinations across US continent to address how expansion of biofuels crops might influence climate mitigation through comprehensively accounting for ongoing carbon flux, soil carbon dynamics and canopy energy balance. Then long term satellite data was used to derive maize plants growth stages information. And we focused on grain filling period, which is supposed to be a critical stage for grain formation and sensitive to heat or drought stress. With various data analysis methods and model simulations, we try to address questions that how much adoption of longer maturity maize cultivars has contributed to the recent US maize increasing trend and whether this variety renewal brought yield benefit is sustainable under future warmer climate to meet the increasing food demand. Finally, we investigated how maize yield was reduced by higher temperature through different growth stages with expected future more frequent heat stress by integrating crop model output and observational data at different spatial scales. With the help of large scale observational data, the relative role of heat stress and water stress induced by warmer climate in regulating crop plants growth and grain formation was untangled. The observational data were also used to constrain model simulated yield reduction across the whole US continent to narrow the uncertainty range and thus improve the credibility of model predictions.

CHAPTER 2.   IMPORTANCE OF BIOPHYSICAL EFFECTS ON CLIMATE MITIGATION POTENTIALS OF BIOFUEL CROPS OVER THE CONTERMINOUS UNITED STATES

Abstarct: Current quantification of Climate Mitigation Potential (CMP) of biomass-derived energy has focused primarily on its biogeochemical effects. This study used site-level observations of carbon, water, and energy fluxes of biofuel crops to parameterize and evaluate the Community Land Model (CLM) and estimate CO_2 fluxes, surface energy balance, soil carbon dynamics of corn, Switchgrass and Miscanthus ecosystems across the conterminous United States considering different agricultural management practices and land-use scenarios. We find that, using carbon as currency, the CMP of energy crops over croplands and marginal lands is significantly changed from -1.9, 49.1 and 69.3 gC/m^2 per year considering only biogeochemical effects to 20.5, 78.5 and 96.2 gC/m^2 per year considering both biophysical and biogeochemical effects for corn, Switchgrass and Miscanthus, respectively. The CMP of biophysical effects is dominated by latent heat fluxes. When fertilization and irrigation is applied, the CMP over croplands and marginal lands reaches 79.6, 98.3 and 118.8 gC/m^2 per year, respectively. We further find that the CMP over marginal lands is lower than that over croplands. This study highlights that biophysical effects induced from altering surface energy and water balance should be considered to adequately quantify CMP of bioenergy crops at regional scales.

2.1   Introduction

Biomass energy has been widely considered as one of the major renewable and sustainable energy sources to increase energy security and contribute to mitigating climate change (Field et al., 2008; Beringer et al., 2011). To provide energy security, bioenergy from crop-based biofuels is currently the most popular biomass feedstock for replacing fossil fuels and its demand is expected to continuingly increase to meet the mandate targets for biofuel production (US Congress, 2007). However, traditional crop-based biofuels have many unintended consequences for feedstock availability, food security, environmental sustainability and societal welfare. Converting lands occupied by natural ecosystems to managed ecosystems for biofuel production

will contaminate water quality with agricultural pollutants, threatening food supplies through competition for land (Clifton et al., 2007; Field et al., 2008; Gibbs et al., 2008).

Recently, perennial grasses such as Switchgrass and Miscanthus have been favored as a better alternative because they are easy to be established and have higher productivity with lower soil moisture request, they also accumulate and store carbon into the soil, enhancing soil organic matter storage (Anderson-Teixeira et al., 2009; Qin et al 2012; Clifton et al., 2007; Valentine et al., 2012). Meanwhile, these grasses could provide abundant biomass but require relatively less nutrient than conventional food crops (Lewandowski et al., 2003; Heaton et al., 2004; Clifton et al., 2007; Stewart et al., 2009; Zeri et al., 2013). Therefore they can grow on degraded agricultural land, i.e. marginal land, including idle or fallow cropland, abandoned or degraded cropland, and abandoned pastureland, where most food crops may not survive due to poor soil or climate conditions (Bandaru et al., 2013; Cai et al., 2010; Gopalakrishnan et al., 2012), which could avoid competing with food crops for land.

It has been widely recognized that perennial biofuel grasses could contribute climate mitigation through biogeochemical pathways by sequestrating carbon while excessive removal of crop residue for biofuel production can impair its ability to sequestrating carbon because residue carbon in biofuels is oxidized to CO_2 at a faster rate than when added to soil so its carbon signal are largely determined by human management practices. (Zeri et al., 2011; Anderson-Teixeira et al., 2011; Liska et al., 2014). Along with biogeochemical effect, biophysical effect due to land conversion leading to a change on surface energy budget has evident impacts on local climate (Loarie et al., 2011; Peng et al., 2014; Zhang et al., 2014; He et al., 2014). Recent studies suggest that land management can also impact surface temperature at a comparable magnitude (Luyssaert et al., 2014). This direct climatic effect can be significant to climate change mitigation and has been investigated in the field of deforestation and afforestation (Loarie et al., 2011; Peng et al., 2014; Lee et al., 2014), but very few researches have been conducted within the framework of biofuel lifecycle analysis under different scenarios (Anderson-Teixeira et al., 2012).

Until now, there have been many bioenergy crop models developed to estimate regional or global scale biomass production and greenhouse gas (GHG) emissions of biofuel crops (Qin et

al., 2014; Surendran et al., 2012; Thomas et al., 2013). However, there are still large uncertainties in the simulated carbon and water balance like biomass production, GHG emissions and water demand due to the different model parameterization such as various feedstock chosen, cultivation practices, harvesting dates, fertilizer application and land-use conversion pattern (Hudiburg et al, 2015). Therefore, the model should be cautiously selected and tested. Generally, the fully coupled earth system model provides a comprehensive evaluation of both biogeochemical and biophysical effects due to land cover change on climate, however, it was too time-consuming. In contrast, most of ecosystem models are sufficient to quantify carbon balance of biofuel ecosystems but often cannot accurately capture the high frequency variation of surface energy due to their simplified surface energy balance schemes. Thus, land surface model which have a higher time frequency and detailed carbon and surface energy parameterization scheme might be more favorable. Based on the revised land surface model, the local scale surface energy change due to biophysical effect was converted into the equivalent carbon flux through accounting of their radiative forcing magnitude and then biogeochemical and biophysical effect are integrated into CMP metric using carbon as the currency.

Using data collected at the University of Illinois Energy Farm, we first parameterize and validate a latest version land surface model CLM4.5 to evaluate ongoing carbon flux, biomass production, surface energy balance of Switchgrass and Miscanthus and then explicit spatial estimation for corn, Switchgrass and Miscanthus across the conterminous United States were conducted to quantify how surface energy change and carbon balance would respond to different land use scenarios and management practices compared to current land use patterns. The surface energy and carbon balance change were finally integrated into CMP. We hypothesize, at the regional scale, that: (1) compared to maize and annual C3/C4 grasses, Switchgrass and Miscanthus will have higher productivity and sequestrate more carbon into soils, (2) CMP of planting biofuels will be enhanced when evaporative cooling effects are accounted; and (3) agricultural management practice like fertilization and irrigation will result in higher total carbon uptake, higher below ground biomass and substantial evaporative cooling due to the sufficient water supply, consequently yield a higher CMP.

2.2   Materials and Methods

2.2.1 Site description

The observational data was obtained at University of Illinois Energy Farm located in central Illinois (40.06°N, 88.19°W, ~220 m above sea level) using eddy covariance and micrometeorological instrumentation placed at the center of four plots (4 ha, 200 m × 200 m). In 2008, four species: corn-soybean rotation, Miscanthus, Switchgrass and a mix of native prairie species were planted to examine bioenergy production and the associated environmental services. The eddy covariance systems were established with a three-dimensional sonic anemometer (model 81000 V, R.M. Young Company, Traverse City, MI, USA) and an infrared gas analyzer (model LI-7500, LI-COR Biosciences, Lincoln, NE, USA). This system was to collect high frequency data (10 Hz) of wind speed, and fluxes of CO_2, H_2O. Other essential meteorological variables to drive our model, including solar radiation (shortwave and longwave, both incoming and outgoing components), precipitation, air temperature, relative humidity, air pressure, were also collected at the center of each plot. The data collected in 2011 was used for model parameterization and evaluation.

2.2.2 Model description and improvement

Model simulations were performed using CLM4.5 to simulate the effects of climate, land use change and agricultural management on carbon budget and surface energy change in bioenergy ecosystems. CLM was initially developed by concurrent effort at NCAR, merging community-developed land model focusing on biogeophysics to expand NCAR Land Surface Model (Bonan 1996). CLM was incorporated with a number of biophysical processes for different plant functional types (PFT) including stomatal physiology, photosynthesis, energy and momentum fluxes with vegetation canopy and soil, heat transfer in soil and snow, and hydrology of canopy, soil, and snow. Carbon allocation and developmental stages are based on temperature thresholds and the accumulation of growing degree-days, which is dynamic throughout the growing season. Soil organic carbon (SOC) is estimated from the turnover of soil organic matter pools, which change with decomposition rate. Version CLM4.5 was released as the land surface component of Community Earth System Model (CESM) with many improvements, including a revised canopy radiation scheme and canopy scaling of leaf processes, co-limitations on photosynthesis and

updated photosynthetic parameters (Bonan et al. 2011). In CLM4.5, there is already a crop submodel, inherited from Agro-IBIS (Foley et al., 1996; Kucharik et al., 2000) to represent the role of agriculture in land surface processes. Processes of land management such as crop type, planting, harvesting, fertilization, and irrigation is added. In this study the two major agricultural management practices: fertilization and irrigation are accounted, since these two management practices are considered to be crucial in determining carbon sequestration potentials of biofuel crops (Elshout et al., 2015). The irrigation parameterization scheme is based loosely on the implementation of Ozdogan et al. (2010). This parameterization did not account for timing and background climate conditions and it responds dynamically to climate. Deficit water can be added to soil through irrigation so that a target soil moisture is reached. Thus irrigation can significantly influence the surface water and energy balances partition in the model and thus has an evident biophysical effect (Ozdogan et al. 2010). Interactive fertilization is also enabled in this version and nitrogen is added directly into the soil mineral nitrogen pool to meet crop nitrogen demands. Total nitrogen fertilizer amounts are 150 g N/m^2 for maize, 80 g N/m^2 for temperate cereals, and 25 g N/m^2 for soybean, representative of central U.S. annual fertilizer application amounts. For biofuel crops, 100g N/m^2 is applied based on previous field experiments (Fike et al., 2006; Heaton et al., 2008; Propheter et al., 2010; Nikiema et al., 2011).

To reach our research goal, a new parameterization scheme for CLM is necessary for those perennial grasses including Switchgrass and Miscanthus, which have different physiological traits. Unlike annual crops, perennial grasses allocate a large amount of resources to belowground organs such as rhizomes (Anderson-Teixeira et al., 2009; Atkinson, 2009). The new scheme was calibrated by adjusting relevant model parameters based on observations of Switchgrass and Miscanthus and then evaluated against observations. Several key parameters and their corresponding values in Switchgrass and Miscanthus parameterization were incorporated into the model (Table 1). These parameters can be generally grouped into three kinds: parameters controlling photosynthesis capacity including Vcmax25, Q and slatop; phenology parameters including lfemerg, hybgdd, mxmat, baset, min_NH_planting_date, min_planting_temp; and allocation parameters including Astem, Aroot, fleafi, Cnleaf. We combined the carbon allocated to rhizome with those to roots to minimize the change of the original model structure. For the simulation at site level, the model is run at a half-hour interval.

The collected meteorological forcing data during 2011 is used to drive the model. At least 500 years of model spin-up is established to allow soil carbon pools to reach equilibrium.

2.2.3 Regional experiments under various land use and management scenarios

Regional simulations were run at half-hourly time step from 2000 to 2010 at $0.5\,°\times0.5\,°$ spatial resolution. This recent 10-year time period was selected to capture the effects of inter-annual variations of climate change. The regional spin-up procedure was the same as the single site and used current vegetation map for each grid cell. In the control run (cntl), each grid cell is initialized with a distribution of plants from current vegetation maps generated from the International Geosphere Biosphere Programme's 1-km DISCover (IGBP) land cover dataset (Loveland et al., 1997). For the remaining 12 simulations, the marginal land distribution utilizes the map estimated from Cai et al (2011). In their study, global marginal lands were classified according to the marginal agricultural productivity based on land suitability indicators such as topography, climate conditions and soil fertility. The scenario 1 in Cai et al. (2011) including marginal lands from abandoned land and mixed crop and vegetation land and yet without sacrificing large amounts of cropland and natural lands (forest and grassland) was used in this study. This scenario was considered as baseline land-use conditions and was used here to represent the spatial distribution of marginal lands in the United States. The data in Cai et al. (2011) was aggregated to $0.5\,°\times0.5\,°$ spatial resolution and then two land conversion scenarios were generated according to the proportion of marginal lands and croplands in each grid : one scenario (Fig. 1a) that both marginal lands and croplands are converted, the other (Fig. 1b) that only marginal lands are converted. The darker pixels in the figure mean higher fractions of convertible land. Compared with Fig. 1a, most of croplands across Midwest remain unchanged and only the scattered marginal lands are converted in Fig. 1b. Soil texture and soil color class for each $0.5\,°$ grid cell are based on the Harmonized World Soil Database (HWSD, Wieder et al 2014) and are used by CLM4.5 to determine soil hydraulic and thermal properties. The climate data needed to drive simulations at the half hourly time steps were obtained from CLM4.5 standard atmospheric forcing data sets CRUNCEP (Viovy 2011), which is a combination of two existing datasets: the CRU TS3.2 $0.5\,°\times0.5\,°$ monthly data covering the period 1901 to 2002 (Mitchell and Jones 2005) and the NCEP reanalysis $2.5\,°\times2.5\,°$ 6-hourly data covering the period 1948 to 2010. 12 experiments were conducted to assess how much climate mitigation can

achieve under different combination of land conversion scenarios and agricultural management practices (Table 2). In addition, the proportion of crop residues removal need to be addressed, which could have a noticeable impact on soil carbon pool (Liska et al., 2014). In the control run, apart from the crop grain was totally harvested, 20% of residue was removed to represent SOC loss by soil disturbance from cultivation, which was neglected by current CLM (Levis et al., 2014). For the remaining 12 experiments, 70% of aboveground biomass was removed to simulate harvest behaviors of biofuel crops. This removal rate is considered to maintain sustainable utilization and can also get as much biomass as possible. Across all of the 13 simulations, natural and crop ecosystems in each grid cell were modelled separately and then aggregated based on their fractions within each grid cell. The following comparison on CMP was based on the difference between 10 year average of the 12 experiments and the control experiments.

2.2.4 Model description and improvement

CMP of growing biofuel crops was often quantified using net GHG fluxes and SOC change, both are important in the lifecycle analysis of biofuel carbon balance. However, the contribution of biophysical effects to CMP was overlooked in previous research (Albanito et al., 2015; Qin et al., 2012; Qin et al., 2015). Here we combine carbon fluxes, soil carbon pool changes, evaporative cooling effects, and net radiation (Rn is the balance between incoming and outgoing longwave and short wave radiation, mainly determined by albedo) changes to construct a synthetic CMP metric by using carbon as the currency. Both biophysical effects and biogeochemical effects can be converted to radiative forcing effects, i.e. biogeochemical effects influence the capacity of absorbing longwave radiation while biophysical effects concerns shortwave radiation and latent heat flux:

$$T\frac{\Delta E}{S} = \frac{\Delta C_e / M_c}{A} R_e$$

(1)

Where ΔE is the surface energy change (W/m^2; $\Delta E = \Delta LE - \Delta Rn$). ΔC_e is the equivalent carbon change. A=1.78 $\times$ 10^8 billion kmol is the moles of air in the atmosphere. Re=1.4 $\times$ 10^4 nW/(m^2·ppb) is the effective radiative forcing efficiency of CO$_2$. S=5.1×10^{10} ha is the global surface area, here acting as scale factor to convert the local ΔE to global radiative forcing effects. Mc is the molar mass of carbon. Since radiative forcing of CO$_2$ has cumulative effect, here T is

multiplied as the time frame to balance the two sides. We choose T to be 50 years as used previously (Anderson-Teixeira et al. 2012) to account the remaining time of CO_2 in atmosphere. Another time frame is needed to stabilize the net carbon flux and SOC to make SOC change be comparable with the change of annual net carbon fluxes over a time span, and we set this time frame as 50 years. Thus CMP can be defined as:

$$CMP = \Delta C_e + \Delta NEP + \frac{\Delta SOC}{50} \qquad (2)$$

According to the conversion equation 1, the surface energy change of 1 W/m^2 is roughly equal to 6 gC/m^2 over a 50-year time span. More technical details of these conversions could be found in Anderson-Teixeira et al. (2011). The CMP of each grid cells occurring in biofuel crops expansion is finally aggregated based on land conversion rate.

2.3   Results

2.3.1. Model evaluation at site

The simulated GPP compared well with measurements for both Switchgrass and Miscanthus with a slight underestimation especially over the maximum carbon uptake period (Fig. 2). Simulated GPP captures the annual variation well over the whole growing season, including the initial rise after leaf emergence, the timing of peak value, and productivity decline after leaf senescence (Fig. 2). For Switchgrass, the simulated timing occurs later for leaf onset and the leaf offset timing matches better with the observations. Similarly, for Miscanthus model performs well in capturing the timing of leaf onset and offset. The simulated result explained 71% and 75% of observed GPP for Switchgrass and Miscanthus, respectively. Miscanthus showed a longer growing season especially for its later leaf offset date, leading to a higher annual GPP (2.34 kg C/m^2 for Switchgrass, 2.88 kg C/m^2 for Miscanthus).

The simulated latent heat (LE) matched well with the observed values at a half hour time step and the timing and magnitude of the simulated NEE also matched the eddy covariance measurements, capturing the transition from winter dormancy to spring uptake and reaching summer maximum uptake (Fig. 3 and 4). Compared to eddy covariance measurements, the simulated LE and NEE was slightly overestimated. The annual LE difference between simulation

and observation were 4.7 W/m^2 and 4.1 W/m^2 while the NEE differences were 32.2 g C/m^2 and 24.3 g C/m^2 for Switchgrass and Miscanthus, respectively. All of these differences were within the 10% of the annual observation.

2.3.2. Model projections of biofuel crop carbon and energy balance

By growing corn and harvesting grain and stove for biofuel production in the Midwest where is known as Corn Belt, our simulation showed that soils acted as a carbon source when no management practices were applied, primarily owing to the higher rate of residue removal for biofuel production (Fig. 5). Due to their higher productivity and longer growing season, soils of Switchgrass and Miscanthus received more litter, leading to soil carbon accumulation, even though much of aboveground biomass was removed (Fig. 6 and Fig. 7). Corn cropland had an increase of soil C in the north while Switchgrass and Miscanthus tended to gain more SOC in the south, which was consistent with previous simulation result (Miguez et al., 2012). There was a substantial increase in SOC when the arid areas like western US were applied with fertilization and irrigation. Corn croplands had a moderate increase in net carbon fluxes than the pristine land and Miscanthus had the largest carbon sequestration potential, followed with Switchgrass and corn (Fig. 8). All of the three biofuel crops showed a larger carbon sequestration from -1.9 gC/m^2, 49.1 gC/m^2, 69.3 gC/m^2 without agricultural management to 49.3 gC/m^2, 66.0 gC/m^2, 84.9 gC/m^2 with agricultural management for corn, Switchgrass, and Miscanthus respectively. Simulated carbon sequestration capacity over croplands were generally larger than that over marginal lands due to its nutrient limitation, implying under a given mitigation target more marginal lands were required compared with cropland whereas marginal land exploitation could relieve the energy-food competition. Our simulations were generally consistent with previous findings (Qin et al, 2012; Qin et al, 2015; Elshout et al., 2015), suggesting that Switchgrass and Miscanthus could sequestrate more carbon and high input increase its carbon sequestration capacity.

The spatial pattern of the simulated Rn and LE was generally consistent with previous modeling result, indicating that annual cumulative ET of Switchgrass and Miscanthus was much larger than corn owing to their longer growing season (Hickman et al., 2010; VanLoocke et al., 2010; Zeri et al., 2013). The distribution of ΔLE generally showed a similar spatial pattern to carbon flux, implying there was a tight nexus between carbon and energy exchanges during biofuel

crops growth (Fig. 9). The three biofuel crops had larger LE due to their higher plant transpiration. Switchgrass and Miscanthus showed a higher net radiation, indicating a lower albedo due to higher LAI. ΔLE of corn, Switchgrass and Miscanthus growing on marginal lands and croplands without management are 3.8 W/m^2, 5.2 W/m^2 and 5.2 W/m^2, respectively. Maximum ΔLE of Switchgrass and Miscanthus were 8.8 W/m^2 and 9.3 W/m^2 in the southeast of the US where also had high ΔRn (Fig. 9 and Fig. 10). The spatial variation of Rn of Switchgrass was similar to Miscanthus, mainly because both were perennial grasses and had the same physiological and phenological traits, while the mean value of Switchgrass was lower than Miscanthus. In most regions covered by biofuel crops, ΔLE typically outweighed ΔRn such that the evaporative cooling effect dominated the biophysical effects induced from land conversion. When agricultural managements were applied, the increase of LE was much greater than Rn, leading to a higher cooling effect. This could be owing to: (1) irrigation keeps soil moisture saturated, supplying more water, (2) fertilization leads to higher LAI and more water is transpired. The spatial pattern of LE change showed larger enhancement in the southern US for the three biofuel crops, which was possibly attributed to the higher evaporative demand in the south of US.

Our simulated annual CMP under various alternatives (Table 3) indicated that CMP could be significantly improved when biophysical effects were added, corn ecosystem even changed from carbon source to carbon sink in the experiment corn1, which affirmed the previous research that biophysical effects of bioenergy crops can be even larger than biogeochemical effects on climate mitigation at regional scales (Georgescu et al., 2011; Anderson-Teixeira et al. 2012). This improvement can be mainly explained by that LE increase accompanied with biofuel crops expansion dominates the biophysical effects so that all land-use change scenarios show cooling effects and contribute to climate mitigation. In addition, fertilization and irrigation significantly improves the CMP of biofuel crops, especially for corn. It is informed that the synergistic effect between fertilization and irrigation might also contribute to this. (Lee et al., 2012). Application of fertilization and irrigation enable CMP of corn more than tripled from 20.5 gC/m^2 to 79.6 gC/m^2 in the scenario converting both croplands and marginal lands. This result is consistent with previous research and confirmed high input could reduce carbon payback time of crop-based biofuel (Elshout et al., 2015). If biofuel crops were planted only on marginal lands and no management practice, their CMP ranged from 33.0 gC/m^2 to 85.1 gC/m^2 while this value will be

elevated to 20.5 gC/m^2-96.2 gC/m^2 when cropland is also converted, implying CMP over marginal lands is lower than that over croplands. The highest CMP of 118.8 gC/m^2 is achieved by mx3 and this value is improved around 50% compared to its biogeochemical effects (84.9 gC/m^2). The simulated CMP of Switchgrass lies between corn and Miscanthus.

2.4 Discussion and Conclusion

In this study, we used revised land surface model to evaluate the climate regulation service of both grain crop and cellulosic crops across conterminous US over a multi-year time frame. Our result suggested that harvesting of corn grain and residual for biofuel production under a scenario without any agricultural management will progressively deplete the soil carbon pool. Previous research showed cultivation of Switchgrass and Miscanthus could increase SOC by an average of 10-100 gC/m^2 per year in the top 30 cm and our modelled SOC change was 16.3-37.7 gC/m^2 per year (Anderson-Teixeira et al., 2009). Our results confirmed that cellulosic crops, which normally had higher nutrient use efficiency and higher water use efficiency, store more carbon, produce more biomass for bioenergy feedstocks (Davis et al., 2011; VanLoocke et al., 2012; Jones et al., 2015). This made both biofuel crops more promising bioenergy crops in areas beyond current cropland area. The results also presented the high spatial variation of carbon sequestration ability which was not only controlled by the climatic and soil conditions but also seriously dependent on the type of land replaced. Previous research demonstrated that the conversion of tropical and temperate forests, savannahs, peatland for biofuel production could even cause net carbon emissions because of the large amount of stored carbon released (Fargione et al. 2008; Elshout et al., 2015). In this study, only marginal land and cropland were taken into account for land conversion, since this tended to be more practical land conversion choices based on previous experimental conclusion that cultivation of biofuels on marginal land can enhance its productivity and minimize environmental degradation (Bhardwaj et al., 2014). Meanwhile, both this and previous researches pointed out that marginal land were less fertile and sustained smaller carbon sequestration capacity (Gelfand et al., 2013), so more marginal land might be reclaimed to achieve the mitigation target.

The proposed CMP here covered ongoing carbon flux, carbon storage and surface energy change, presents a new perspective of evaluating climate mitigation of biofuel crops, which might conduce to formulate a more reasonable land use policies (Anderson et al., 2010; Knoke et al., 2012). CMP of both cellulosic crops and maize significantly increased after biophysical effects are accounted. One aspect of biophysical effect Rn, determined by albedo, was increased when land was displaced by biofuel crops, which meant part of evaporative cooling was offset and this was consistent with a previous study using a land surface model as well (Anderson-Teixeira et al., 2012). However, latest observed experiment indicated Miscanthus and Switchgrass had a higher albedo, meaning Rn was reduced (Miller et al., 2015). This discrepancy was likely to originate from the wrong parameters used in current model, controlling leaf transmittance and reflectance, leaf angle and canopy structure (Lawrence et al., 2011). Thus further efforts need to be done to improve surface energy processes of biofuel crops, whereas this aspect is minor relative to LE. Another aspect of biophysical effect LE is tightly correlated with water cycle so irrigation application can not only improve the crop productivity but also LE especially in arid environment (Roncucci et al., 2014). Experiments suggest Miscanthus has larger transpiration due to the higher stomatal conductance to support its high carbon assimilation rate (Dohleman et al., 2009), which is reproduced in our simulation. The LE change induced by biofuel crops expansion might also impact hydrological cycle and this influence is highly spatially dependent implying there might be little impact at certain site (Abraha et al., 2015), but possibly deteriorate the water resources in other area (Vanloocke et al., 2010).

While this study indicates that both biogeochemical and biophysical feedbacks should be considered in evaluating biofuel crops on the climate, several limitations are also identified in our analysis. First, another important GHG from agroecosystems, N_2O, is neglected in this study. When fertilization is applied, it stimulates more N_2O emissions and thus weaken the CMP of bioenergy ecosystems (Crutzen et al., 2008; Roth et al., 2015; Davis et al, 2014), which should be addressed in the future research. Meanwhile, this research mainly focused on climate mitigation service of ecosystem, so we overlooked the environmental impact of increasing nitrate leaching induced by fertilization application, which is also a serious problem during biofuel production (Chamberlain et al., 2011). Second, previous research also implied that soil carbon storage is heavily dependent on crop residual remove rate (Liska et al., 2014; Smith et al., 2012),

while we here set crop residual remove rate as a constant value across the US, which might be too arbitrary. More flexible removal rates should be introduced in the future research. Third, the irrigation in CLM4.5 is automatically triggered based on soil water status. Although irrigation is shown to improve CMP of biofuel crops and might save more lands, its possible threat to local water resource is not accounted. Recent research highlighted to institute policies so as to balance the water and land requirements during bioenergy production (Bonsch et al., 2014). Finally, we used land surface energy change to represent total cooling effects of growing biofuel crops on the climate. It is desirable to use dynamic climate models to examine how these land use change and management scenarios affect the climate in terms of air temperature and precipitation. For instance, the changed evapotranspiration due to growing biofuel crops will impact water vapor in air. Especially irrigation impacts soil moisture, ultimately influences clouds and precipitation (Lobell et al., 2009; Puma and Cook, 2010). More clouds formed will affect the shortwave radiation and impact air temperature while these climate process and dynamics are omitted in our analysis.

Previous researches have demonstrated that integrating the proper farming practices like improving harvesting techniques, altering harvest timing, organic matter amendments, reduced-till coupled with straw return, rotating cereals with grain legumes can reduce the GHG emissions and improve soil carbon sequestration capacity and soil quality and also benefit to environmental protection and biodiversity conservation (Gan et al., 2014; Cheng et al., 2013; Hudiberge et al; Davis et al., 2013). Our research confirmed the importance of agricultural management in enhancing CMP especially when biophysical effect is accounted. Besides climate mitigation, we suggest improving current farming practices to better manage the environmental impact of bioenergy production. Faced with increasing land-use pressures driven by growing population, our spatially explicit result accounting both biophysical and biogeochemical effect enable policy makers to make wiser decisions on the landscape planning of biofuel crops expansion to accomplish climate mitigation target (Campbell et al., 2010).

Table 2. 1 New parameter values for Switchgrass and Miscanthus calibrated from site observational data

Parameter name	Description	Switchgrass	Miscanthus
Vcmax25	Maximum rubisco activity at 25 °C at top of canopy (μmol/ (m^2 s))	75	92
Q	Intrinsic quantum efficiency (dimensionless)	0.04	0.04
slatop	Specific leaf area (m^2/gC) at top of canopy	31	70
laimx	Maximum leaf area index (LAI) allowed (m^2/ m^2)	6.5	8.5
hybgdd	Maximum growing degree days (base 0 °C) required for physiological maturity	3700	3820
mxmat	Maximum number of days allowed past planting for physiological maturity to be reached	260	260
fleafi	Fraction of assimilated carbon allocated to leaves	0.6	0.7
Astem	fraction of assimilated carbon allocated to stems	0.2	0.2
Aroot	fraction of assimilated carbon allocated to roots	0.15	0.12
Cnleaf	C:N ratio of leaf biomass	100	80
baset	Base temperature for GDD calculation	0	0
min_planting_temp	Average 5 day daily minimum temperature needed for planting (K)	274.1	275
min_NH_planting_date	Minimum planting date for the Northern Hemipsphere	301	301
lfemerg	Leaf emergence parameter	0.02	0.03

Table 2. 2 12 Experiments allowing for biofuel crop types, land conversion scenarios and management practices mainly irrigation and fertilization.

Experiments	Biofuel Type	Land Conversion Scenarios	Management Practices
corn1	corn	marginal land and cropland	No
corn2	corn	marginal land	No
corn3	corn	marginal land and cropland	Yes
corn4	corn	marginal land	Yes
sw1	Switchgrass	marginal land and cropland	No
sw2	Switchgrass	marginal land	No
sw3	Switchgrass	marginal land and cropland	Yes
sw4	Switchgrass	marginal land	Yes
mx1	Miscanthus	marginal land and cropland	No
mx2	Miscanthus	marginal land	No
mx3	Miscanthus	marginal land and cropland	Yes
mx4	Miscanthus	marginal land	Yes

Table 2. 3 The simulated CMP change based on 10-year (2000–2010) means under various alternatives

Experiment	Carbon flux (gC/m²)	SOC (gC/m²)	LE (W/m²)	Rn (W/m²)	CMP (gC/m²)
corn1	24.4	-26.3	4.3	0.30	20.5
corn2	21.5	-8.3	3.8	0.26	33.0
corn3	37.5	11.8	5.8	0.38	79.6
corn4	32.1	8.2	4.9	0.32	65.9
sw1	30.6	18.5	5.6	0.35	78.5
sw2	28.7	16.3	5.2	0.32	71.3
sw3	39.2	26.8	6.2	0.42	98.3
sw4	34.1	22.2	5.8	0.37	86.7
mx1	38.5	30.8	5.7	0.67	96.2
mx2	32.4	27.2	5.1	0.55	85.1
mx3	47.2	37.7	6.9	0.87	118.8
mx4	43.5	32.4	6.3	0.68	107.3
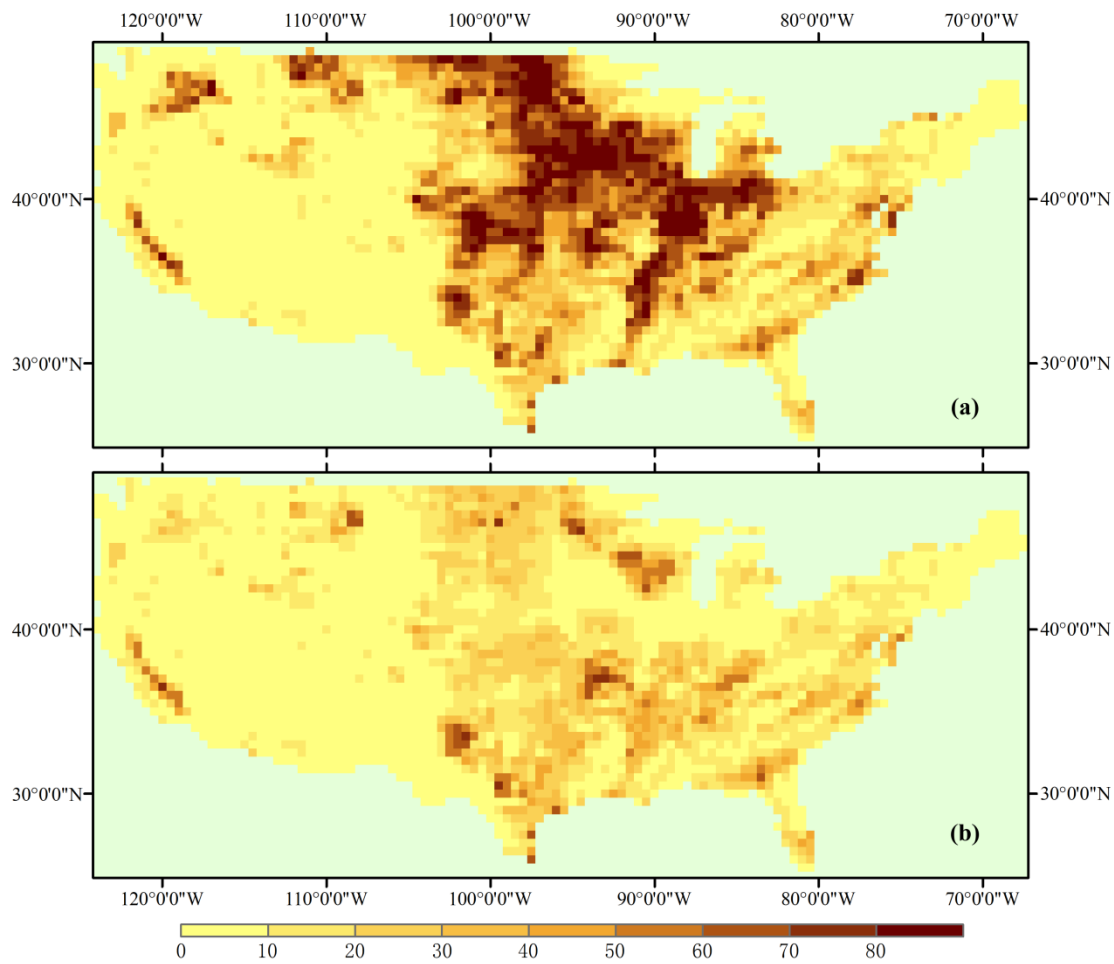
Figure 2. 1 Two scenarios of land conversion fraction: (a) both marginal lands and croplands are converted, (b) only marginal lands are converted.
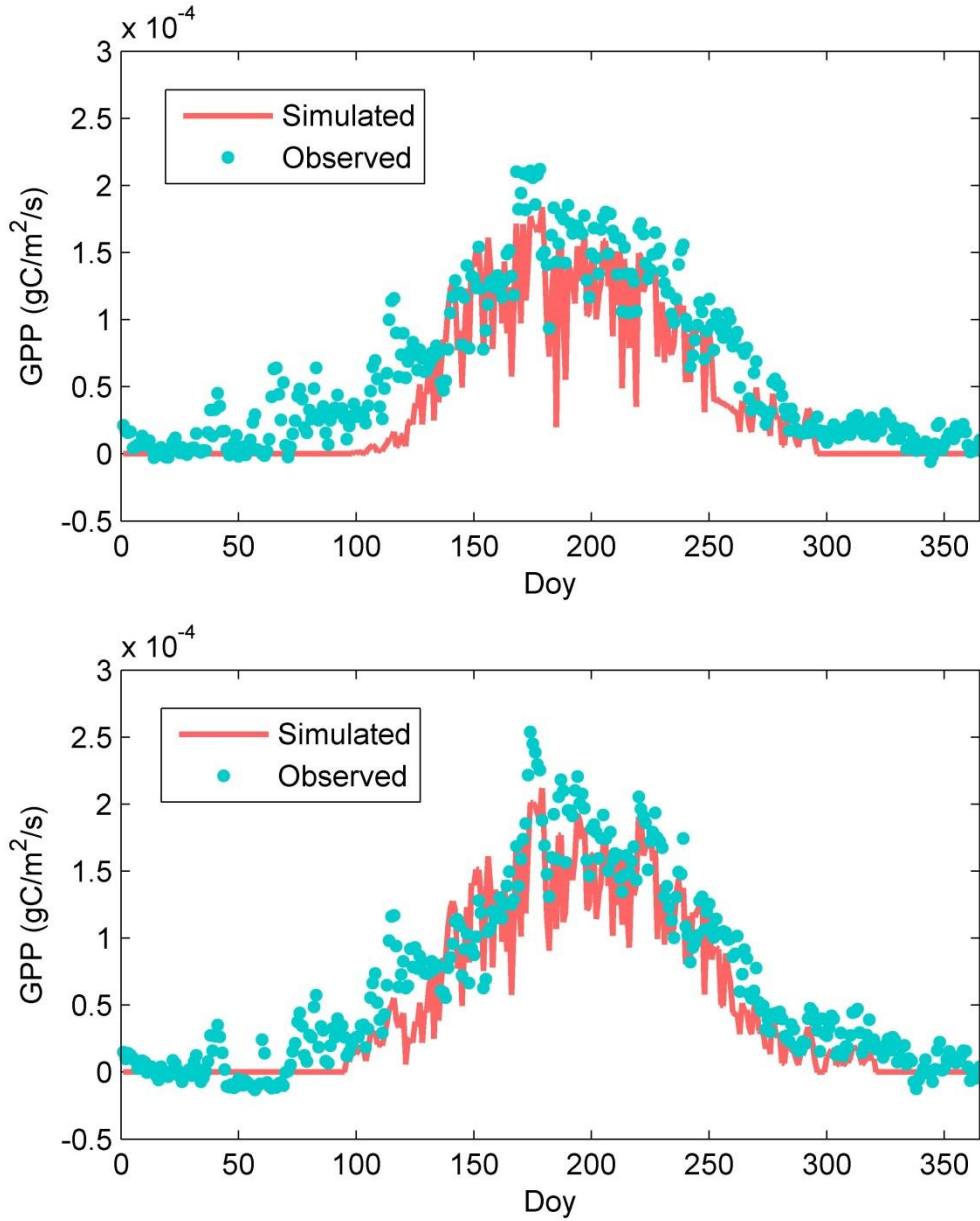
Figure 2. 2 Simulated daily photosynthesis (GPP) vs observed GPP: Switchgrass (upper panel, model = $0.92 \times$ obs + 0.000017, R^2 = 0.71, RMSE=4.47×10^{-6} gC/(m^{2}s)), Miscanthus (lower panel, model = $0.94 \times$ obs + 0.000013, R^2 = 0.75, RMSE==3.78×10^{-6} gC/(m^{2}s)).
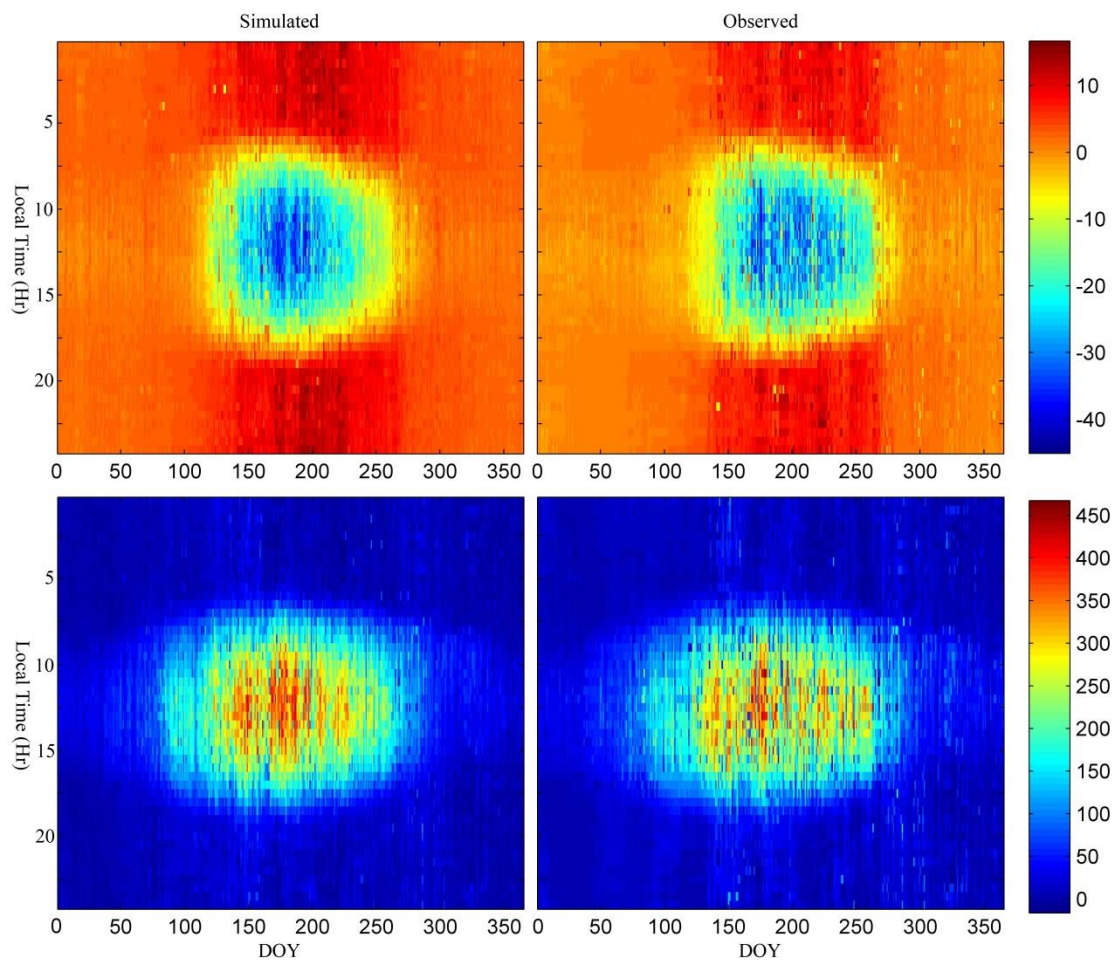
Figure 2. 3 Observed (left column) and simulated (right column) net ecosystem exchange (NEE, top row), latent heat flux (LE, bottom row) at half hour interval for Switchgrass in 2011
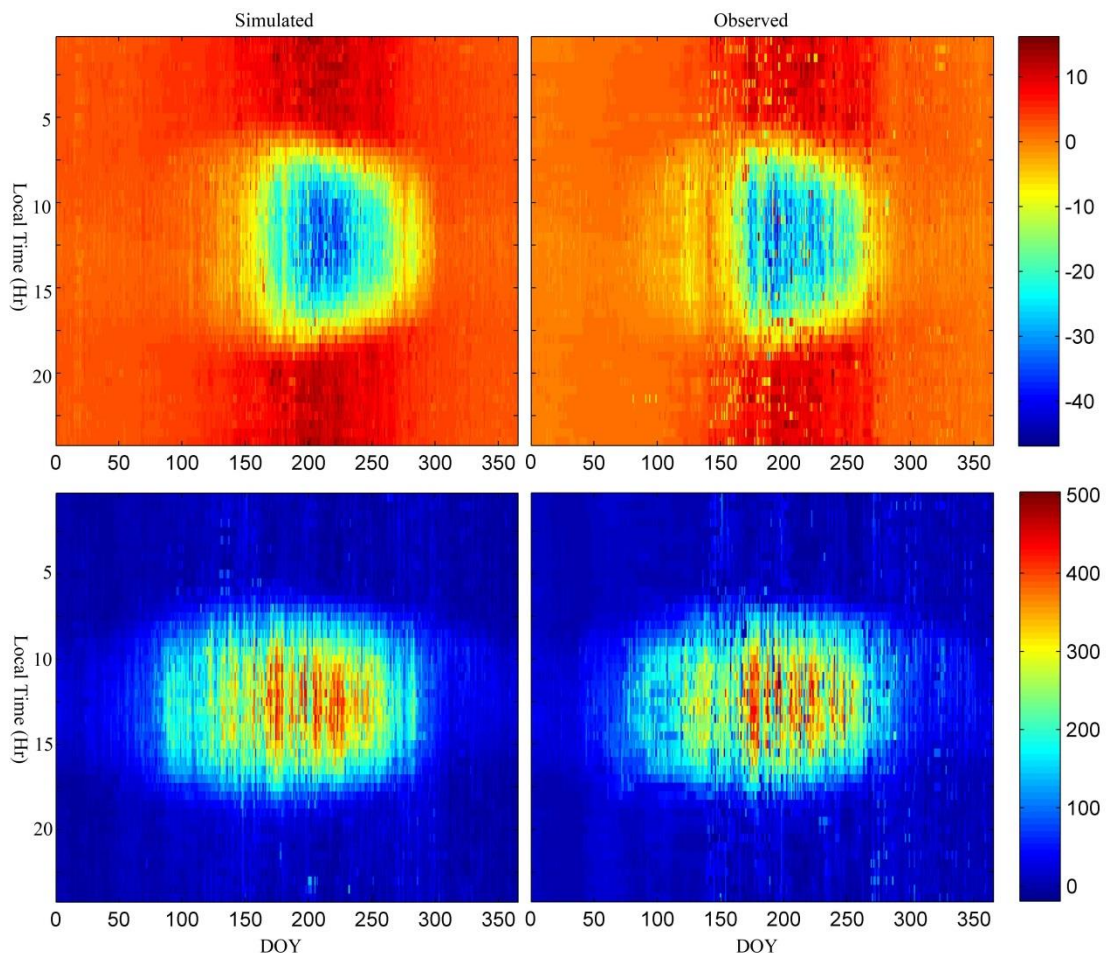
Figure 2. 4 Observed (left column) and simulated (right column) NEE (top row), LE (bottom row) at half hour interval for Miscanthus in 2011
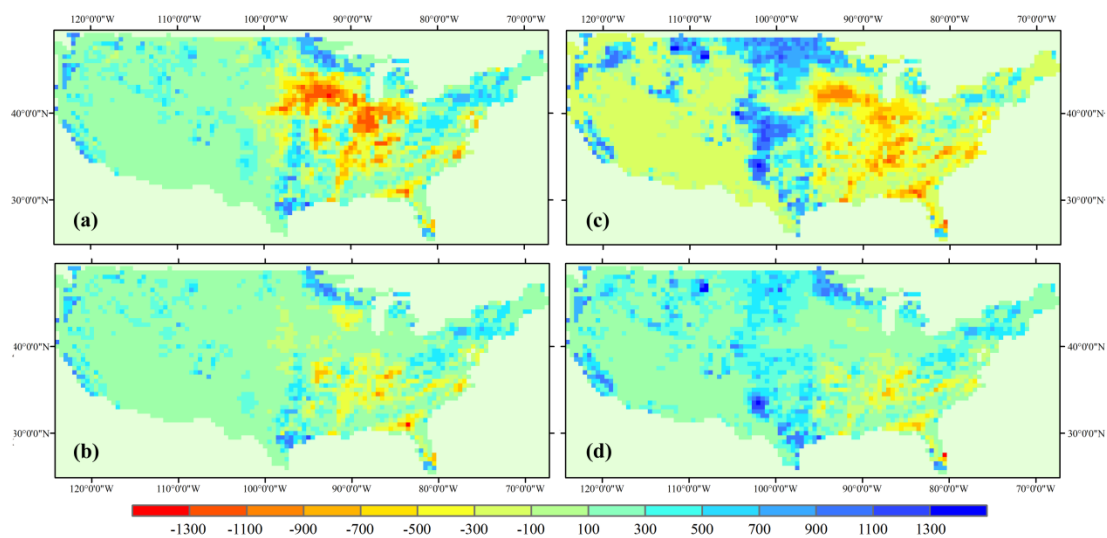
Figure 2. 5 Simulated difference of SOC (gC/m2) based on 10-year (2000–2010) climate forcing data when the soil carbon pool reaches equilibrium for corn1-cntl (a), corn2-cntl (b), corn3-cntl (c), corn4-cntl (d).
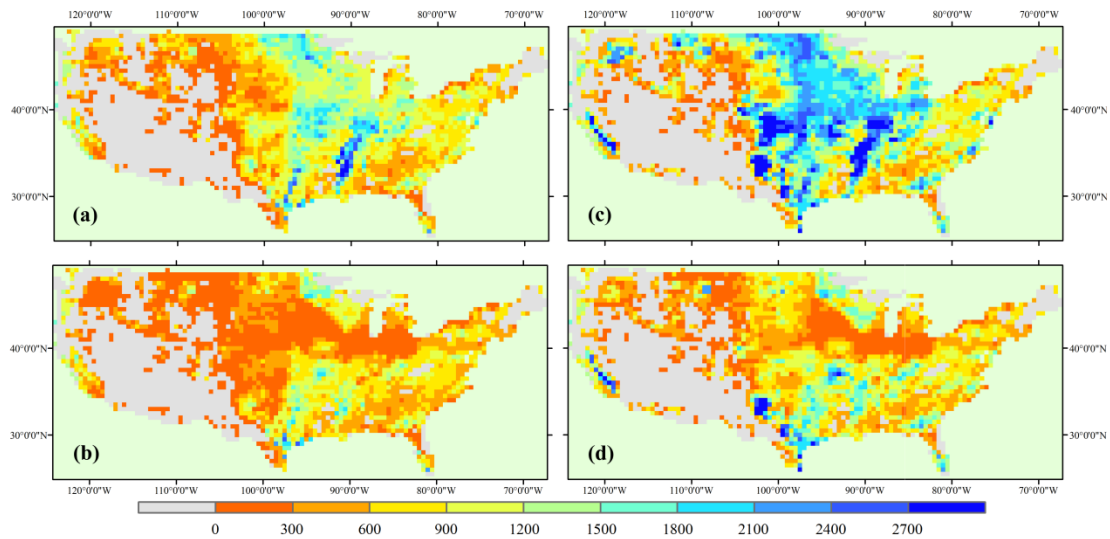
Figure 2. 6 Same as Figure 5, but for Switchgrass.
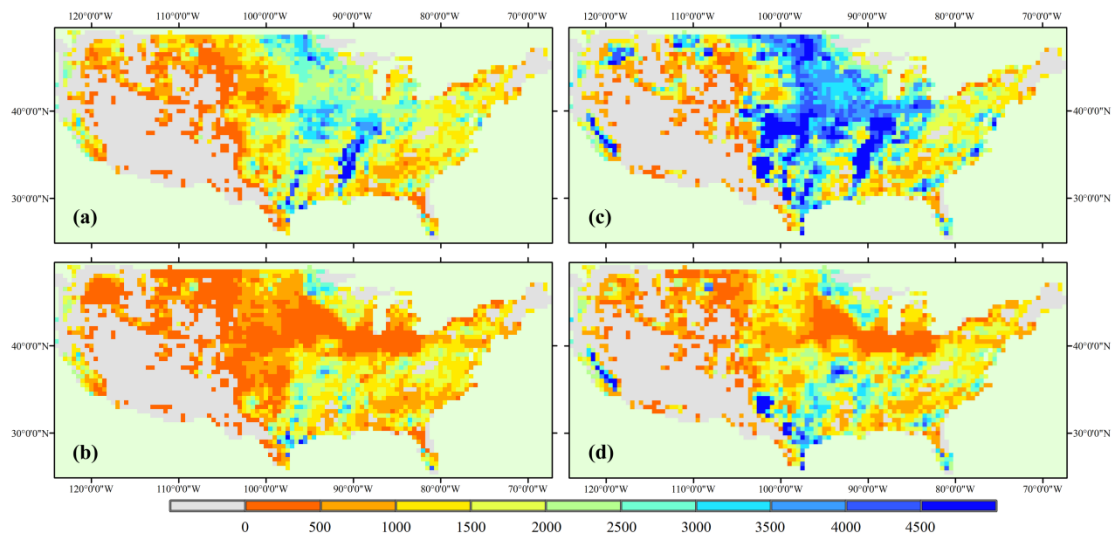
Figure 2. 7 Same as Figure 5, but for Miscanthus.
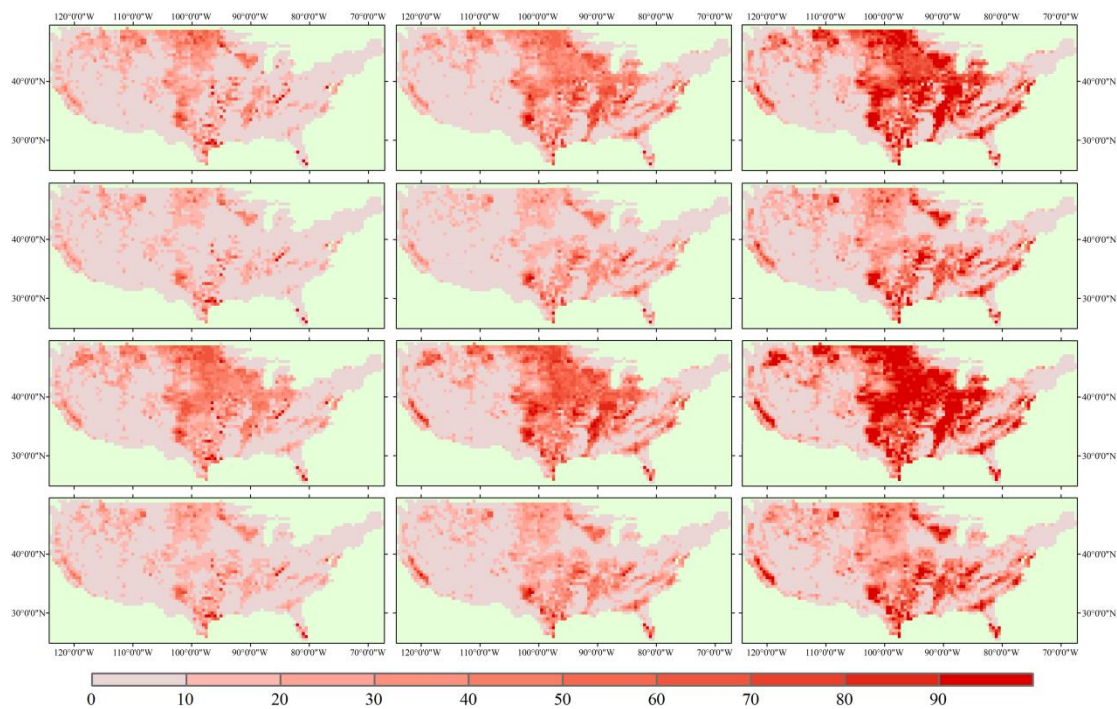
Figure 2. 8 The simulated difference of annual net carbon flux (gC/m^2) based on 10-year (2000–2010) climate forcing data among each experiments, (a)-(l) corresponds to the difference between corn1, corn2, corn3, corn4, sw1, sw2, sw3, sw4, mx1, mx2, mx3, mx4 and cntl, respectively.
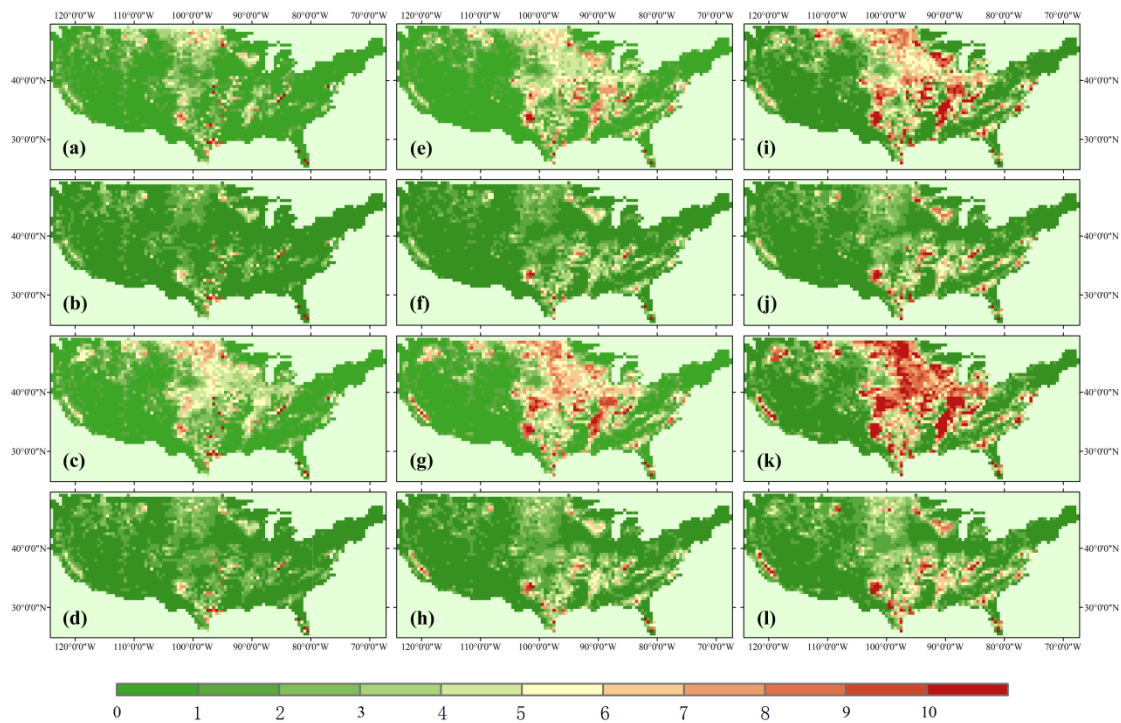
Figure 2. 9 Same as Figure 8, but for LE (W/m^2).
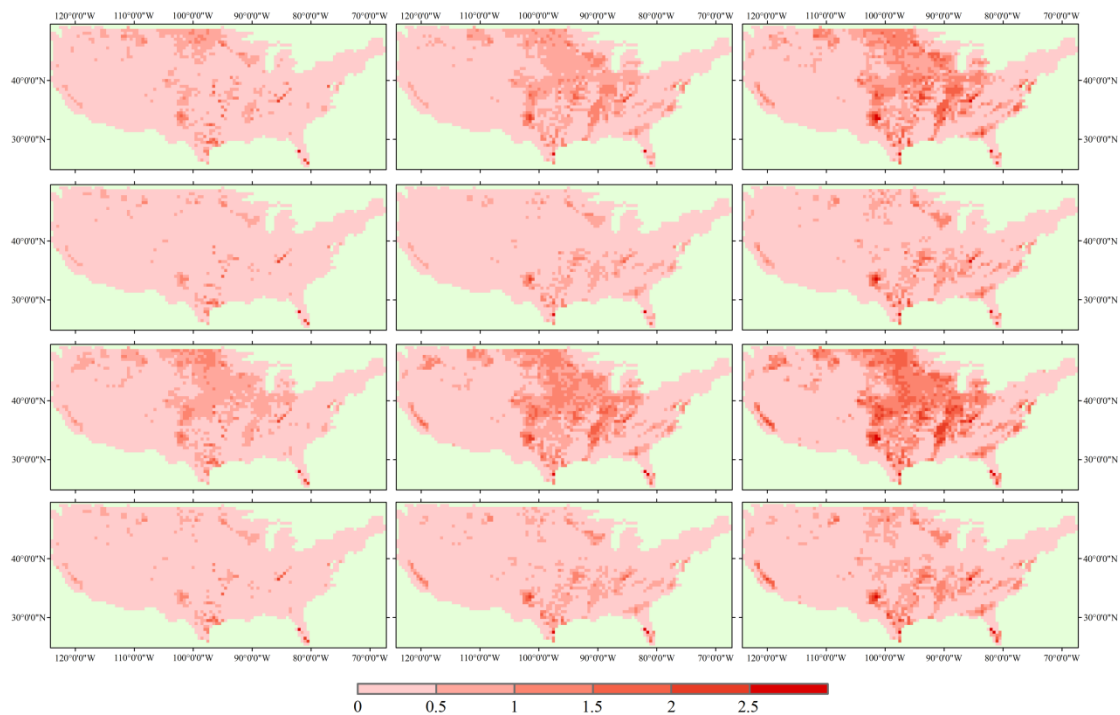
Figure 2. 10 Same as Figure 8, but for Rn (W/m^2).

CHAPTER 3.   THE IMPORTANT BUT WEAKENING MAIZE YIELD BENEFIT OF GRAIN FILLING PROLONGATION IN THE US MIDWEST

Abstract: A better understanding of recent crop yield trends is required for sustaining the yield progress and maintaining food security. Several possible mechanisms have been investigated recently in order to explain the steady growth in maize yield over the US Corn-Belt, but a substantial fraction of the increasing trend remains elusive. In this study, we argue that shift towards varieties with prolonged grain filling period (GFP) had a much greater contribution to the recent yield trends than previously thought. By using long term satellite data from 2000 to 2015, we identified an average lengthening of GFP of 0.37 days per year over the region, which probably results from variety renewal. An empirical statistical model demonstrated that longer GFP contributed roughly one-quarter (23%) of the yield increase trend by promoting kernel dry matter accumulation, yet less yield benefit was identified in hotter counties. Both official survey data and crop model simulations estimated a similar contribution of GFP trend to yield. If growing degree days that determines the GFP continues to prolong at the current rate for the next 50 years, yield reduction will be lessened with 25% and 18% longer GFP under Representative Concentration Pathway 2.6 (RCP 2.6) and RCP 6.0, respectively. However, this level of progress is insufficient to compensate yield losses in future climates, because drought and heat stress during the GFP will become more prevalent. Our study highlights devising multiple effective adaptation strategies is necessary to withstand the upcoming challenges in food security.

3.1   Introduction

Agricultural systems in many regions may be negatively impacted by increasing temperature especially when accounting for the nonlinear effect of climate extremes such as heat waves and droughts (Rattalino and Otegui, 2013; Porter and Semenov, 2005; Sánchez et al., 2014; Schlenker and Roberts, 2009), which are predicted to become increasingly frequent in a warmer climate. Higher-than-optimal temperature negatively impacts maize yield through affecting reproductive structures (Siebers *et al.,* 2015; Siebers *et al.,* 2017), decreasing the Rubisco activation (Crafts-Brandner, 2002), and increasing water stress (Lobell *et al.,* 2013). Thus, to

maintain or potentially increase productivity, agricultural systems must adapt to upcoming warmer and more extreme climates.

As the world's largest producer of maize, the US has seen a steady increase in maize yield since the 1950s through improvements in agronomic practices, genetic technology and favorable growing conditions despite interannual yield variability related to hot and dry summers (USDA, 2015). Several possible mechanisms have been investigated in order to understand this increasing trend in yields, including: expansion of more heat tolerant cultivars (Driedonks *et al.,* 2016), delayed foliar senescence or stay-green traits (Thomas and Ougham, 2014), new cultivars adapted to higher sowing density (Duvick, 2005; Tollenaar and Wu, 1999), development of pest resistant maize cultivars through genetically engineering (NRC, 2010), enhanced water use efficiency under rising atmospheric CO_2 (Lobell and Field, 2008; Jin *et al.,* 2017), and increase in accumulated solar radiation during the post-flowering phase (Tollenaar *et al.,* 2017). A drought sensitivity analysis over US Midwest based on field maize yield data showed, however, higher sowing density brought about side effect that field maize yield sensitivity to water stress became increased (Lobell *et al.,* 2014). In this context, it is necessary to understand the response of maize yield in farmers' fields to climate variation over time and thereby allowing crops more effectively to adapt to the future climate change.

Crop phenological development is an essential reference for agricultural management practices (Irmak *et al.,* 2000), and reflects the combined effect of climate exposure and plant physiological traits (McMaster *et al.,* 2005). Specifically, this study focused on GFP, a critical kernel development stage when plant growth and grain formation is sensitive to stress *(*Badu-Apraku, 1983; Çakir, 2004; Cheikh, 1994*)*. In addition, because there is a tight positive correlation between the grain filling length (GFL*)* and the final crop yield *(*Tollenaar *et al., 2017;* Badu-Apraku, 1983*)*, characterizing recent trends in GFL may also help explain yield trends.

Satellite remote sensing observations such as the vegetation index derived from moderate-resolution imaging spectroradiometer (MODIS) reflectance data provide the opportunity to characterize the regional-scale spatiotemporal patterns of field crop growth status information, in particular phenological transition dates (Sakamoto *et al.,* 2010). In this study, 8-day Wide

Dynamic Range Vegetation Index (WDRVI) derived from MODIS reflectance data (MOD09Q1 and MYD09Q1) from 2000 to 2015 was used to map trends in maize phenology in Illinois, Indiana, Iowa, Nebraska across the US Midwest, which collectively account for half of the total US maize production. To extract maize phenology, shape model fitting (SMF) has been shown as an effective approach and was validated at both site and state level (Sakamoto *et al.,* 2010; Sakamoto *et al.,* 2014; Zeng *et al.,* 2016). On the other hand, threshold based methods can be used to extract the starting and ending of growing season more flexibly. Thus, we developed and implemented a hybrid method combining SMF and threshold-based analysis to generate 8 million samples of maize phenological date from MODIS WDRVI data at 250×250 m spatial resolution from 2000 to 2015. This satellite data produced spatially explicit maize phenological date then was used to understand the relationship between GFP prolongation and yield increase.

3.2   Materials and Methods

3.2.1   Satellite data

In this study, the 8-day time series of 250 m daily surface reflectance MODIS data on board Earth Observing System (EOS) Terra and Aqua satellite platforms: MOD09Q1 (2000-2015) and MYD09Q1 (2002-2015) Collection 6, was used. Four tiles MODIS data (h10v04, h11v04, h10v05, h11v05) covering the study area (4 states: Indiana, Illinois, Iowa, Nebraska) were downloaded from NASA Land Processes Distributed Active Archive Center. Although the daily satellite observations can better capture the phenological phase transition during maize growth, the 8-day composite products in MOD09Q1 and MYD09Q1 are selected to minimize the impact of clouds and haze. Generally, the MODIS 8-day composite products were systematically corrected for the effects of aerosol light scattering (Vermote and Vermeulen, 1999). Meanwhile, the constrained view-angle maximum value composite method guarantee the quality of surface spectral reflectance data for each 8-day period   (Huete *et al.,* 2002). Both 250m MOD09Q1 and MYD09Q1 data consists of red (R) and near-infrared (NIR) bands with an actual spatial resolution of 231.7 m. Here a scaled WDRVI (Wide Dynamic Range Vegetation Index) is used to monitor the growing status of maize plants (Zeng *et al.,* 2016), because WDRVI is supposed to have a better performance in characterizing seasonal biomass dynamics than normalized difference vegetation index (NDVI), which is often saturated for dense vegetation and a linear

relationship was identified between WDRVI and the green leaf area index (LAI) of both maize and soybean (Gitelson, 2004; Gitelson *et al.,* 2007). The scaled WDRVI is calculated by the following equation:

$$\text{WDRVI} = 100 * \frac{\left[(\alpha - 1) + (\alpha + 1) \times \text{NDVI}\right]}{\left[(\alpha + 1) + (\alpha - 1) \times \text{NDVI}\right]} \tag{1}$$

$$NDVI = (\rho_{NIR} - \rho_{red})/(\rho_{NIR} + \rho_{red}) \tag{2}$$

Where ρ_{red} and ρ_{NIR} are the MODIS surface reflectance in the red and NIR bands, respectively. A comparison of multiple vegetation indexes indicates WDRVI with α=0.1 showed a strong linear correlation with corn green LAI (Guindin-Garcia *et al.,* 2012). Here we also set α as 0.1 for WDRVI calculation. Before WDRVI calculation, the reflectance data were quality-filtered using the band quality control flags. Only the data passing the highest quality control test is retained.

3.2.2   Crop location information

A cropland dynamic layer (CDL) spanning from 2000 to 2015 generated by USDA/NASS is used to be as maize mask (The time span of NASS-CDL for Nebraska is from 2001 to 2015). The spatial resolution of the original products of NASS-CDL varied from year to year due to different satellite data being used. The satellite data sets used to generate NASS-CDL over 2000–2005 and 2010-2015 were obtained from Landsat/TM with 30 m resolution. Those used to generate NASS-CDL over 2006–2009 were obtained from Resourcesat-1/AWiFS with 56 m resolution. The CDL data was firstly projected to MODIS sinusoidal projection and then aggregated to 231.7 m. We only extracted the phenological information over the MODIS pixels with the corresponding maize fraction surpassing 80% determined by CDL aggregation, which can thus suppress the mixing effect of other vegetation types like grasses and soybean. The classification errors in the CDL data might mix non-crops signal into the WDRVI calculation. However, previous study showed that the influence of classification errors on maize phenological extraction can be minimized at regional scale (Sakamoto *et al.,* 2014), especially when a high threshold value (here it is 80%) was applied to filter mixing pixels.

3.2.3   Maize phenology and yield statistics data

USDA/NASS surveys crop progress and condition based on questionnaires and publishes percent complete (area ratio) of crop fields that have either reached or completed a specific phenological stage, on Agricultural Statistics Districts (ASD) or state level, in a weekly report called the Crop Progress Report (CPR). The state level phenology information is available in the USDA/NASS Quick Stats 2.0 database. This weekly reported area ratios were interpolated using sigmoid function. The target phenological stages (emerged, silking, dent, and mature stages) were then determined as the date when the interpolated area ratio reached 50% on a state level (Tollenaar et al., 2017). The phenological dates from CPR were used as a reference to evaluate the MODIS based estimations.The county-level corn grain yield data covering the 4 states (IL, IN, IA, NE) were obtained from the Quick Stats 2.0 database. The selected data period was from 2000 to 2015. The unit system for corn grain yield is bushel per acre (bu/ac).

3.2.4   Climate data

Daily precipitation, minimum and maximum temperatures and relative humidity data at 4km resolution was obtained from University of Idaho Gridded Surface Meteorological Data (Abatzoglou, 2013) (http://metdata.northwestknowledge.net/). It is a gridded product covering the US continent and spanning from 1979 to 2016. This dataset is created by combining attributes of two datasets: temporally rich data from the North American Land Data Assimilation System Phase 2 (Mitchell, 2004) (NLDAS-2), and spatially rich data from the Parameter-elevation Regressions on Independent Slopes Model (Daly et al., 2008) (PRISM). After validated using extensive network of weather stations across the United States, this dataset is proved to be suitable for landscape-scale ecological model. To be consistent with the climate data resolution, MODIS derived maize phenology information is aggregated to 4 km by averaging all available maize phenological date. Then the climate variables like mean temperature, mean VPD and mean precipitation during the vegetative period, grain filling period and total growth period are estimated by integrating daily climate data over the corresponding period according to MODIS derived phase starting and ending date. VPD is estimated from relative humidity and temperature data.

Here GDD, a commonly used metric as the cumulative warmth for a crop having experienced over the growing season for maize, is calculated from daily temperature values. It is defined as the sum of all daily average temperatures over the growing season in excess of 8 °C. A base temperature of 8 °C and a maximum temperature of 35 °C for maize were used (Kiniry and Bonhomme, 1991).

3.2.5   Maize growing phase extraction

A shape model fitting (SMF) (Fig. 1), which represents the general pattern of corn growth characterized by time-series WDRVI, was created using a similar procedures as previous study (Sakamoto *et al.,* 2010). The shape model was defined by averaging 10 years (2001 to 2010) of 8 days WDRVI observations from the irrigated continuous corn field at Mead, Nebraska operated by the University of Nebraska Agricultural Research and Development Center. The dates of the key phenological stages on the shape model were empirically determined based on the ground-based phenology observations. In the original study (Sakamoto *et al.,* 2010), the preliminarily defined dates of emerged, silking, dent, and mature stages is set as 150, 200, 240 and 265, respectively. These parameters are also used in this study. Then, the shape model was geometrically scaled and fitted to 8-day time series WDRVI data, which is generated by combining Terra and Aqua observations, with the following equation:

$$h(x) = yscale \times \{ g(xscale \times (x + tshift)) \} \tag{3}$$

where the function g(x) refers to the preliminarily defined shape model function and x refers to WDRVI acquiring date. The function h(x) is transformed from the shape model g(x) in time- and VI-axis directions with the scaling parameters xscale, yscale, and tshift. The scaling parameters were optimally estimated by using 'fminsearch' function in Matlab R2015b to minimize the discrepancy between the scaled shape model h(x) and the WDRVI data. Here the root mean square error (RMSE) between the scaled shape model h(x) and the WDRVI data is used to quantify the discrepancy.

Although the previous study showed this SMF based method had a good estimation of corn phenology at site and state level and the RMSE of maize phenological stage estimation at ASD-level ranged from 1.6 (silking date) to 5.6 days (dent date) (Zeng *et al.,* 2016), there is an

inevitable problem in this method that the linear scaling method only depending on two parameters (xscale and tshift) is too stiff and leads to identical trends in the 4 phenological dates (emerged, silking, dent, and mature date). However, the US maize plants seems to have different or even opposite temporal shifts in different phenological dates as reported by Sacks and Kucharik (2011) like an advance in planting and emergence date while delay in maturity date during 1981-2005. So we need a more flexible way to characterize the different trends in the four phenological dates.

Among the numerous methods for deriving seasonal parameters from the time-series vegetation index, the threshold method, which assumes that a specific phenology will start when the vegetation index value exceeds a threshold, is widely used because it generally keeps dates within a certain reasonable range and can achieve relatively high accuracies. In general, threshold is usually selected based on crop types. In this study, the WDRVI of 18 is set as threshold based on trials when comparing the estimation with NASS reported emergence date and maturity date for 4 states. We used a hybrid method by merging the advantage of SMF in extracting the silking and dent dates and the threshold method in extracting the growing start (emergence) and ending (maturity) date (Fig. 1). Furthermore, SMF was restricted to only fit WDRVI curve for a specific range, where WDRVI is above its 40% peak value, so the estimated parameters are mainly relevant to the silking and denting phenological information. Before applying the threshold method, the WDRVI curve is firstly smoothed using a robust smoothing-spline approach to reduce the signal noise (Keenan *et al.,* 2014). To minimize the impact of maize pixels contaminated by clouds, cloud shadow and aerosol loading, a 3*3 windows is used to filter the data. In each 3*3 windows, only those with more than 4 maize pixels were selected for phenology extraction, so there were multiple observational vegetation index data to constrain the optimization model, which can thus improve the stability of parameters estimation. In addition, the searching boundary for the scaling parameter yscale and xscale was empirically set as [0.4, 1.8] to ensure the extracted phenological date within a reasonable range. Finally, approximate 8 million grids containing the 4 critical phenological date over 16 years were retrieved. When the MODIS extracted emergence date was aggregated to the state level and compared with the NASS CPR, we found a systematic bias in emergence dates that MODIS estimated emergence dates were 7.6 days later than the NASS report date. This systematic bias

might result from the selection of WDRVI threshold. Then this systematic bias was deducted from the MODIS derived emergence date before comparison. Nevertheless, the bias will not influence the estimation of grain filling starting and ending date. The state level comparisons show a good agreement for the four key phenological stages with the RMSE ranging from 1.6 (silking date) to 4.4 days (dent date) (Table 1).

Finally, the GFP and grain filling GDDcrit trend was analyzed in 4km grid cell to keep consistent with the spatial resolution of climate data. This larger grid size than the orignal resolution of MODIS data (250m) brings more phenological samples for trend analysis, thus a stronger statistical inferences can be made.

3.2.6   Yield stability and GFP

Generalized additive regression model (GAM), an effective and flexible method to characterize nonlinear effects of explanatory variables, was used here to explore the relationship between yield stability and GFP. Coefficient of variation and standard deviation of county yield over time were alternatively used to represent the temporal stability of maize yield. The model was constructed based on R package "mgcv" (Wood, 2006). The spline method was used as the smooth term. In addition to GFP, climatic variables including multi-year mean precipitation, mean daily temperature and vapor pressure deficit (VPD) during GFP over 2000-2015 were also selected as the covariates. Both county level GFP and the trends in GFP were alternately used as the explanatory variables, so the influence of the longer GFP in space and GFP extension over time on yield stability can be analyzed.

3.2.7   Crop model simulations

An agricultural system modeling platform APSIM version 7.7 is used here to simulate the benefit of GFP extension under future climate. APSIM can simulate a number of crops under different climatic and management conditions, and hence is used worldwide to address a range of research questions related to cropping systems (Holzworth *et al.,* 2014). In particular, maize is simulated by the APSIM-Maize module. The APSIM-Maize module is inherited from the CERESMaize, with some modifications on the stress representation, biomass accumulation and phenological development (Hammer *et al.,* 2010). This flexible process-based model allows us to separately

estimate the yield benefit of agronomic practices like the cultivar shift indicated by higher thermal time requirement during grain fillling.

The MODIS data showed both the grain filling GDD_{crit} and GFP increased, suggesting the GFP extension is likely to be associated with variety change, such as the adoption of longer maturity variety. We designed three simulations to explore the contribution of GFP extension to recent decades yield increase. GDD_{crit} was increased to drive a prolonged GFP to emulate the adoption of longer maturity variety over this period. Simulation sim1 is the control with no increase in variety GDD_{crit}; simulation sim2 sets an increase in variety GDD_{crit} by 0.65% per year which charasterized the observed increasing rate in all counties; simulation sim3 sets an increase in GDD_{crit} by 0.82% per year which represented the observed increasing rate in GFP prolonged counties. All of the simulations were forced with University of Idaho Gridded Surface Meteorological Data. The soil parameters, like soil hydraulic properties and soil organic matter fractions were extracted from the State Soil Geographic (STATSGO) data base, as collected by the National Cooperative Soil Survey over the course of a century. For each simulation grid, the soil information was queried through R package 'soil DB' (http://ncss-tech.github.io/AQP/). Management information like planting density and fertilizer application amount was taken from the USDA NASS survey report at state level. Crop sowing date was derived from the Crop Calendar Dataset (Sacks *et al.,* 2010). We used generic maize hybrids ('B_110') provided by APSIM version 7.7 to run the simulation.

To investigate the yield benefit of longer GFP until 2060-2070, we constructed two simulations for climate forcing data from historic (2000-2015) period and two future climate scenarios (RCP2.6 and RCP6.0), respectively: one is the control simulation, where the maize GDD_{crit} was set as a constant using generic cultivar parameters ('B_110'); the other one is the GFP prolonged simulation, where GDD_{crit} was increased by 0.82% per year to be consistent with the current advance in maize cultivar based on historical MODIS image analysis. For historic period simulation, the climate forcing data during 2000-2015 was recycled until 2070. For the future climate scenarios, three climate forcing data was used to account for the climate model uncertainty in global temperature: Institute Pierre Simon Laplace CM5A Earth system model (IPSL-CM5A-LR), Geophysical Fluid Dynamics Laboratory Earth System Model with

Generalized Ocean Layer Dynamics component (GFDL-ESG2G) and the Hadley Centre Global Environment Model, version 2-Earth System (HadGEM2-ES). As a C_4 plants, maize plants loss less water in response to future enriched atmospheric CO_2, which is modeled by enhanced transpiration efficiency in APSIM. The CO_2 concentration is set as 380 ppm for historic simulation while increased to follow the concentration trajectory defined in RCP2.6 and RCP6.0 (Meinshausen *et al.,* 2011). The soil parameters and management information followed the above simulation for historic period. Then yield increasing rate in 2060-2070 is calculated by (yield with prolonged GFP - yield in control simulation)/(yield in control simulation) with three climate forcing data: historic period, RCP2.6 and RCP6.0.

3.2.8   Conceptual model of GFP trend analysis

Although there are many kinds of equations to estimate GDD, GDD during GFP can be generally written as:

$$GDD_8^{35} = \int_{silking}^{maturity} DD_t, DD_t = \begin{cases} 0, when\, Tmean < 8 \\ Tmean - 8, when\, 8 \leq Tmean < 35 \\ 27, when\, Tmean \geq 35 \end{cases} \tag{4}$$

8, 35 means the lower and upper boundary of daily mean temperature (Tmean) to calculate GDD. As most of Tmean is within this range, it can be approximately written as:

$$GDD_8^{35} \approx GFP \cdot (Tmean - 8) \tag{5}$$

Then the GFP trend can be rearranged as:

$$\frac{dGFP}{GFP \cdot dt} \approx \frac{dGDD}{GDD \cdot dt} - \frac{d(Tmean - 8)}{(Tmean - 8) \cdot dt} \tag{6}$$

So GFP trend ($\frac{dGFP}{GFP \cdot dt}$) can be approximately estimated by GDD trend minus Tmean trend. As Tmean trend is very small (Fig. 4), GFP trend is mostly driven by GDD trend.

3.3   Results and Discussion

The verification at state level showed a good agreement between MODIS derived maize phenology and the National Agricultural Statistics Service (NASS) reported state mean phenological dates for the four key maize growth stages of emergence (late May), silking (Middle July), dent (late August) and maturity (late September) (Fig. 2). The root mean square error (RMSE) of the 4 phenological dates estimated over the four states ranged from 1.6 days (silking date in Nebraska) to 4.4 days (dent date in Nebraska) (Table 1). The duration between emergence and maturity is used to represent maize total growth period, and the duration between silking and maturity dates is used to define the GFP. Across the four states, GFP generally starts from around day of year (DOY) 200 and ends by DOY 260 but varied interannually (Fig. 2).

GFP trend was analyzed on a 4km grid to keep consistent with the spatial resolution of climate data (Abatzoglou, 2013). We found significant trends of maize phenology, with silking dates becoming earlier in 61% of the pixels and more pixels (84%) exhibiting a later maturity date (Fig. A2). This resulted in a significant extension of the GFP over 81% of the pixels during the 16-year analysis (Fig. A2). This trend of GFP obtained from satellite data is similar to NASS reports when aggregated to state level (Fig. 3). This is also in line with the study over the U.S. Corn Belt from Sacks and Kucharik (Sacks and Kucharik, 2011) that was conducted for the earlier period of 1981-2005 based on NASS state reports.

The spatial variation of the GFP trends shows increasing trends in most Midwest areas and decreasing trends in drier areas like western Nebraska (Fig. 4a). The spatial mean of the GFP trends across the four states is 0.37 days per year with interquartile values ranging from 0.09 to 0.68 (Fig. 4b). When aggregated to the county level, 79% of the counties exhibit significant increase in GFP (Fig. 4a). As the longer GFP might be a result of increased variety thermal time accumulation, we also looked into growing degree days (GDD). GDD is a commonly used metric to measure thermal time accumulation of crops and the critical threshold GDD_{crit} at which GFP is fulfilled is an important physiological trait of maize cultivars. The GDD_{crit} calculated from satellite and climate data shows trends that have a similar spatial structure than the GFP trends, with a mean rate of increase of 0.65% per year (Fig. 4c and d). The small warming trend observed in the study area (Fig. A4) would have shortened GFP (Egli, 2004), if GDD_{crit} keeps

constant. Thus the observed longer GFP is likely to be associated with variety shifts, marked by the concurrently increasing GDD$_{crit}$. As GDD$_{crit}$ reflects the thermal time requirement of a specific cultivar to achieve grain filling, the increasing GDD$_{crit}$ over time (Fig. 4c) and the higher GDD requirement from emergence to maturity in south counties with warmer temperature (Fig. 5 and Fig. A5) suggest that farmers have switched to use longer maturity cultivars which compensated for the negative impact of warmer temperatures shortening the overall growing season length and the GFP (Çakir *et al.,* 2004; Dwyer *et al.,* 1994; Egli, 2004; Sacks and Kucharik, 2011).

Evidence from agronomical research shows that extended GFP contributes a higher yield by providing more time to translocate photosynthates to kernels (Crosbie and Mock., 1981; Wang *et al.,* 1999). We conducted a panel analysis to quantify the statistical contribution of increasing GFP to the observed increase of maize yield. A linear model considering the fixed effects in each year and county was used:

$$log(Yield_{i,t}) = \beta_1 * GFP_{i,t} + Year_t + County_i + \varepsilon_{i,t} \tag{7}$$

where $Year_t$ and $County_i$ specify independent intercept of each year and county. The estimated yield benefit β_1 (% per day) defining the sensitivity of yield to GFP is 0.86±0.03% (±standard error, SE), indicating that one additional day of GFP increased maize yield on average by 0.86%. According to this empirical relationship and the estimated total yield trend (1.4% per year), the lengthening of GFP observed in the MODIS data is inferred to have contributed to 23±0.7% (±SE) of the maize yield trend for all of the studied counties (Fig. 6a). This contribution was computed as:

$$\beta_1 \times GFP \text{ increasing trend / Yield increasing trend} \tag{8}$$

Equation (8) was also applied to the NASS reported maize phenological data at state level. In this application, the fixed effect term $County_i$ for each county was replaced by the state fixed effect $State_i$, and the estimated value of β_1 was slightly higher (1.08 ± 0.18% per days) compared to the above estimation (Fig. 6a). Given the mean GFP trend (0.43±0.12 days per year), which is also based on NASS report, this empirical estimation solely based on NASS report suggests GFP prolongation contributed 31±4.8% of the maize yield trend, which is slightly higher than the above estimation based on satellite data analysis.

A previous study suggested the solar brightening during GFP is responsible for about 27% of the observed increase in US maize yield from 1984 to 2013 (Tollenaar *et al.,* 2017). However, we did not find a significant increase in solar radiation across the four corn states considered during the study period when using the same solar radiation dataset integrated over the grain filling period (Fig. A6).

When counties were grouped based on whether their GFP has increased or not, counties where GFP increased showed on average higher increasing rates of GDD_{crit} (0.82% per year) and grain yield (1.5% per year) compared to the mean of all the counties (Fig. 6b). According to the estimated β_1, the mean increase in GFP for those counties is estimated to have contributed to $27\pm0.8\%$ ($\pm$SE) of the yield trend. Alternatively, counties with decreasing GFP trend, perhaps resulting from the effects of climatic warming overwhelming those of cultivars, showed a smaller yield trend of 1.0% per year (Fig. 6b). Alternatively, when equation (8) was applied to counties grouped by warmer and cooler growing season mean temperature separately, a significant ($p<0.01$) lower yield benefit (β_1) was found in warmer counties (Fig. 6b). This result implies that the yield benefit of GFP extension might be weakened in future warmer climate. This analysis also explained why the yield benefit in GFP prolonged counties was higher than the one estimated in GFP shortened counties (Fig. 6b), since the GFP shortened counties generally have a warmer background climate (Fig. A8).

To account for possible omitted variables in the above analysis, for instance if an unobserved factor such as pest resistance affects both GFP and yield on a year-to-year basis, we also conducted a regression comparing linear yield trends with GFP trends over the study period as follows:

$$Yield\ trend_i = \beta_1 * GFP\ trend_i + \varepsilon_i \qquad (9)$$

where *i* is the county indices. In this second statistical model, the effect of year-to-year variation in each county is minimized, thus the significant slope (0.82% per day) primarily quantifies the contribution of GFP trend to yield trend (Fig. 6c), which was close to the one of the panel analysis (0.86% per day). The intercept term in this regression (1.1% per years) indicates the

yield trend with no GFP extension and is 27% lower than the trends of GFP extended counties (1.5% per year), which is also consistent with the above estimation.

To further guard against the impact of potential confounding factors which might be not fully separated in the statistical models, the process-based crop model APSIM was then applied to simulate the contribution of GFP extension to yield trend. In this analysis, the variety GDD_{crit} parameter of the model was increased to simulate the observed variety shift caused GFP extension. Three simulations were conducted: sim1 has no increase in GDD_{crit}; sim2 assumes an increase GDD_{crit} of 0.65% per year from the observed mean GDD_{crit} trend in all counties; sim3 sets a larger increase of GDD_{crit} of 0.82% per year consistent with observed mean GDD_{crit} trend over a subset of counties showing significant GFP increase. Compared to the results of sim1, the modelled increasing trends of GFP in sim2 and sim3 were close to the observed GFP trend (Fig. 7). The yield increase in sim2 and sim3 attributable to GDD_{crit} presents a positive trend of 0.24% and 0.34% per year, respectively (Fig. 8), which thus produces a close estimation of the contribution of GFP extension to yield trend (Table 2). The results from sim1 also confirm that the GFP extension was caused by shift in varieties because the GFP is shortened by climatic warming where there is no increase in variety GDD_{crit} (Fig. 7).

Climate change is also expected to exacerbate the variability of crop yields (Ray *et al.,* 2015; Wheeler and Braun, 2013). Therefore, we analyzed the influence of a prolonged GFP on yield stability, another important dimension of food security (Campbell *et al.,* 2016). We used the coefficient of variation (CV) of yield in each county during 2000-2015 as an index of stability. A generalized additive regression model (GAM), suitable to account for nonlinear effects of explanatory variables, was employed to relate yield CV with GFP. We found that a longer GFP (Fig. 9a) and an increase of GFP over time (Fig. 9b) correspond to lower CV of yield when accounting for the climatic covariates, suggesting that longer GFP in both space and time is associated with more stable yields. The reason might be that the selection of longer GFP cultivars is associated with increasing stress tolerance and thereby reduces the negative impact of warming on yield stability (Tollenaar and Lee, 2002).

Finally, the APSIM model was used to investigate the future benefit of maize production across the US Midwest with three ensembles of future climate forcing data to account for the climate model uncertainty in global temperature. The simulations for the next 50 years suggest that if farmers are able to switch to longer maturity variety (at the GDD_{crit} current rate of 0.82% per year), the maize GFP in 2060-2070 will be lengthened by 25% and 18% under the RCP 2.6 and RCP 6.0 (Fig. 10a), respectively. This means an approximate 15 days extension of GFP under the RCP 2.6, so the future maturity date still falls in a reasonable period for harvesting in these simulations. Simulations indicate that a continuation of the GFP prolongation rate would continue to benefit yields (Fig. 10b), albeit by a smaller amount in future climate conditions compared to the historic period (Fig. 10c). Specifically, the predicted 10.8% and 13.6% yield loss under RCP 2.6 and RCP 6.0 could be partially offset by longer GFP, with a benefit of 7.2% and 5.6% under RCP 2.6 and RCP 6.0, respectively. The reduced benefit of GFP results in part from the increasing water and heat stress under a future warmer climate (Fig. A9), which could decrease yield significantly during maize grain formation (Siebers *et al.,* 2017).

Overall, we found a significant GFP extension and concurrent increasing GDD_{crit} during the last 16 years across the U.S. Midwest Corn Belt, which is likely to reflect changes in the traits of maize cultivars. The GFP prolongation shows the potential to increase the maize yield and also to stabilize the yield variability but its yield benefit might diminish under future warmer climate. Although the GFP information extracted here is mainly based on satellite observed canopy chlorophyll content but not on ground identified kernel color development, this method estimated a similar GFP trend and contribution of GFP prolongation to yield increase across US Midwest when compared with the state level statistical data and more importantly it provided more detailed spatial information. Our study suggests that the historic satellite data can be utilized to map field crop phenological traits at large scales with fine spatial resolution to understand how farm management influence yield trend and the climatic response of crop growth in specific stage. When the observed GFP prolongation rate is applied up to 2070, the negative impact of climatic warming is partially offset by lengthening the GFP, but the grain yield still decreased even in the mild emission climate scenario, highlighting multiple adaptation strategies are necessary in future agricultural system.

Table 3. 1 RMSE (days) of 4 phenological stages estimation over four states

State	Emergence	Silking	Dent	Maturity
Illinois	4.0	1.9	2.8	3.4
Indiana	4.2	2.2	4.0	3.2
Iowa	2.9	4.3	3.3	3.6
Nebraska	3.1	1.6	4.4	3.0

Table 3. 2 The contribution of grain filling length extension to the maize yield increasing trend estimated using APSIM (± indicates the SE)

	GFP prolonged counties	All counties
GDDcrit increasing rate (% per year)	0.82	0.65
Simulated yield increase rate (% per year)	0.34	0.24
Observed yield trend (% per year)	1.5±0.07	1.4±0.08
Contribution	23±1.6%	17±1.1%
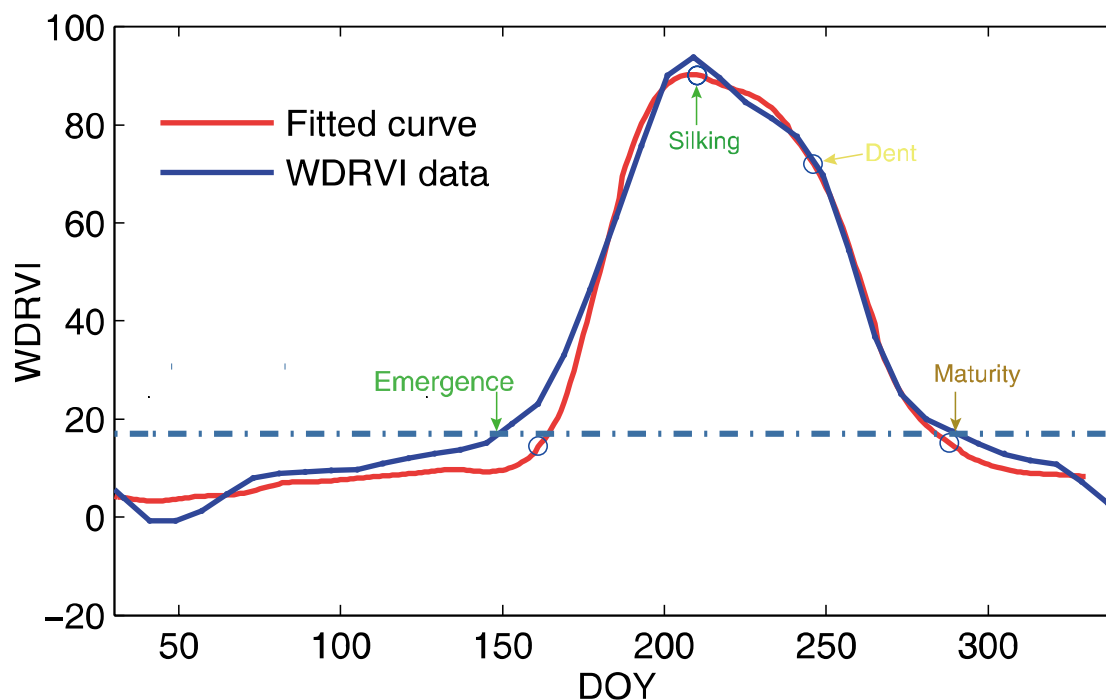
Figure 3. 1 The procedure of hybrid maize phenological extraction by merging shape model fitting and threshold based method. The blue line is the spline approach smoothed WDRVI time series data and the red line is the scaled shape model fitting and the dashed blue line indicates the threshold, which is set as 18 based on trials when compared with the NASS reported emergence and maturity date for 4 states. The circle on red curve indicates the phenological date determined by shape model fitting. Here the silking and dent date were determined by shape model fitting and the emergence and maturity date were determined by the threshold.
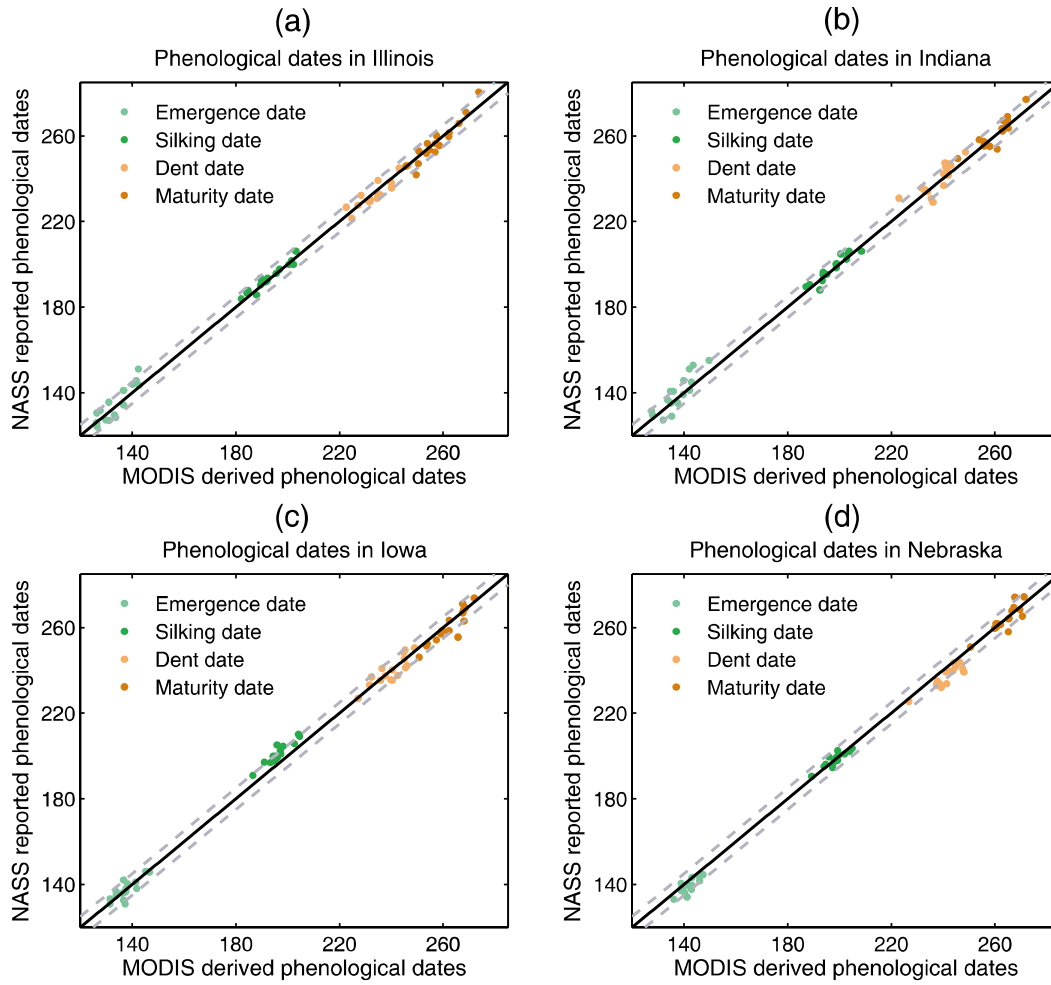
Figure 3. 2 Comparison of maize phenological dates between NASS statistical data and MODIS-derived estimation aggregated over state level. The two dashed lines in each figure define the region where the errors between MODIS-derived estimation and NASS statistical data are less than 5 days.
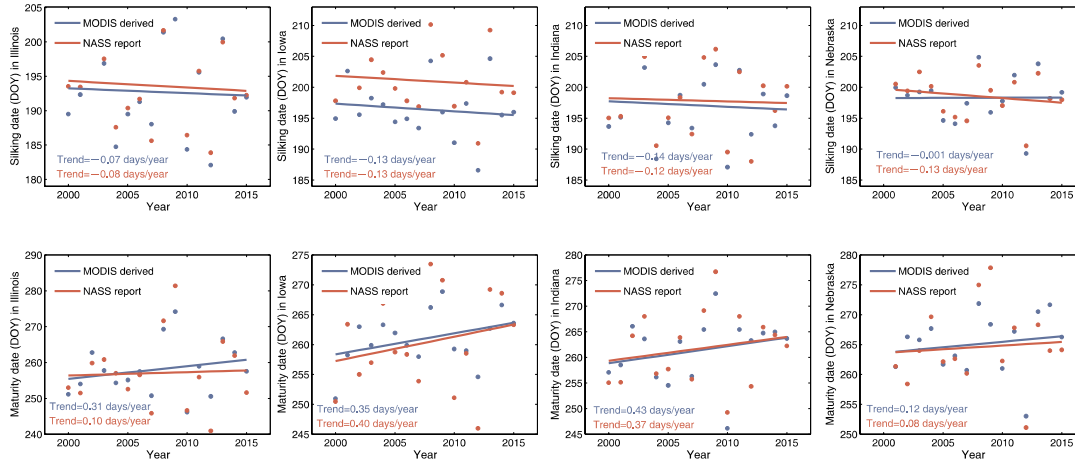
Figure 3. 3 Time series of MODIS derived (blue) and NASS reported (red) silking and maturity date for 4 states during 2000-2015. The lines show the GFL trend estimated by the non-parametric Theil-Sen fitting.
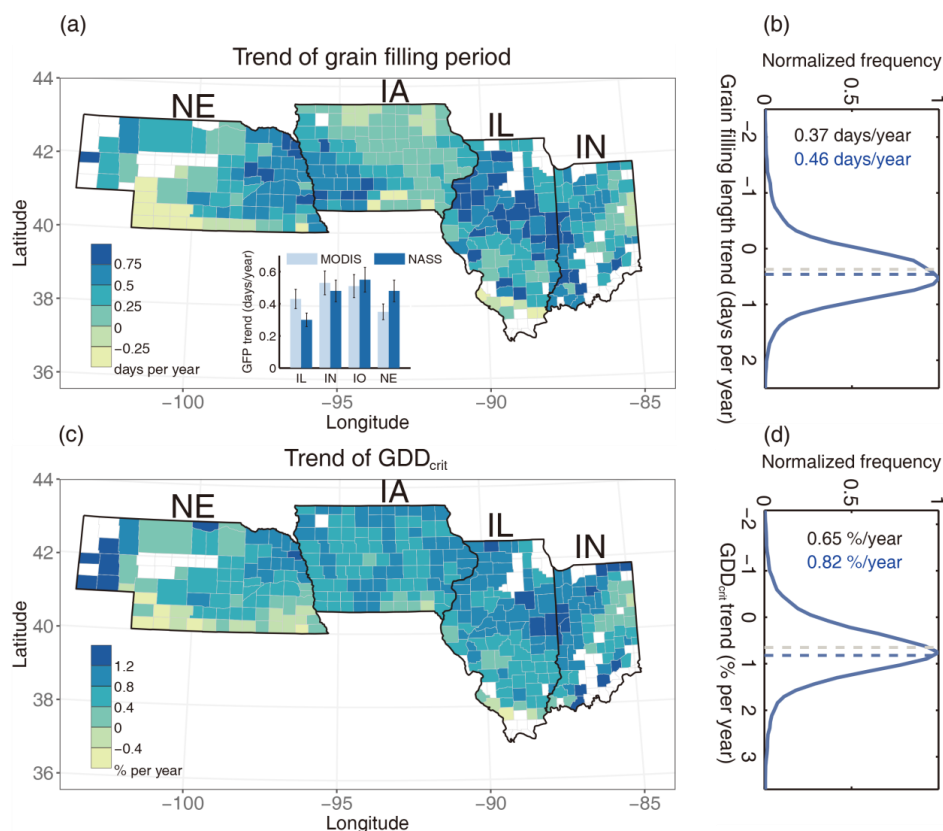
Figure 3. 4 Trends in grain filling length and grain filling GDD$_{crit}$. Trends in county-level grain filling length and grain filling GDD (GDD$_{crit}$), (a) and (c), where the empty counties mean that county has less than 12 years available data. For a specific year, a county with a number of maize grid cells less than 100 is regarded as unavailable. When estimating the trend, all of the grid cells in a county were pooled. And all of the trends shown are significant. The inset in (a) indicates GFP trend for the 4 states derived from NASS report and satellite data. The error bars indicate standard deviation of spatially estimated GFP trend. The distribution of grain filling length and GDD$_{crit}$ trend in each 4km grid, (b) and (d). The grey horizontal line illustrates the mean trend of GDD$_{crit}$ or grain filling length for all counties and the blue horizontal line illustrates the mean trend of GDD$_{crit}$ or grain filling length for the counties where GFP has extended. GFP is defined as the period from silking to maturity. The grain filling length and GDD$_{crit}$ trend was estimated by the non-parametric Theil-Sen fitting.
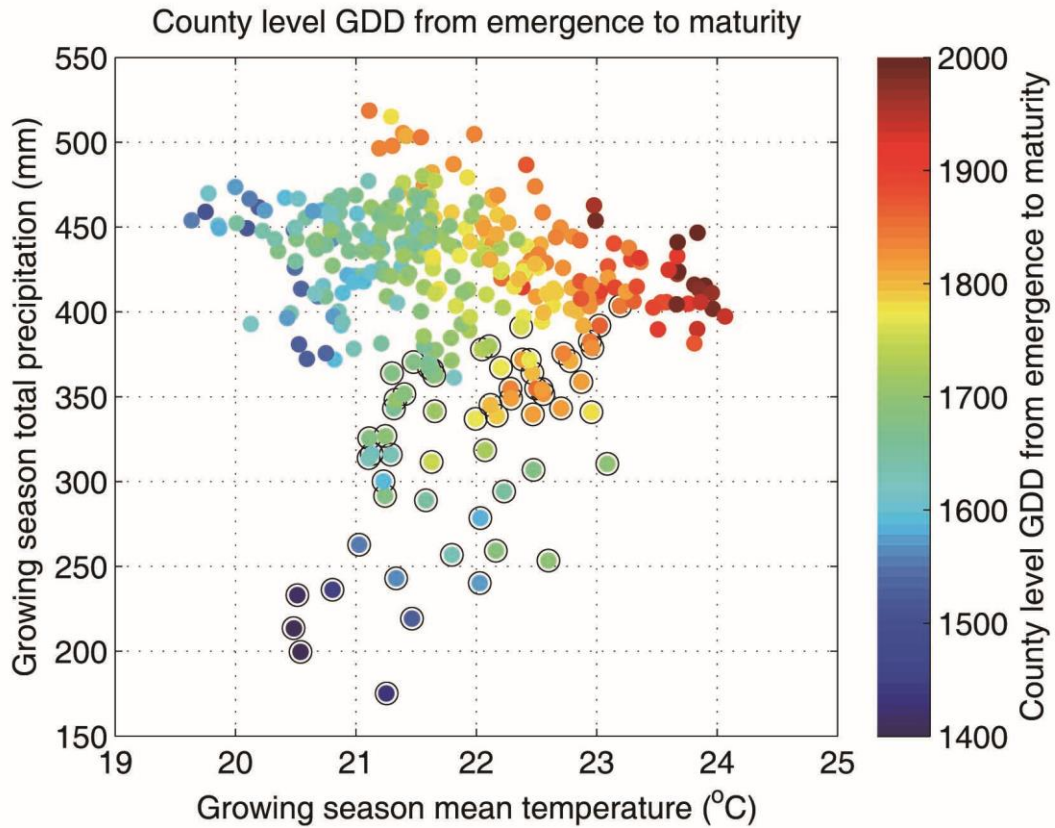
Figure 3. 5 Scattering of county level (332 counties) multiple year mean GDD from emergence to maturity in temperature and precipitation space (points with black circles indicate the counties with irrigated area > 50%).
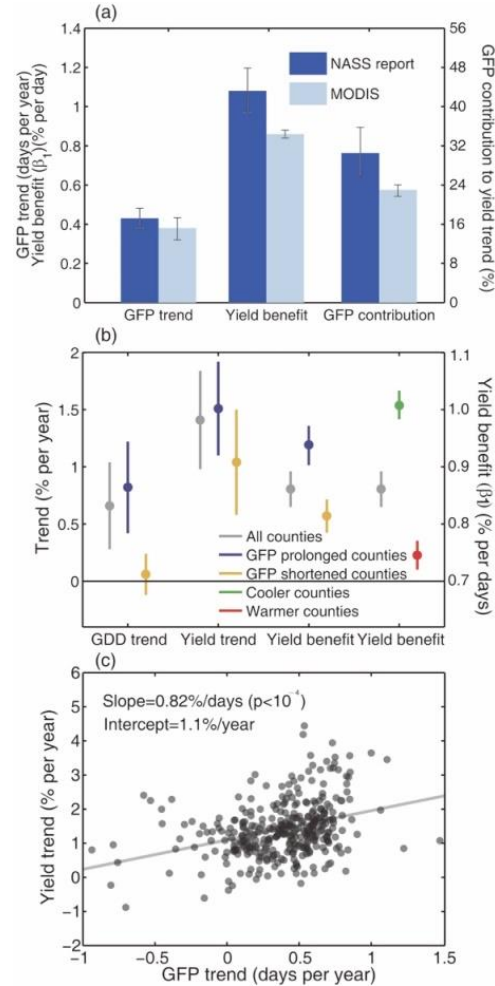
Figure 3. 6 GFP trend, yield benefit of GFP prolongation and contribution of GFP prolongation to yield increase. (a) GFP trend, yield benefit (β_1) and GFP contribution to yield increase estimated from NASS report and MODIS derived maize phenological progress data. GFP contribution was computed as: $\beta_1 \times$ GFP increasing trend / Yield increasing trend. The scales for GFP contribution to yield increase are shown in right y-axis. (b) GDD_crit trend, yield trend and yield benefit of GFP extension (β_1) based on counties grouped by whether their GFP have prolonged or not. Yield benefit was also separately estimated by grouping growing season mean temperature. Warmer and cooler counties were divided according to the median value of growing season mean temperature. The yield benefit is then estimated by applying equation (1) to each group. The scales for yield benefit are shown in right y-axis. The error bars in (a) and (b) indicate the SD of each estimation. (c) The effect of GFP trend on maize yield trend. Each point corresponds to one county's trend in GFP and yield during 2000-2015.
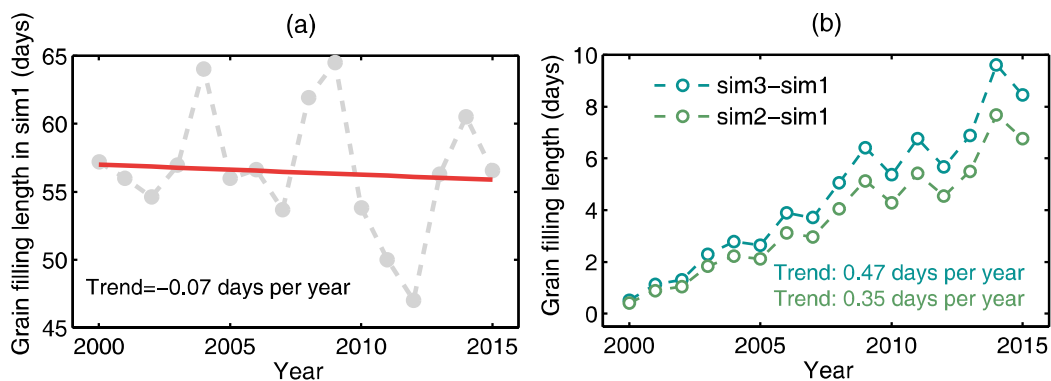
Figure 3. 7 Simulated grain filling length to explore the contribution of grain filling length to the growing maize yield using APSIM 7.7. sim1 is the control without grain filling prolongation; sim2 is to increase GDDcrit by 0.65% per year to characterize the observed GDDcrit trend in all counties; sim3 is to increase GDDcrit by 0.82% per year to characterize observation of GFP prolonged counties. The left panel shows the mean time series of GFL in simulation 1 and the right panel shows the GFL difference.
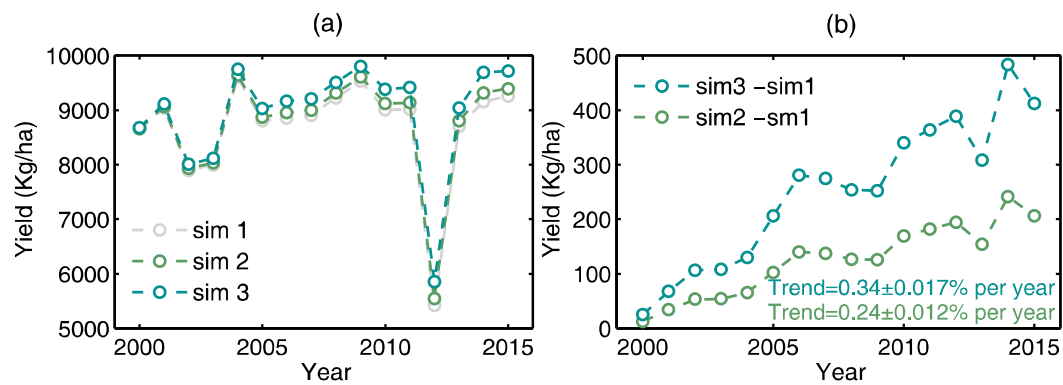
Figure 3. 8 APSIM 7.7 simulated maize grain yield with different rate of GFP prolongation to explore the contribution of grain filling length to growing maize yield.
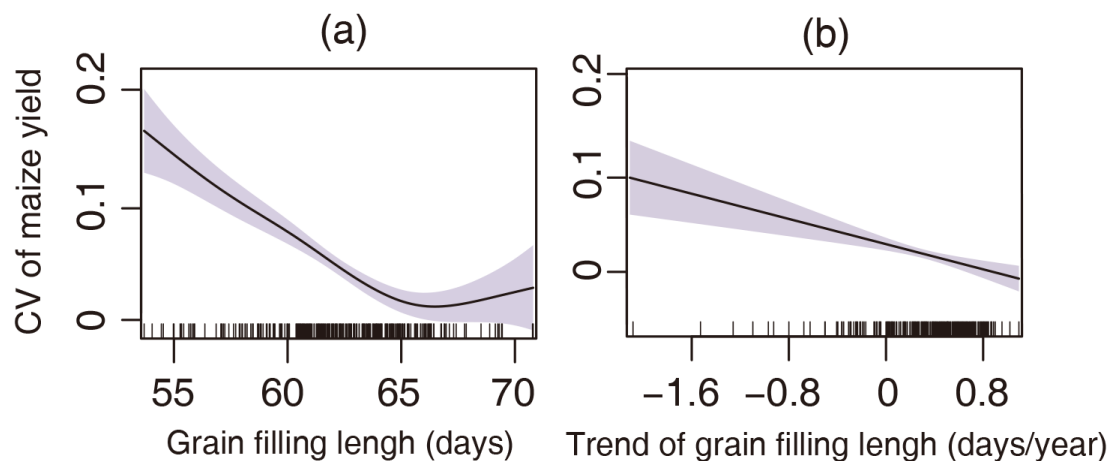
Figure 3. 9 The effect of grain filling length on maize yield stability. Coefficient of variation (CV) of the yield in each county over 2000-2015 as a function of (a) the multi-year mean grain filling length, and (b) the trend of the grain filling period. Both longer GFP across different counties in space (a) and time (b) are associated with a smaller CV of yield, that is, more stable yields. The shaded areas indicate the 95% confidence interval. Each small bar next to the horizontal line is a value observed for a county.
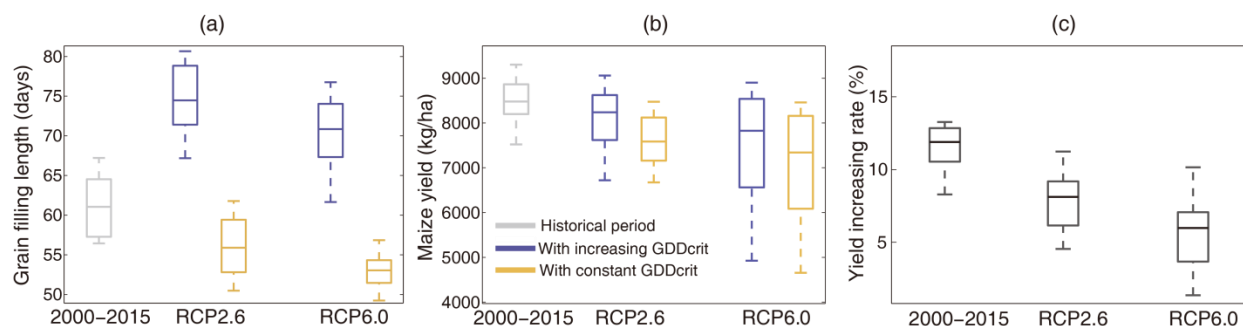
Figure 3. 10 The benefit of prolonged grain filling period for maize yield in future climate. Boxplot of grain filling length (a) and maize yield (b) simulated with the APSIM model running up to 2060-2070 assuming constant (yellow) or linearly increasing GDD_{crit} at the same rate than during the past 16 years (blue) in comparison with the historic period 2000-2015. (c) Comparison of maize yield benefit with GDD_{crit} increase at the rate of 0.82% per year in historic and future climate conditions. Here yield increasing rate up to 2060-2070 is calculated by (yield with prolonged GDD_{crit} ‐ yield with constant GDD_{crit})/(yield with constant GDD_{crit}) using three climate forcing data: 2000-2015, RCP2.6, RCP6.0 (see Method). The lines in the middle of box represent median projection, boxes show the interquartile range, and whiskers indicate the 5th–95th percentile of projections.

CHAPTER 4. HIGH TEMPERATURE NONLINEARLY DECREASES MAIZE YIELD PRIMARILY THROUGH GRAIN FORMATION

Abstract: Multiple lines of evidence have consistently suggested the reduction in global crop productivity under warmer climate (Schlenker and Roberts, 2009; Lobell et al., 2011; Zhao et al., 2017). However, there is still limited knowledge about which crop growth process is negatively or positively impacted by an increase in temperature, between biomass growth rate (BGR), growing season length (GSL) and grain formation, which is necessary to develop targeted crop adaptation strategy for future warming (Hatfield and Prueger, 2015; Siebers et al, 2015; Siebers et al., 2017). We integrated crop models, satellite data, statistical data and field experiment data to investigate how increasing temperature influences maize yield through various processes across the US Midwest. Observational data suggests a nonlinear increasing temperature sensitivity of maize yield as temperature goes up, which is predominantly determined by sensitivity of harvest index (HI), while the response of BGR and GSL is relatively small. Although model ensemble exhibited a similar pattern of temperature sensitivity, the negative impact of warming on HI is underestimated. Further analysis shows that the enhanced temperature sensitivity of HI mainly results from a higher sensitivity of yield to temperature stress during grain filling period (GFP), which accounts for approximate 63% yield reduction. Future warming might influence yield directly through frequent heat stress or indirectly through water stress. Analysis of observational data suggests that high temperature stress is more influential than water stress, especially with warmer climate, while model ensemble shows an opposite result. This discrepancy implies that the yield benefit of increasing atmospheric CO_2 might have been overestimated in crop models while direct temperature stress during grain formation is underestimated, because water conservation effect of increasing CO_2 brings more yield benefit under water stress conditions but shows limited benefit under heat stress. Our results suggest that, although maize yield has increased significantly in the US, limited progresses have achieved when confronted with heat stress during grain formation, highlighting more efforts are required for future climate adaptation during maize grain formation.

4.1   Introduction

Historical warming trend have resulted in stagnated crop production in some countries (Olesen et al., 2011). Further warming might nonlinearly decrease crop yield with increasing extreme heat events (Stefan and Dim, 2011; Schlenker and Roberts 2009), which causes oxidative damage to chloroplasts (Crafts-Brandner, 2002; Siebers, et al., 2015), destroy reproductive structures (Commuri and Jones, 2001) and facilitate crop plants senescence (Lobell et al., 2012). Faced with the challenge of meeting increasing food demands, we need to upgrade current farming system to better cope with future warmer climate. In recent decades, multiple ways have been adopted to sustain crop production increase through genetic technology and improved agronomic practices, while the actual effect could be complex due to different levels of field management and diverse natural environmental factors (Lobell et al., 2014). Therefore, it is necessary to better understand the response of crop yield to climatic variation in field conditions.

As a C_4 plant, maize often has a higher optimal temperature for photosynthesis but it is generally more sensitive during its reproductive stage than vegetative stage (Cheikh and Jones, 1994; Siebers, et al. 2017). Thus, the same level of warming treatment in different stages could result in different and even opposite influence on maize yield. In particular, a targeted adaptation strategy to deal with future warming should be on the premise of a clear understanding of how crop yield responds to warming during different development stages. Due to limited knowledge on crop stages information (Butler and Huybers, 2015), the commonly used total temperature sensitivity analysis of maize yield ignoring the stage-dependent response precluded a detailed understanding. This might bring considerable uncertainties when predicting future crop yield and developing adaptation methods. Field warming experiments were suggested to shed light on understanding climatic warming effects on crop yield in different growth stages (Siebers, et al. 2017; Hatfield and Prueger, 2015), but were often limited to small scales, which makes it insufficient to represent complex crop landscapes and diverse levels of agronomic management.

Here we combined regional crop models output, satellite derived crop stage information, yield statistical data from United States Department of Agriculture (USDA) and site level experiment data to investigate how temperature influence maize yield during different stages. Statistical yield data, together with satellite data derived crop biomass which was calibrated against site

measured standing crop biomass, enabled us to estimate county level GSL, BGR and HI (defined as ratio of yield to total aboveground biomass). Then the temperature sensitivity of yield (S_T^{Yield}) can be decomposed to temperature sensitivity of BGR (S_T^{BGR}), temperature sensitivity of GSL (S_T^{GSL}) and temperature sensitivity of HI (S_T^{HI}). We further investigated the underlying driver of nonlinear response of maize yield to high temperature stress using statistical analysis and crop model simulation. Model outputs from crop model inter-comparison project, built on existing knowledge of maize yield response to environmental drivers, were analyzed here as a compliment. In this study, we focused on three states dominated by rainfed maize in the US Midwest: Indian, Illinois and Iowa, which accounted for approximate 40% of US Maize production (USDA, 2015). Thus, the conclusion drawn from this study is likely to provide insight for the temperature response of whole US rainfed maize production.

4.2   Methods and Dataset

4.2.1 Satellite date derived crop stage information

In this study, 8-day time series of 250 m daily surface reflectance MODIS data on board Earth Observing System (EOS) Terra and Aqua satellite platforms: MOD09Q1 (2000-2015) and MYD09Q1 (2002-2015) Collection 6, was used. Here a scaled WDRVI (Wide Dynamic Range Vegetation Index) is used to monitor the growing status of maize plants (Gitelson, 2004), because WDRVI has a higher sensitivity to changes at moderate to high biomass than the normalized difference vegetation index (NDVI) and has been found to have a linear relationship with the green leaf area index (LAI) of both maize and soybean (Gitelson et al., 2007). The scaled WDRVI is calculated by the following equation:

$$\text{WDRVI}=100*\frac{\left[(\alpha-1)+(\alpha+1)\times\text{NDVI}\right]}{\left[(\alpha+1)+(\alpha-1)\times\text{NDVI}\right]} \tag{1}$$

$$NDVI = (\rho_{NIR} - \rho_{red})/(\rho_{NIR} + \rho_{red}) \tag{2}$$

Where ρ_{red} and ρ_{NIR} are the MODIS surface reflectance in the red and NIR bands, respectively. A comparison of multiple vegetation indexes indicates WDRVI with α=0.1 showed a strong linear correlation with corn green LAI (Guindin-Garcia et al., 2012). Here we also set α as 0.1 for WDRVI calculation. Before WDRVI calculation, the reflectance data were quality-filtered

using the band quality control flags. Only the data passing the highest quality control test is retained. To extract maize phenology, shape model fitting (SMF) has been shown as an effective approach and was validated at both site and state level (Sakamoto T, et al. 2010). On the other hand, threshold based methods can be used to extract the starting and ending of growing season more flexibly (Keenan TF, et al. 2014). Here we developed and implemented a hybrid method combining SMF and threshold-based analysis to derive maize phenology from MODIS WDRVI data at 250 ×250 m spatial resolution data from 2000 to 2015. More details can be found in Zhu et al., 2018. We have derived four key maize growth stages of emergence (late May), silking (Middle July), dent (late August) and maturity (late September) across 4 states: Indianan, Illionis, Iowa and Nebraska. The verification at state level showed a good agreement between MODIS derived maize phenology and the National Agricultural Statistics Service (NASS) reported state mean phenological dates (Zhu et al., 2018). In this study, we only focused on the 3 states (Iowa, Illinois and Indiana) rain-fed maize.

4.2.2 USDA crop yield statistic

The county-level corn grain yield data covering the 3 states (IL, IN, IA) were obtained from the Quick Stats 2.0 database. The selected data period was from 2000 to 2015. The unit system for corn grain yield is bushel per acre (bu/ac). This data is used associated with remote sensing modeled county level biomass data to calculate the harvest index, which is the ratio of yield to aboveground biomass and generally represents the resource conversion efficiency of maize variety to reproductive yield.

4.2.3 Site level maize yield and biomass data

31 site-year measurements on maize yield, aboveground biomass (AGB) close to maturity and associated daily climate variables (temperature and precipitation data) across US Midwest were compiled. Firstly, this dataset was used to construct a regression model between WDRVI and AGB and then we also calculated the temperature sensitivity of yield and HI at site level as a compliment for the regional temperature sensitivity analysis, which provides direct evidence at site level.

To construct the regression model between WDRVI and AGB, WDRVI for 3×3 pixels centered on the site with measured AGB was extracted and then quality control procedure was applied to the time series WDRVI to remove low-quality, cloud/aerosol contaminated observations. Then Pearson correlation was estimated between the time series WDRVI of center pixel and the surrounding 8 pixels. 3 Pixels scoring the highest correlation together with the center pixel were averaged for regression use. Previous studies have showed integrated EVI over the growing season is a good proxy of vegetation AGB (Ponce-Campos et al., 2013). Here we integrated WDRVI (IWDRVI) by summing WDRVI over the whole growing season. The growing season start and end date has been derived based on threshold-based method (Zhu et al., 2018). Finally, a linear regression model was constructed between IWDRVI and *in-situ* measured AGB. The model shows IWDRVI have a very good explaining power (R^2=0.76, p<0.0001) with equation: AGB=15.97IWDRVI$^{0.8}$ (Figure 1). We also applied the same method to normalized difference vegetation index (NDVI) and enhanced vegetation index 2 (EVI2), which are also two common used vegetation indexes for temporal monitoring of vegetation greenness or productivity, but the performance is not so good as WDRVI.

Then the 16 years satellite data derived GSL and aboveground biomass was integrated to county level to get HI (Yield/AGB) and mean daily biomass growth rate BGR (AGB/GSL) for each county.

4.2.4 Crop Model output

Crop models generally represent our understanding of response of crop plants growth to climatic variation and soil nutrient and hydrological conditions, agronomic management practices, while some basic knowledge might have not been updated for decades. The parameters related with the crop varieties might be not able to reflect the recent progress in breeding techniques. Thus, when using those models to reproduce historic or predict future crop yield, there are often considerable mismatch between simulation and field observations. Model ensemble is often supposed to be an effective way to narrow down the mismatch. Here 9 global gridded crop model simulation outputs are used in this study, which results from the joint effort of Agricultural Model Intercomparison and Improvement Project (AgMIP) (Rosenzweig et al., 2013) and Inter-Sectoral

Impact Model Intercomparison Project 1 (Warszawski et al., 2014) for assessing the impact of climate change and management practices on global staple crop production.

In terms of the 9 crop models used here, it can be generally divided into two groups: (1) designed solely for agricultural systems, like APSIM, DSSAT, DSSAT-pt, GEPIC, PEGASUS and WOFOST (2) evolved from terrestrial ecosystem mode and covering both natural and agro ecosystems, like CLM-crop, LPJ-GUESS, LPJ-ml. The first group often have a more detailed representation of crop development and temperature stress influence was parameterized differently over crop vegetative and reproductive stages. The Table 4.1 gives an overview of how temperature stress is implemented in 9 crop models. Each model selected in this study outputs maize yield, total biomass and growing season duration. The daily climate data (temperature and precipitation) was integrated over the growing season and temperature sensitivity of yield, BGR, HI, GSL thus can be estimated for each model.

4.2.5 Temperature sensitivity analysis

We used different sensitivity analysis to understand how temperature influences maize yield across different physiological processes. Firstly, we estimated the temperature sensitivity for maize yield, BGR, HI and GSL using a panel data analysis with growing season mean surface air temperature (Tsa) and precipitation (Prcp) as the explanatory variables:

$$\log(Yield_{i,t}) = \gamma_1 t + \gamma_2 Tsa_{i,t} + \gamma_3 Prcp_{i,t} + County_i + \varepsilon_{i,t} \tag{3}$$

$\gamma_1 t$ captures the yield increasing trend in recent years. $County_i$ corresponds to fixed effects of county i. This county specific intercept ($County_i$) accounts for time-invariant county differences, like the soil quality. γ_2 defines the temperature sensitivity of yield S_T^{Yield}. The temperature sensitivity of BGR (S_T^{BGR}), HI (S_T^{HI}) and GSL (S_T^{GSL}) can be estimated similarly. Here the dependent variable Yield and other variables BGR, GSL and HI were logged, so the estimated temperature sensitivity γ_2 represents percentage change with 1 ℃ temperature increase.

The climate data used here was obtained from University of Idaho Gridded Surface Meteorological Data (http://metdata.northwestknowledge.net/) with a spatial resolution of 4km

(Abatzoglou, 2013). It is a gridded product covering the US continent and spanning from 1979 to 2016. This dataset is created by combining attributes of two datasets: temporally rich data from the North American Land Data Assimilation System Phase 2 (Mitchell, 2004), and spatially rich data from the Parameter-elevation Regressions on Independent Slopes Model (PRISM) (Daly et al., 2008). After validated using extensive network of weather stations across the United States, this dataset is proved to be suitable for landscape-scale ecological model. Then growing season mean Tsa and Prcp were estimated by integrating daily climate data according to MODIS derived growing season starting and ending date.

As Yield $=$ HI $\cdot$ BGR $\cdot$ GSL, temperature sensitivity of Yield can be written as follows:

$$\frac{\partial \ln(Yield)}{\partial Tsa} = \frac{\partial \ln(\text{HI})}{\partial Tsa} + \frac{\partial \ln(BGR)}{\partial Tsa} + \frac{\partial \ln(GSL)}{\partial Tsa} \tag{4}$$

$$\frac{\partial Yield}{Yield \cdot \partial Tsa} = \frac{\partial HI}{HI \cdot \partial Tsa} + \frac{\partial BGR}{BGR \cdot \partial Tsa} + \frac{\partial GSL}{GSL \cdot \partial Tsa} \tag{5}$$

This means the percentage of yield change with 1degree warming can be decomposed into percentage changes in HI, BGR, GSL, which generally corresponds to physiological processes of maize reproductive growth like grain size and grain number determination, carbon assimilation rate through photosynthesis and crop plants development rate, respectively. We further divided the total dataset into 5 groups according to the quintile of mean growing season temperature. This separation enables us to understand how maize physiological processes respond to warming as temperature goes up.

Although the coefficient in linear model is better to interpret, the actual response of crop yield and related physiological processes to climate variables is more likely to be nonlinear. Therefore, an alternative model was used to capture this nonlinear relationship:

$$\log(Yield_{i,t}) = \gamma_1 t + \gamma_2 Tsa_{i,t} + \gamma_3 Tsa_{i,t}^2 + \gamma_4 Prcp_{i,t} + \gamma_5 Prcp_{i,t}^2 + County_i + \varepsilon_{i,t} \tag{6}$$

We can see the main difference between (3) and (6) is that a quadratic function of Tsa and Prcp was added to capture the nonlinear response of yield. The climatic influence on HI, GSL and BGR can be modeled similarly by replacing Yield with the corresponding variables.

The total temperature sensitivity estimated above can be regarded as a synthetic effect of temperature stress across different stages on maize yield. Then the total temperature sensitivity of yield was written as:

$$\frac{\partial Yield}{\partial Tsa} = \frac{\partial Yield}{\partial HDD}\frac{\partial HDD}{\partial Tsa} + \frac{\partial Yield}{\partial GDD}\frac{\partial GDD}{\partial Tsa}$$
$$= \frac{\partial Yield}{\partial HDD^{VP}}\frac{\partial HDD^{VP}}{\partial Tsa} + \frac{\partial Yield}{\partial HDD^{An}}\frac{\partial HDD^{An}}{\partial Tsa} + \frac{\partial Yield}{\partial HDD^{GFP}}\frac{\partial HDD^{GFP}}{\partial Tsa} + \frac{\partial Yield}{\partial GDD^{VP}}\frac{\partial GDD^{VP}}{\partial Tsa} + \frac{\partial Yield}{\partial GDD^{An}}\frac{\partial GDD^{An}}{\partial Tsa} + \frac{\partial Yield}{\partial GDD^{GFP}}\frac{\partial GDD^{GFP}}{\partial Tsa} \tag{7}$$

High temperature degree days (HDD) represents the higher-than-optimal thermal time accumulation. Here we use 30 degree as the threshold to represent high temperature stress. Growing degree days (GDD) represents the thermal time requirement which drives crop development. $HDD^{VP} or GDD^{VP}$, HDD^{An} or GDD^{An} and HDD^{GFP} or GDD^{GFP} represents HDD or GDD during vegetative period (VP), anthesis (An) and grain filling period (GFP). The three periods are generally distinguished by their main roles in determining the final yield: vegetative period is mainly related with foliation and leaf expansion, anthesis is mainly related with pollination and determines grain number and grain filling period is related with grain size through translocating photosynthates to kernels. The crop growth stage information was derived from above remote sensing data: VP is defined as duration from emergence to 10 days ahead of silking, anthesis is defined as duration between 10 days before and after silking, GFP is defined as duration from 10 days after silking to maturity. Although we did not exactly extract flowering timing from the remote sensing data, previous study generally shows that the anthesis is around one week before silking. Thus here we use 10 days before and after silking date as a conservative estimation of anthesis.

We then applied another panel data analysis to directly regress the maize yield over growing degree days during different periods:

$$Yield_{i,t} = \alpha_0 t + \alpha_1 GDD_{i,t}^{VP} + \alpha_2 HDD_{i,t}^{VP} + \alpha_3 GDD_{i,t}^{An} + \alpha_4 HDD_{i,t}^{An} + \alpha_5 GDD_{i,t}^{GFP} + \alpha_6 HDD_{i,t}^{GFP} + County_i + \varepsilon_{i,t} \tag{8}$$

Where $\alpha_0 t$ captures the yield increasing trend, $County_i$ corresponds to county fixed effects. $\alpha_1 - \alpha_6$ defines the sensitivity of yield to GDD and HDD during the three periods. Thus, the yield sensitivity of HDD can be estimated by its first order difference:

$$\alpha_2 = \frac{\partial Yield}{\partial HDD^{VP}} \; ; \; \alpha_4 = \frac{\partial Yield}{\partial HDD^{An}} \; ; \; \alpha_6 = \frac{\partial Yield}{\partial HDD^{GFP}} \tag{9}$$

The sensitivity of GDD and HDD in VP, anthesis and GFP to 1 ℃ (2 ℃) warming is estimated by uniformly increasing daily temperature by 1 ℃ (2 ℃) for the three stages and then get the GDD or HDD difference between 1 ℃ (2 ℃) warming and the original GDD or HDD. Thus the sensitivity of yield to high temperature stress in different growth stages can be separately estimated by the equation (6).

GDD and HDD were estimated from hourly temperature values obtained by fitting a sine function to daily maximum Tsa and minimum Tsa with the following equations:

$$GDD_8^{30} = \sum_{t=1}^{N} DD_t, DD_t = \begin{cases} 0, when\, Tsa < 8 \\ Tsa - 8, when\, 8 \leq Tsa < 30 \\ 22, when\, Tsa \geq 30 \end{cases} \tag{10}$$

$$HDD_{30}^{\infty} = \sum_{t=1}^{N} DD_t, DD_t = \begin{cases} 0, when\, Tsa < 30 \\ Tsa - 30, when\, Tsa \geq 30 \end{cases} \tag{11}$$

where t represents the hourly time step, N is the total number of hours in each growing period and DD is degree days. It has been proved that interpolating daily temperature to hourly value is better in capturing sub-daily heat stress (Jack et al., 2015).

Warming trend increases extreme heat events and also water stress (WS) by regulating both water demand and water supply (Lobell et al., 2013). Thus the temperature influence on yield can be interpreted as the joint effect of high temperature stress and water stress with the following equation:

$$\frac{\partial Yield}{\partial Tsa} = \frac{\partial Yield}{\partial HDD} \frac{\partial HDD}{\partial Tsa} + \frac{\partial Yield}{\partial GDD} \frac{\partial GDD}{\partial Tsa} + \frac{\partial Yield}{\partial WS} \frac{\partial WS}{\partial Tsa} \tag{12}$$

Here HDD, GDD and WS are climate variables integrated over the whole growing season.

When we construct another panel data model to regress yield over HDD, GDD, WS using:

$$Yield_{i,t} = \beta_0 t + \beta_1 GDD_{i,t} + \beta_2 HDD_{i,t} + \beta_3 WS_{i,t} + County_i + \varepsilon_{i,t} \tag{13}$$

Where $\beta_0 t$ captures the linear increasing trend of yield and $County_i$ corresponds to county fixed effects. Then, the yield sensitivity to HDD, GDD and WS can be estimated by its first order difference:

$$\beta_1 = \frac{\partial Yield}{\partial GDD}, \beta_2 = \frac{\partial Yield}{\partial HDD}, \beta_3 = \frac{\partial Yield}{\partial WS} \tag{14}$$

Here, the ratio of evapotranspiration (ET) to potential ET (PET), which generally characterizes the soil water availability, derived from MODIS ET product MOD16 from 2001 to 2015 was used to represent growing season water stress. This product has a spatial resolution of 1 km and its 8-days temporal resolution is used. ET and PET in MOD16 is estimated using Mu et al.'s improved ET algorithm (2011) developed from the Penman–Monteith equation based on MODIS derived land surface temperature, vegetation cover and global meteorology data. Although various metrics have been proposed to measure water stress or climatic drought, there is no consensus that one is superior to the others. Currently, this observational data based ET product is the only one at high spatial and temporal resolution. We also evaluated the MOD16 based ET/PET at Ameriflux tower site (US-bo1) in Illinois from 2004-2012, where ET is estimated by eddy-covariance technique and PET is also estimated by Penman–Monteith equation with site measured meteorological forcing data. MODIS based ET/PET is calculated during growing season for each pixel with 70% area covered by maize cropland and then averaged to county level to be consistent with the other variables.

When applying the equation (12) and (13) to AgMIP model outputs to evaluate the relative contribution of temperature stress and water stress to maize yield in crop models, we employed model output ET and estimated PET with Penman–Monteith equation using the corresponding climate forcing data.

4.2.6 APSIM model analysis

APSIM model is a process crop model, which explicitly accounted for the temperature stress and water stress during different crop growth stages. It can simulate a number of crops under various climatic, soil physical and management conditions, and therefore is used widely to address a range of research questions related to agricultural systems (Holzworth et al., 2014). In particular, maize is simulated by the APSIM-Maize module. The APSIM-Maize module is inherited from the CERESMaize, with some modifications on the stress representation during grain set and grain filling, biomass growth rate and phenological development. This flexible process-based

model allows us to investigate the different role of temperature stress in determining maize yield variation.

The water stress in APSIM is calculated by the ratio of water supply to water demand. Water demand is driven by both biomass growth rate and transpiration efficiency (TE), and TE is inversely correlated with vapor pressure deficit (VPD). Water supply is related with hydraulic conductance, roots depth and the amount of water above wilting point in soil layers containing roots. As temperature goes up, it will increase water demand through VPD and thus reduce future supply of soil water through high ET. Here we designed two grid-based simulation experiments to further investigate how water stress and high temperature stress influence maize yield as temperature goes up: sim1 is a control simulation with active default temperature stress and water stress; sim2 is a simulation with temperature stress blocked. Here we only block temperature stress, because water stress is controlled by both temperature and precipitation, which is more complex to control. As sim1 includes both temperature stress and water stress during photosynthesis, anthesis and grain filling while sim2 only includes water stress, temperature stress can be separately estimated by comparing the two simulations. The simulation is run for the 3 states over 2000-2015 and forced with PRISM climate data at about 10km. The soil parameters, like soil hydraulic properties and soil organic matter fractions were extracted from the State Soil Geographic (STATSGO) data base, as collected by the National Cooperative Soil Survey over the course of a century. For each simulation grid, the soil information was queried through R package 'soil DB' (http://ncss-tech.github.io/AQP/). Management information like planting density and fertilizer application amount was taken from the USDA NASS survey report at state level. Crop sowing date was derived from the Crop Calendar Dataset (Sacks et al., 2010). The generic maize hybrids ('B_110') provided by APSIM version 7.7 was used for the simulation but its phenology related parameters like 'tt_emerg_to_endjuv' and 'tt_flower_to_maturity' was assigned based on the MODIS derived crop stage information, which could match the maize development with the actual situation better.

4.3 Results and Discussion

S_T^{Yield}, S_T^{BGR}, S_T^{HI} and S_T^{GSL} were estimated by equation (3). As shown in equation (5), S_T^{Yield} can be decomposed into three components S_T^{BGR}, S_T^{HI} and S_T^{GSL}. S_T^{BGR}, S_T^{HI} and S_T^{GSL} generally represent different physiological controls of temperature on maize yield through reproductive growth during anthesis and grain filling period (S_T^{HI}), photosynthesis dominated carbon assimilation (S_T^{BGR}) and plants development rate (S_T^{GSL}). Although S_T^{Yield} varies considerably among individual crop models, the model ensemble mean ($-7.1\pm3.1\%$ per ℃) shows a consistent estimation of yield sensitivity with the one based on observational evidences ($-7.3\pm0.6\%$ per ℃) (Figure 2). When we looked into the three components, model ensemble mean generally overestimated S_T^{GSL} while underestimated S_T^{HI} when compared with the observational evidences. As model parameters are normally based on the knowledge of crop physiological processes decades ago, this discrepancy suggests the crop systems in recent years seems to become more adapted to warmer climate in crop development possibly by adoption of more heat tolerance varieties while the management practices intended to improve the yield like more application of nitrogen fertilizer increased the sensitivity of heat stress during grain formation processes, (Wahid et al., 2007; Ordóñez et al., 2015). In terms of the sensitivity of BGR, both models and observational evidences show a weak response, consistent with the fact that maize photosynthesis has a high optimal temperature (Dekov et al., 2000). However, some models overestimated the temperature influence on BGR but underestimated its influence on HI, like LPJ-GUESS and LPJml, which suggests that in these models excessive temperature stress is imposed to processes associated with photosynthesis while the stress during grain formation is overlooked.

The temperature sensitivity analysis is further divided into 5 groups based on the quintile of growing season mean temperature, which provides an insight on how temperature sensitivity evolves as the mean temperature goes up in the future. Generally, S_T^{Yield} is significantly enhanced in warmer divisions by analysis using NASS report yield, which changed from $0.3\pm1.1\%$ per ℃ to $-16.6\pm4.3\%$ per ℃ from the lowest to highest temperature quintile (Fig 4a). It is also noted that increase in S_T^{Yield} was mainly driven by S_T^{HI}, which varied from $1.5\pm1.4\%$ per ℃ to $-12.6\pm3.8\%$ per ℃ in the course of temperature increase. While S_T^{GSL} keeps a

relatively stable value of approximate -2.6% per ℃ despite of increasing background temperature and S_T^{BGR} shows a small decrease as temperature goes up. Thus, in the lower temperature division (the first 3 temperature quintiles in Fig 4a), it can be inferred that temperature influence on yield is mainly driven by influence on GSL while in higher temperature division, temperature influence on HI become more dominant (Fig 4a).

When each model output was similarly divided based on the quintile of growing season mean temperature, model ensemble mean of S_T^{Yield}, S_T^{BGR}, S_T^{GSL} and S_T^{HI} was used to gain insight on how temperature stress was represented in crop models. The individual model performance was shown in Supplementary Figure S2. Generally, compared with the estimations by observational data, the model ensemble mean reproduced the patterns of S_T^{Yield}, S_T^{BGR}, S_T^{GSL} and S_T^{HI} across the temperature gradient (Fig 4b). Change in model ensemble mean S_T^{Yield} is mainly driven by S_T^{HI} (Fig 4b), which is supported by field warming experiment (Edreira et al., 2012). But S_T^{GSL} was overestimated for all five temperature quintiles (approximate -5.4% per ℃ relative to -2.6% per ℃ in observational data estimation). The stable S_T^{GSL} estimated by both crop models and observational data suggests maize plants development is quasi-linearly driven by temperature (Edreira et al., 2012; Hatfield and John, 2015) and relatively more heat tolerance compared with wheat plants (Lobell et al., 2012). The small change in S_T^{BGR} estimated by both crop model and observational data suggests photosynthesis dominated BGR might be minimally influenced in future warmer climate, which might be the result of higher optimal temperature of C_4 plant during photosynthesis.

We also used an alternative panel model (Equation 6 in Method) by adding quadratic function of Tsa and Prcp to capture the nonlinear response of yield, HI, BGR and GSL to climate variables. This model was applied to the observational data based yield, HI, BGR and GSL. The temperature response of yield, HI, BGR and GSL was characterized by the normalized quadratic functions associated with temperature in (6). This alternative analysis demonstrated that as temperature goes up, temperature response of GSL was generally linear while response of yield and HI became nonlinear, which is in line with the above analysis by grouping the temperature (Figure 3). By this method, the temperature response curve also suggests the optimal temperature for BGR is higher than the one for HI and yield (Edreira and Otegui, 2012).

The reason why yield and HI is nonlinearly decreased by warming remains unclear. Using equation (7), S_T^{Yield} was decomposed into the response of yield to HDD (GDD) and the response of HDD (GDD) to temperature during the three stages. When a panel data model was used to investigate the different sensitivity of yield to HDD during vegetative period ($\frac{\partial Yield}{\partial HDD^{VP}}$), HDD during anthesis ($\frac{\partial Yield}{\partial HDD^{An}}$) and HDD during grain filling period ($\frac{\partial Yield}{\partial HDD^{GFP}}$), it suggests yield is most sensitive to HDD during GFP ($-0.46\pm0.04\%$ per degree days) (Figure 5a), which is in line with the field heating experiment (Edreira et al., 2014). The yield sensitivity to HDD during anthesis ($-0.33\pm0.07\%$per degree days) is slightly higher than HDD during VP ($-0.30\pm0.08\%$ per degree days) (Figure 5a). The yield sensitivity to GDD is relatively small in all three periods and even shows a positive response for GDD in VP and GFP (Figure 5a). Meanwhile, HDD also increases non-uniformly among the three stages with rising temperature (Figure 5b). The increase in HDD during GFP is the largest than the other two stages (Figure 5b).

As S_T^{Yield} is mainly characterized by the high temperature stress $\frac{\partial Yield}{\partial HDD}$, a statistical method is used to estimate impact of HDD during the three stages on yield. A uniform 1 ℃ and 2 ℃ warming is applied to the whole growing season temperature, according to equation (7), yield is reduced by 5.8% and 20.4%. When temperature increase was applied only for HDD during 'VP', 'Anthesis' and 'GFP' , maize yield was reduced by 1.8% (7.1%), 1.1% (5.2%) and 3.2% (12.4%) in the 1 ℃ (2 ℃) warming scenarios, suggesting that the increase HDD solely during GFP by warming might contribute more than half of total yield reduction.

Previous study has suggested that extreme heat event might threaten maize yield through water stress (Lobell et al., 2013) and a better discernment of the effect of water stress and heat stress might also help farmers to make proper decisions to deal with future warming. A panel data analysis was also used here to estimate the relative contribution of water stress (AET/PET) and high temperature stress (HDD) on yield. Our model suggests that 1 ℃ warming will change GDD, HDD and AET/PET by 50 ± 1.7 degree days, 17 ± 0.27 degree days and $-0.011\pm6\times10^{-4}$, respectively (Fig 6a). And a unit increase in GDD, HDD and AET/PET will cause yield change

by -0.0054 ± 0.003%, -0.27 ± 0.0016% and 154 ± 6% (Fig 6a). Taking this together, the regression model suggests 1 ℃ warming will reduce yield by 0.27 ± 0.15%, 4.6 ± 0.34% and 1.7 ± 0.16% through GDD, HDD and AET/PET, respectively (Fig 6a), suggesting that warmer temperature reduce maize yield mainly through the direct heat influence.

When the same panel model is applied to crop model from AgMIP, the model and ensemble results generally showed a small temperature influence through GDD but varied substantially with regard to the temperature influence through AET/PET and HDD. Compared with the observational evidences, crop model ensemble underestimated the direct heat influence through HDD while overestimated the indirect influence through AET/PET (Fig 6b). As the field warming+CO_2 enrichment experiment suggested, water conservation effect of increasing CO_2 in future scenario might result in more yield benefit under water stress conditions but its yield benefit under heat stress is limited (Siebers et al., 2015). This implies in current crop models the direct high temperature stress on yield might be underestimated while the yield benefit of increasing atmospheric CO_2 might be overestimated. This discrepancy could bias the projection of maize yield given future higher atmospheric CO_2 and more frequent heat waves.

Although the model ensemble suggests a lower influence of temperature through HDD, some individual model estimation is close to the observational evidences. As shown in Figure 6b, estimation by APSIM crop model suggests a higher influence of temperature through HDD than through water stress (AET/PET). In addition, we also used APSIM model default water stress metric, ratio of water supply to water demand, to construct an alternative panel model, this water stress metric produced a similar estimation of temperature influence through GDD, HDD and AET/PET as using water AET/PET as the water stress metric (Figure S5).

To better understand how water stress and heat stress influence maize yield through different physiological processes, we designed a model experiment: sim1 is the control run with both temperature stress and water stress; sim2 is the simulation with temperature stress blocked. When we used the same method as equation (3) to estimate the temperature sensitivity of yield, HI, BGR and GSL, it is noted that as temperature goes up, there is no significant change between the two simulation in S_T^{BGR} and S_T^{GSL} while the S_T^{HI} is significantly reduced in sim2. As S_T^{GSL} is

almost constant with increasing background temperature, it can be regarded as mainly driven by thermal time accumulation. Thus, the other two components S_T^{BGR} and S_T^{HI} represent the main effect of high temperature stress on yield. The comparison between two simulations suggests as temperature goes up, increased high temperature stress reduces yield mainly through grain formation process including the process of grain set and grain filling while the high temperature induced water stress influences yield mainly through processes related with BGR, such as photosynthesis or respiration.

Finally, employing the emergent constraint technique, this dataset was used to constrain the whole US S_T^{Yield}, S_T^{BGR}, S_T^{GSL}, and S_T^{HI} with the above estimated S_T^{Yield}, S_T^{BGR}, S_T^{GSL}, and S_T^{HI} of the three states across US Midwest. Due to different model structures and parameters, crop model simulated S_T^{Yield}, S_T^{BGR}, S_T^{GSL}, and S_T^{HI} for the US and US Midwest spread widely. But there is a good relationship between sensitivity estimations for US Midwest and the whole US across models (Figure 8 a-d), which is utilized to constrain sensitivity for the whole US. After emergent constraint, the estimation of S_T^{Yield}, S_T^{BGR}, S_T^{GSL}, and S_T^{HI} was changed and the uncertainty of S_T^{Yield}, S_T^{BGR}, S_T^{GSL}, and S_T^{HI} was also significantly narrowed (Figure 8 e). For S_T^{Yield}, it was changed from $-5.38\pm2.5\%$ per ℃ to $-5.14\pm0.5\%$ per ℃. S_T^{BGR} was changed from $-0.55\pm3.2\%$ per ℃ to $0.38\pm0.2\%$ per ℃. S_T^{GSL} was changed from $-5.5\pm3.2\%$ per ℃ to $-2.3\pm0.1\%$ per ℃. S_T^{HI} was changed from $-1.36\pm1.7\%$ per ℃ to $-3.8\pm0.4\%$ per ℃. After constraint, we can give a more confident estimation of warming influence on US maize yield, which is important for future prediction of maize yield.
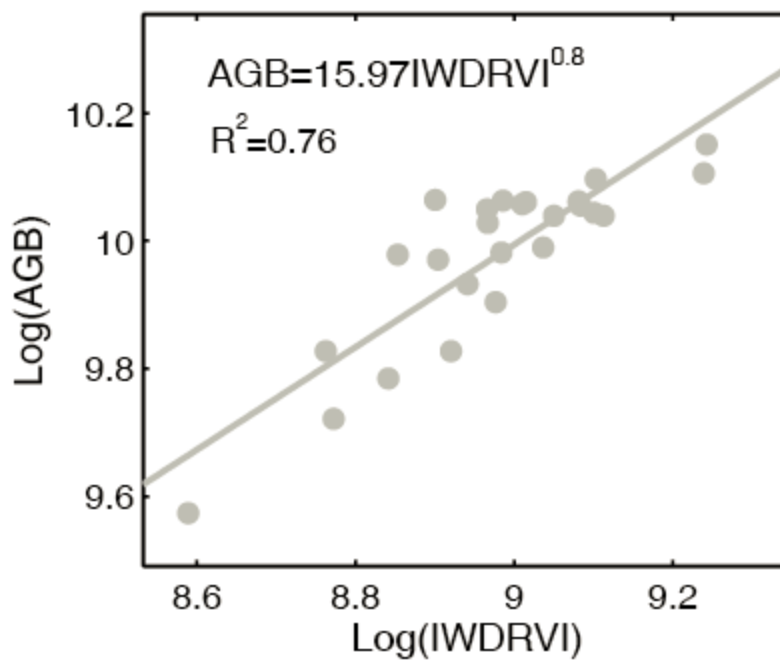
Figure 4. 1 The regression model used to relate IWDRVI with AGB. Each point corresponds to a site measured AGB and MODIS derived IWDRVI.
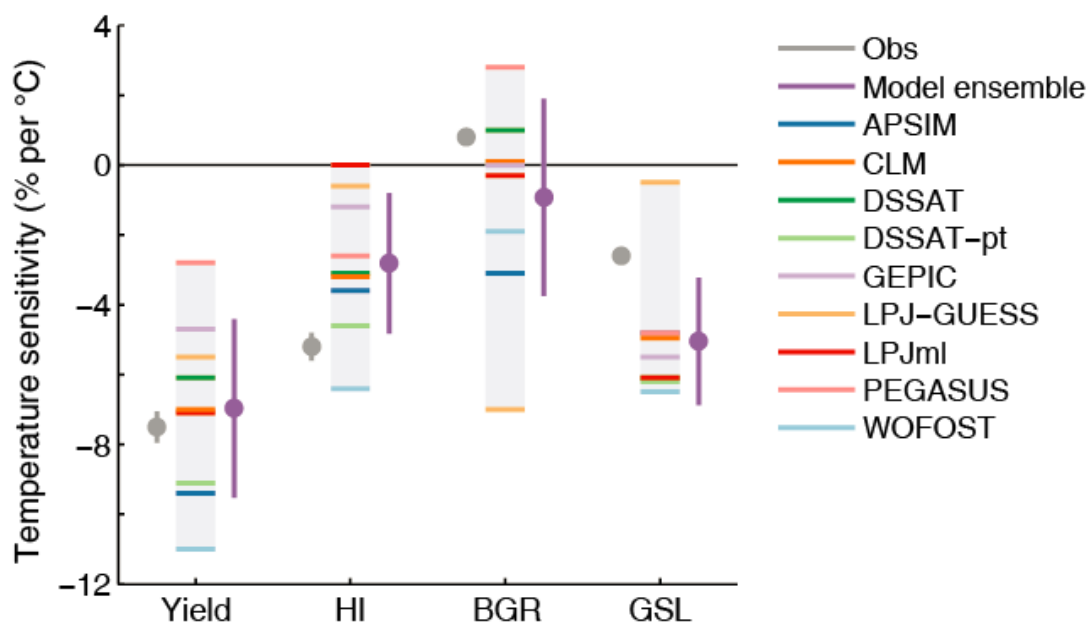
Figure 4. 2 Temperature sensitivity of yield, HI, BGR and GSL based on satellite data and NASS reported yield (grey line) and crop models, where the horizontal line indicates sensitivity estimation in each model. The error bars in a and b represent the 95% confidence interval of estimated sensitivity.
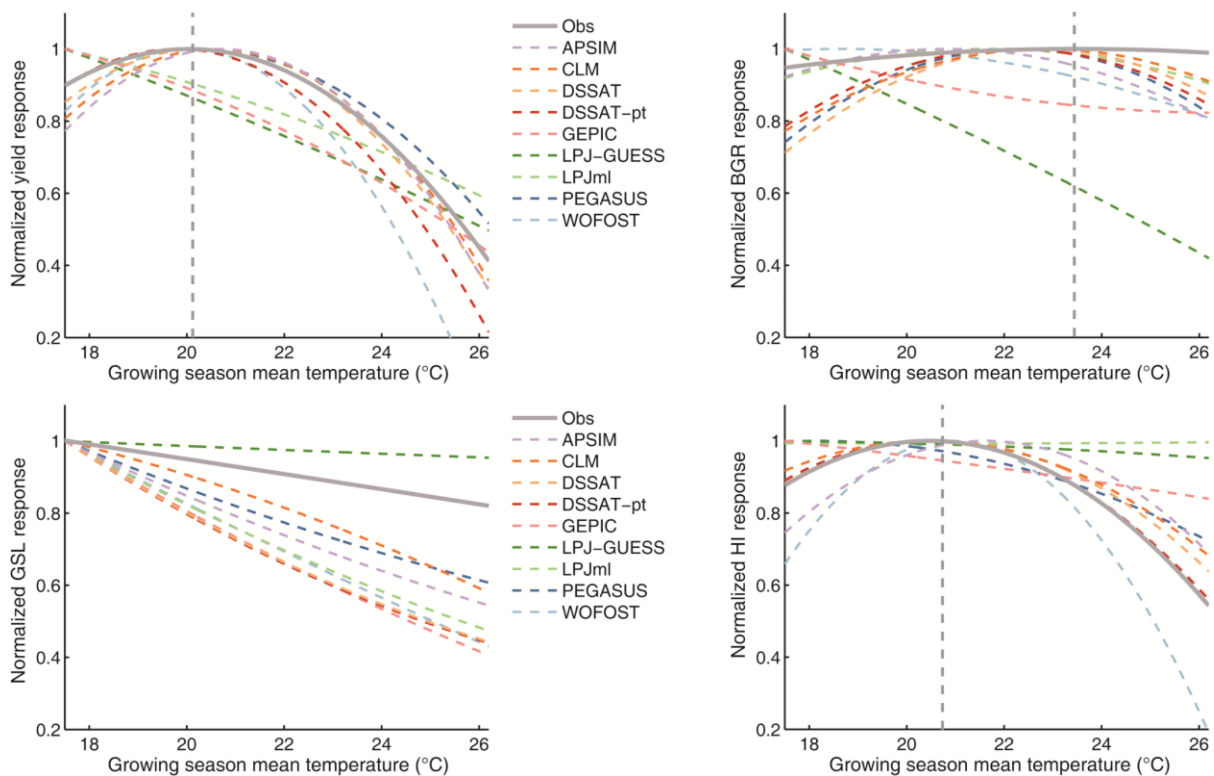
Figure 4. 3 The response of Yield, HI, GSL and BGR to growing season mean temeprature. The vertial dashed lines indicate the optimal mean temperature derived from the observational evidences where Yield, HI or BGR peaks. The response function is normalized by maximum value in each response. The temperature range here is determined by the maximum and minimum mean growing season temperature across US Midwest during the period of 2000-2012.
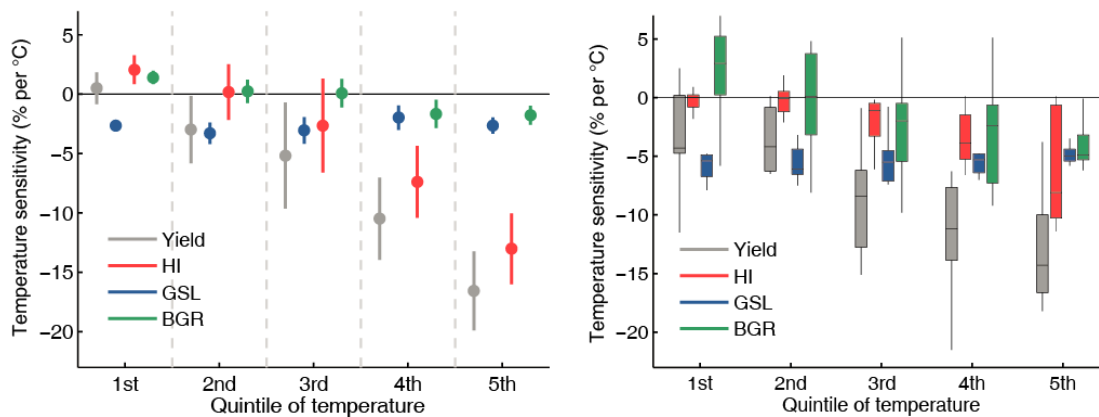
Figure 4. 4 Satellite data and NASS yield derived temperature sensitivity of yield, HI, BGR and GSL when the data was divided by the quintile of growing season temperature (a). The error bars in a and b represent the 95% confidence interval of estimated sensitivity. Box plot of temperature sensitivity of yield, HI, BGR and GSL output from crop models when the data was divided by the quintile of growing season temperature during 2000-2012 (b). Boxplots indicate the median, 25–75th percentile, and 5–95th percentile of crop model estimated temperature sensitivity.
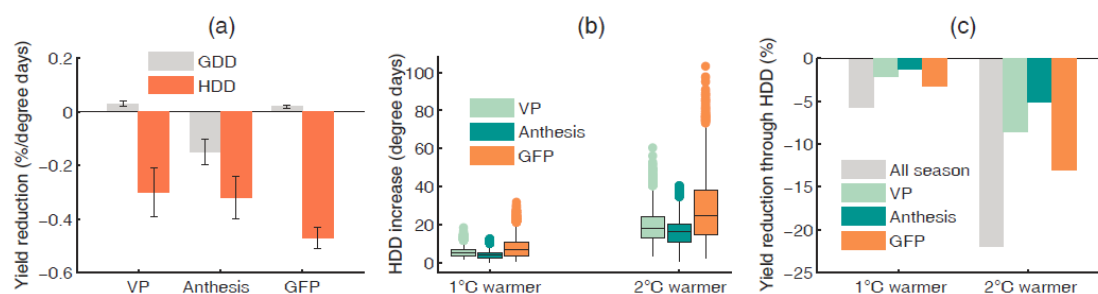
Figure 4. 5 Sensitivity of maize yield from NASS to GDD and HDD in different growing stages: vegetative period (VP), anthesis and grain filling period (GFP) (a). Boxplot of HDD increase in response to 1 ℃ and 2 ℃ warming (b). Boxplots indicate the median, 25–75th percentile, and 5–95th percentile of HDD increase across all counties during 2000-2012. Estimation of yield reduction according to the regression model (equation 7). Yield reduction of 'All season' indicates the temperature was increased uniformly across the whole growing season, while 'VP', 'Anthesis' and 'GFP' means temperature was increased solely for HDD during 'VP', 'Anthesis' and 'GFP'. As temperature was only increased during the calculation of HDD, the yield reduction characterizes the relative contribution of high temperature stress during a specific maize stage.
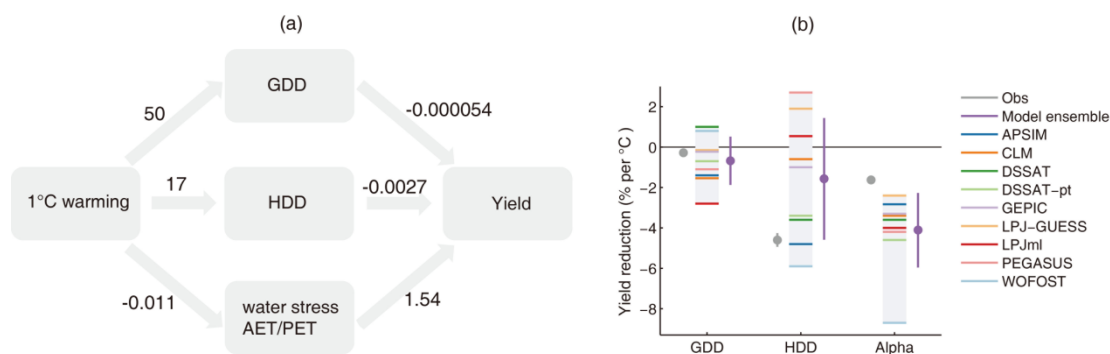
Figure 4. 6 The direct (HDD) and indirect (WS) effect of temperature increase on maize yield based on NASS yield report, MODIS derived crop stages information and MODIS ET/PET product MOD16 (a). The numbers marked on the arrows indicate the effects of 1 ℃ warming on yield through GDD, HDD and WS, corresponding to the coefficients in equation (12). Comparison of maize yield response to GDD, HDD and Ws estimated from observational evidences and crop models. The error bars in model ensemble (b) represent the stand deviation of multi-model estimated yield responses.
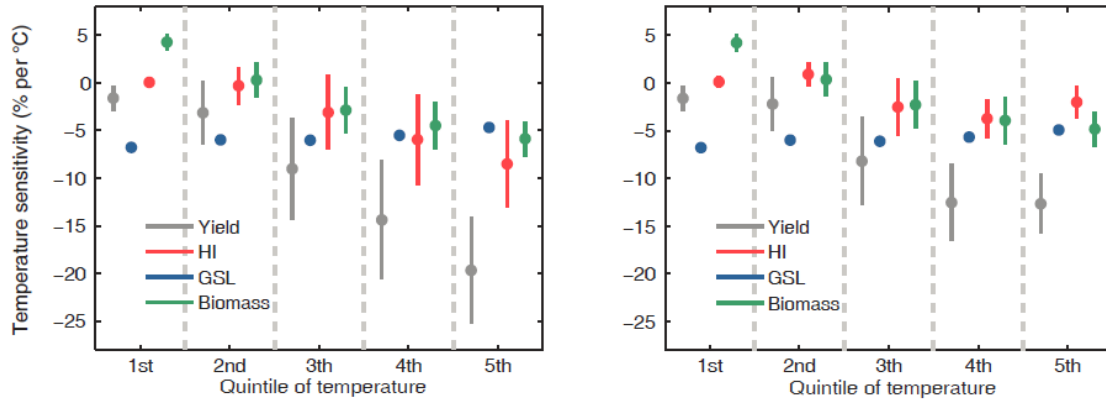
Figure 4. 7 Temperature sensitivity of yield, HI, GSL and BGR divided by quintile of growing season temperature in two APSIM simulation results. Left one is the simulation with both water and temperature stress and the right is the simulation with only water stress.
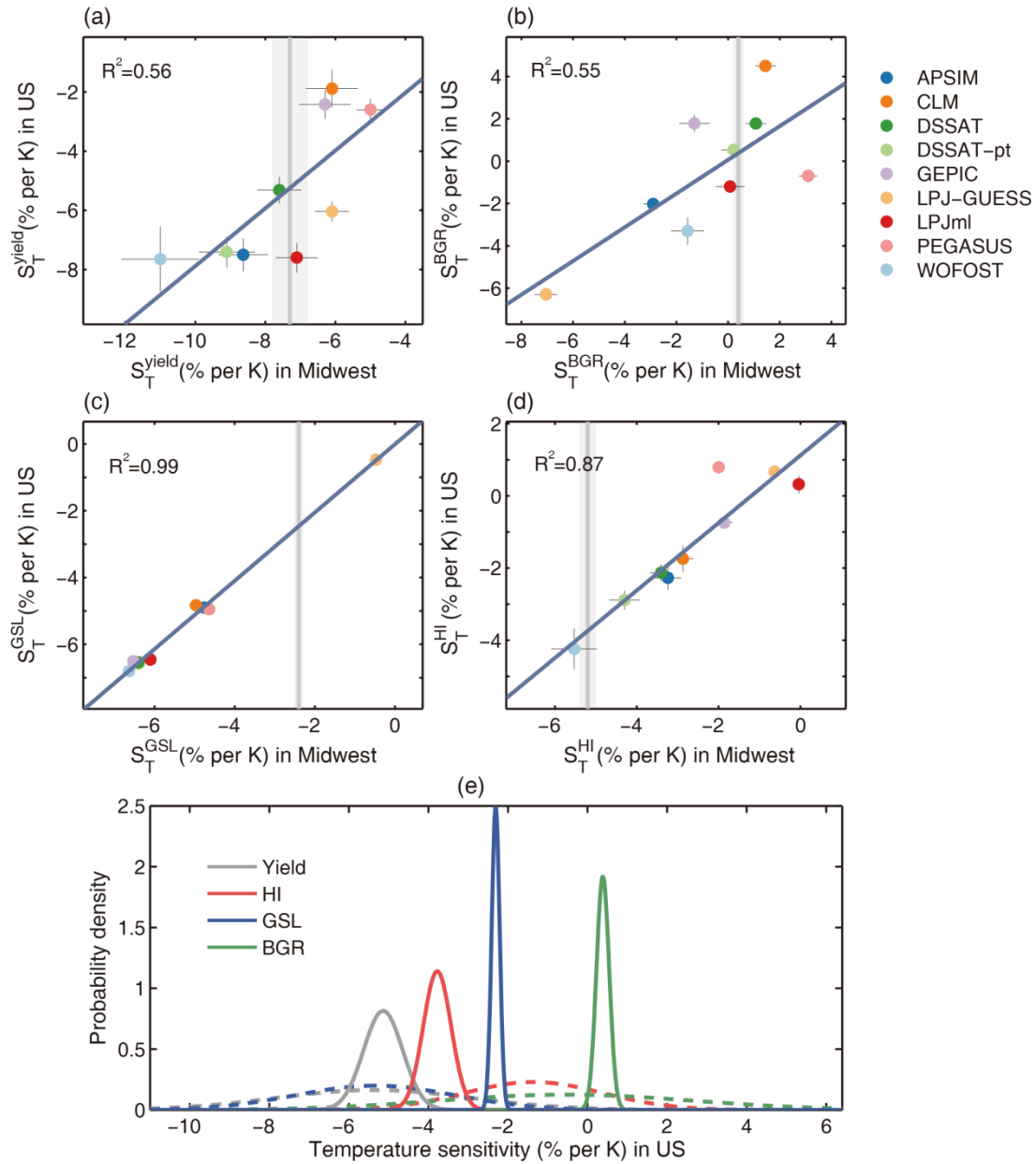
Figure 4. 8 Emergent constraint of the whole US S_T^{Yield}, S_T^{BGR}, S_T^{GSL}, and S_T^{HI} with the observational evidences. Relationships between temperature sensitivity of yield (a), BGR (b), GSL (c), HI (d) in US Midwest and those estimated for the whole US. The vertical grey lines indicate S_T^{Yield}, S_T^{BGR}, S_T^{GSL}, and S_T^{HI} estimated from observational evidences with its uncertainty represented by the standard deviation. Probability density function of S_T^{Yield}, S_T^{BGR}, S_T^{GSL}, and S_T^{HI} before and after emergent constraint (e). The dashed line represents the estimation before constraint and the solid line is the estimation after constraint.

CHAPTER 5.   CONCLUDING REMARKS AND FUTURE WORK

5.1 Summary and conclusions

In the context of growing global food demand and warming trend, agricultural system must be upgraded to reduce the farming practice related greenhouse gas emissions and simultaneously keep the sustainable yield increase under more extreme climate environment. In this study, we addressed three questions: (1) how and to what extent the climate mitigation potential can be achieved with different levels of management intensity and land conversion scenarios when accounting for both biogeochemical and biophysical effects collectively; (2) how much the adoption of longer maturity maize cultivars has contributed to the recent US maize increasing trend and whether this variety renewal brought yield benefit is sustainable under future warmer climate to meet the increasing global food demand; (3) how heat stress influences maize grain yield across different maize growth stages and how the management practices might regulate the response of maize yield to heat stress.

For the first question, we focused on the whole US continent. The crop module in a land surface model was revised to reflect the difference between perennial biofuels crops and ordinary C_4 crop plants. After the calibration and validation against site observed carbon and energy flux, the revised model was applied to the whole US continent with different scenarios of land conversion and management practices combinations. Our study concludes that: (1) using carbon as currency, the CMP of energy crops over croplands and marginal lands is significantly enhanced from -1.9, 49.1 and 69.3 gC/m^2 per year considering only biogeochemical effects to 20.5, 78.5 and 96.2 gC/m^2 per year considering both biophysical and biogeochemical effects for corn, Switchgrass and Miscanthus, respectively; (2) the CMP of biophysical effects is dominated by latent heat fluxes; (3) when fertilization and irrigation is applied, the CMP over croplands and marginal lands reaches 79.6, 98.3 and 118.8 gC/m^2 per year, respectively; (4) the CMP over marginal lands is lower than that over croplands. Our study highlights that biophysical effects induced from altering surface energy and water balance should be considered to adequately quantify CMP of bioenergy crops at regional scales.

In the next two studies, we focused the adaptation issues of agricultural system in the US Midwest. Our analysis is based on the long term satellite data derived vegetation spectral data, site measured maize biomass and yield and multiple process based crop models. With the satellite data informed maize plants growth trajectory, four critical growth path transitional dates were identified. The change in grain filling duration and its contribution to maize yield increase was investigated. Our study concludes that: (1) silking dates become earlier in 61% of the pixels and more pixels (84%) exhibit a later maturity date. This resulted in a significant extension of the GFP over 81% of the pixels with an average lengthening of GFP of 0.37 days per year, which probably results from variety renewal; (2) empirical statistical model demonstrated that longer GFP contributed 23% of the yield increase trend by promoting kernel dry matter accumulation, while less yield benefit was identified in hotter counties; (3) both official survey data and crop model simulations estimated a similar contribution of GFP trend to yield; (4) if growing degree days that determines the GFP continues to prolong at the current rate for the next 50 years, GFP will be 25% and 18% longer under RCP 2.6 and RCP 6.0, respectively. However, this level of progress is insufficient to compensate yield losses in future climates, because end-of-season stresses become more common. This study has important implications for developing effective adaptation strategies to sustain food productivity in future warmer climate.

Thirdly, influence of temperature stress on maize yield through different growth stages was investigated. Satellite data was used to fill the gap that there is often limited spatial data on crop stages and biomass information. The total effect of temperature stress on maize yield was decomposed into three components: temperature stress on HI, GSL and BGR. By integration of crop models and observational based evidences, we concludes that (1) a nonlinear increasing temperature sensitivity of maize yield was identified as temperature goes up, which is predominantly determined by temperature stress on HI, while the response of BGR and GSL is relatively small; (2) model ensemble exhibited a similar pattern of temperature sensitivity, however, the negative impact of warming on HI is underestimated and temperature stress through GSL was overestimated; (3) the enhanced temperature sensitivity of HI mainly results from a higher sensitivity of yield to temperature stress during grain filling period and 1 degree warming during this period could explain approximate 63% yield reduction; (4) high temperature stress is more influential than warming induced water stress, especially as temperature goes up,

while model ensembles reaches an opposite conclusion. As the explored three states: Indiana, Illinois and Iowa accounted for approximate 40% of US Maize production (USDA, 2015), the conclusion drawn from this study is likely to provide insight for the temperature response of the whole US rain-fed maize production and our study is necessary to develop targeted crop adaptation strategy for future warming.

5.2 Reflections and future work

For the climate mitigation study, the simulation results indicates the necessity of considering both biogeochemical and biophysical feedbacks when evaluating climate mitigation potential of biofuel crops, however, several limitations are also identified. First, another important GHG from agroecosystems, N_2O, is neglected in this study. When fertilization is applied, it stimulates more N_2O emissions and thus weaken the CMP of bioenergy ecosystems (Crutzen et al., 2008; Roth et al., 2015; Davis et al, 2014), which should be addressed in the future research. Meanwhile, this research mainly focused on climate mitigation service of ecosystem, so we overlooked the environmental impact of increasing nitrate leaching induced by fertilization application, which is also a serious problem during biofuel production (Chamberlain et al., 2011). Second, previous research also implied that soil carbon storage is heavily dependent on crop residual remove rate (Liska et al., 2014; Smith et al., 2012), while we here set crop residual remove rate as a constant value across the US, which might be too arbitrary. More flexible removal rates should be introduced in the future research. Third, the irrigation in CLM4.5 is automatically triggered based on soil water status. Although irrigation is shown to improve CMP of biofuel crops and might save more lands, its possible threat to local water resource is not accounted. Recent research highlighted to institute policies so as to balance the water and land requirements during bioenergy production (Bonsch et al., 2014). Finally, we used land surface energy change to represent total cooling effects of growing biofuel crops on the climate. It is desirable to use dynamic climate models to examine how these land use change and management scenarios affect the climate in terms of air temperature and precipitation. For instance, the changed evapotranspiration due to growing biofuel crops will impact water vapor in air. Especially irrigation impacts soil moisture, ultimately influences clouds and precipitation (Lobell et al., 2009; Puma and Cook, 2010).

For the adaptation study, we used MODIS 8-days vegetation index to capture the maize plants growth cycling across the US Midwest. The derived maize growth stages information is validated against state level crop progress report. Although the validation process suggests a quite good consistency between progress report and MODIS derived crop stage information, more site level data comparison and validation is still desirable. Thus our study suggests more efforts are required on field measurement to obtain the crop growth stages information, which will facilitate model calibration and improve the performance of remote sensing data derived crop phenology.

In addition, the analysis in this study was confined by the dynamic crop type maps. To our knowledge, US Midwest is the only region in the world with public available long term crop type maps. Thus, future work dedicated to extend to the other regions must get over this barrier. Recently, the emergent progress in computation ability and big data platforms, like Google earth engine makes it possible to transform crop type monitoring and mapping from medium to high spatial resolution (Azzari and Lobell, 2017). The data fusion technology combines the advantage of different satellite platforms in capturing heterogeneous landscape with finer spatial information and more frequent monitoring (Gao, et al; 2017).

With technology advancement and more data becoming available, it is possible to extend our current study to other regions and other crop types, like wheat and sorghum (Tack et al., 2015; Tack et al., 2017). For example, the winter growing crop wheat, it is also the staple food crop and is shown to be not only vulnerable to the heat stress around anthesis but also to the exposure in days to freezing temperatures during autumn period. So more spatially explicit crop stage information will help us to better understand such stage dependent temperature sensitivity and developing adaptation strategy accordingly. Such spatially explicit crop stage information from remote sensing could provide a scalable and efficient way for crop yield prediction and quantifying the crop yield gap due to physical environment and insufficient water/nutrient management at large scale (Edreira et al., 2017; Estel et al., 2016; Duncan et al., 2015), especially for those less developed countries.

In addition to capturing the crop plants growth cycling, thermal band in satellite data could be used to detect land surface temperature anomaly and thus could quantify influence of irrigation, another important management practices in relatively dry regions, on crop yield. Previous study often overlooked the irrigation regulated canopy energy balance which could substantially change leaf temperature and thus relieve heat stress on crop plants. At the same time, satellite data can be utilized to generate irrigation/non-irrigation map (Deines et al., 2017). With this map, we could get a better understanding on the relative contribution of irrigation on crop yield through relieving water stress and heat stress.

The temperature sensitivity analysis in the third study suggests current crop models need to improve its module related with crop development and grain formation. When models switch from natural terrestrial ecosystem to agro-systems, more detailed processes on crop growth stage and associated stress parameterization is required. This study depends on satellite derived growing season duration and crop biomass. The regression between satellite derived IWDRVI and site measured biomass showed a good statistical power, which extends previous studies only employing several sites measured biomass and crop stage information. But the errors and uncertainty rooted in satellite data might still be propagated to the downstream analysis. In addition, the vegetation index WDRVI derived biomass could be further improved with recent advancement in new satellite spectral information acquisition, like the ESA operated Sentinel series. Its finer spectral resolution with the spectral information in red-edge region enables us to better characterize vegetation photosynthesis dynamics and stress response (Delegido et al., 2013; Chemura et al., 2017). The recent advances in obtaining space based solar-induced fluorescence (SIF) signal provides an alternative way to estimate the crop photosynthesis/biomass and crop yield (Guanter et al., 2014; Guan et al., 2015). All of these emergent satellite signals provide the possibility to better characterize crop plants growth status and final yield.

Current studies in evaluating the food security when faced with global warming are often focused on crop yield, the crop production per unit area, which is surely worth delving into. However, these studies overlooked the cropping area response of global warming. Cropping area can be varied through actual harvesting rate (harvesting area/planting area) and cropping frequency (harvesting times per year). Until recently, the climate warming effects on cropping

frequency and harvesting area are assessed in tropical area (Cohn et al., 2016). This study suggests that the cropping frequency and area response to climate variability might exceed the yield response in tropical region. It has important implications that future warming might exacerbate global food security with more crop production reduction than previously thought, which was mainly based on crop yield analysis. Thus, it is necessary for the future study to account for the cropping area based response to global warming at global scale when predicting global food production.

APPENDIX A
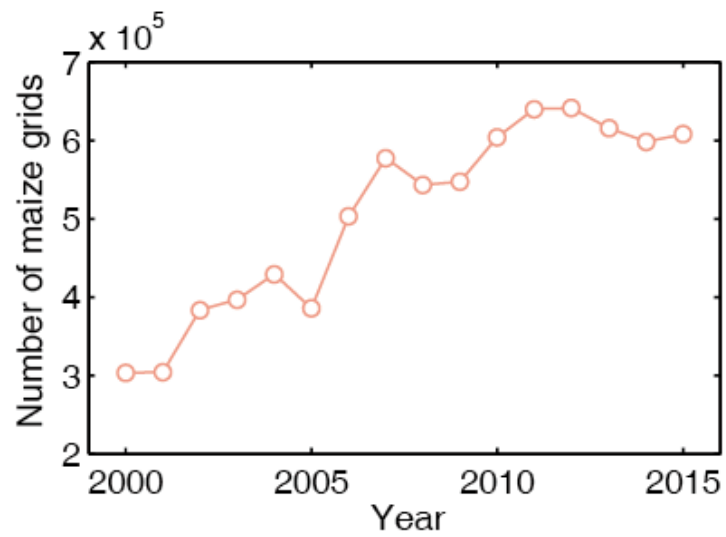
Figure A1 Number of pixels for estimating phenological date in each year over the studied 4 states
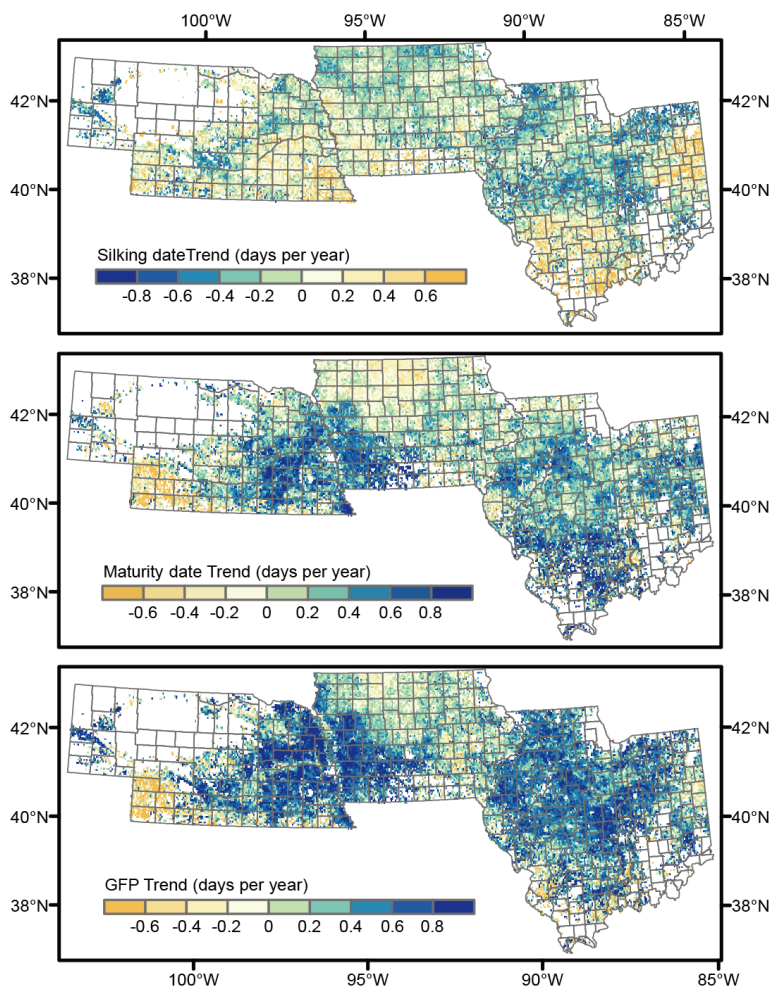
Figure A2 Trend of silking date, maturity date and GFP based on MODIS WDRVI data during 2000-2015.
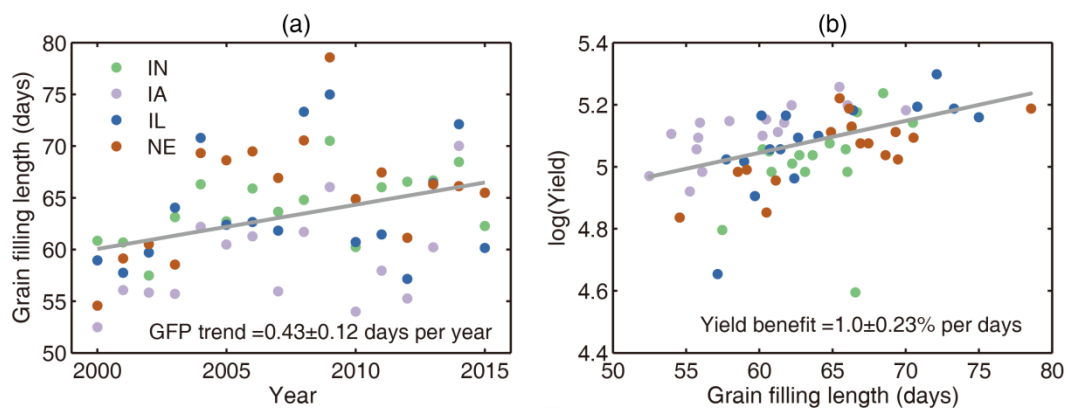
Figure A3 Grain filling length from 2000 to 2015 estimated from NASS reported crop progress data (a). The yield benefit of GFP extension based on state level yield data and crop progress data (b). Both slopes were estimated using a non-parametric Theil-Sen fitting.
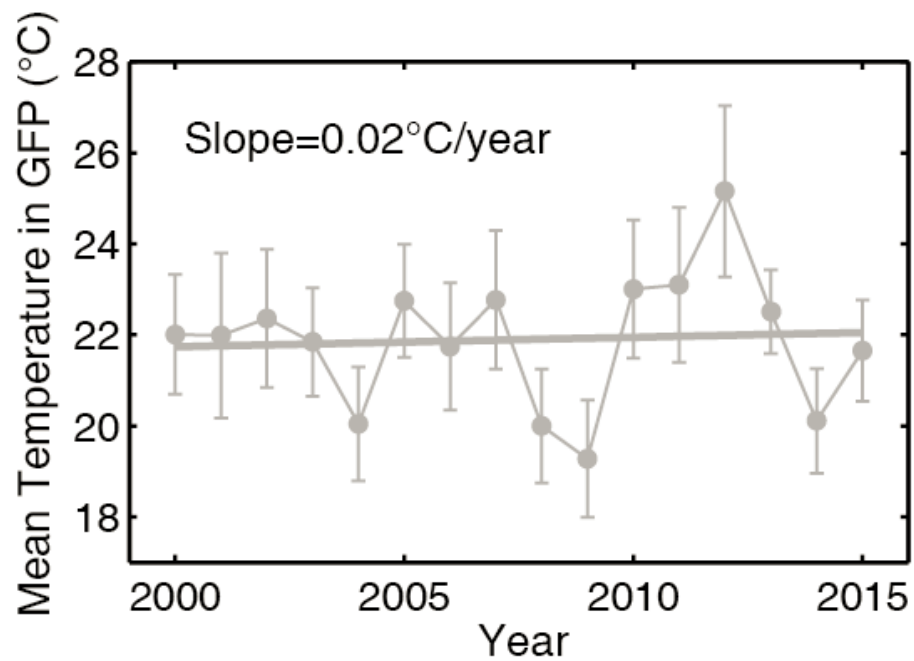
Figure A4 The mean temperature during grain filling period from 2000 to 2015. The error bars indicate the spatial variation (SD) of temperature.

(a)
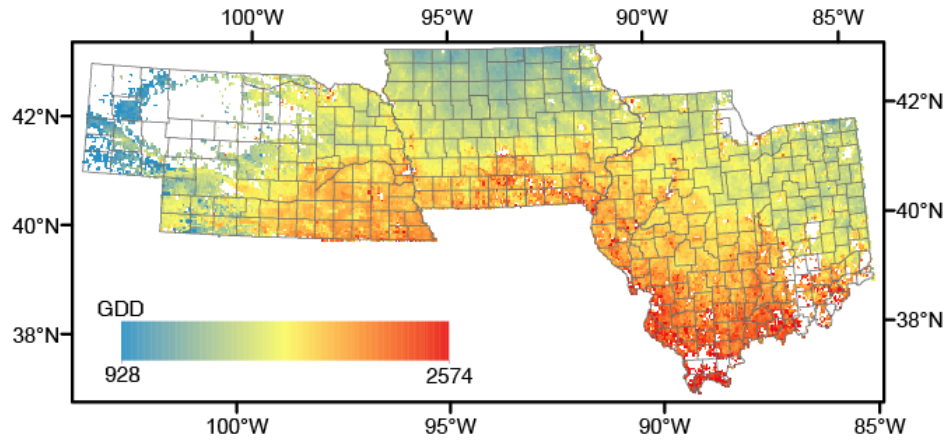
(b)
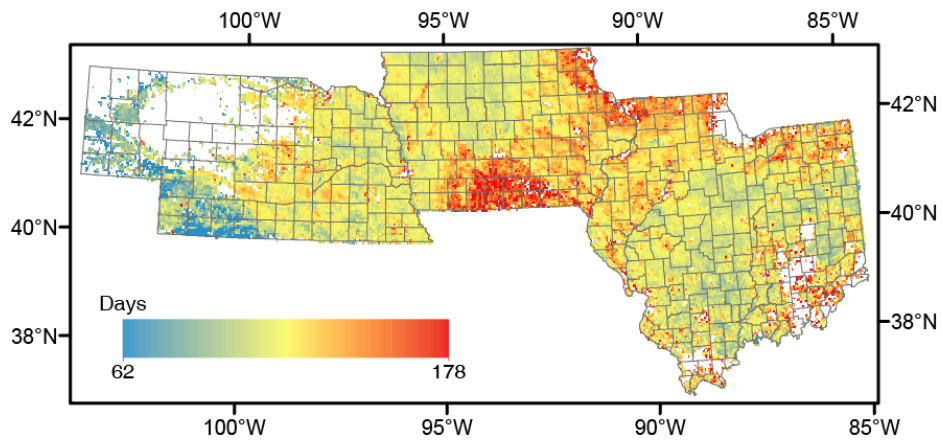
Figure A5 Spatial pattern of multi-year mean emergence to maturity GDD (a) and duration (days, b) for the period 2000-2015 in the U.S. Midwest.
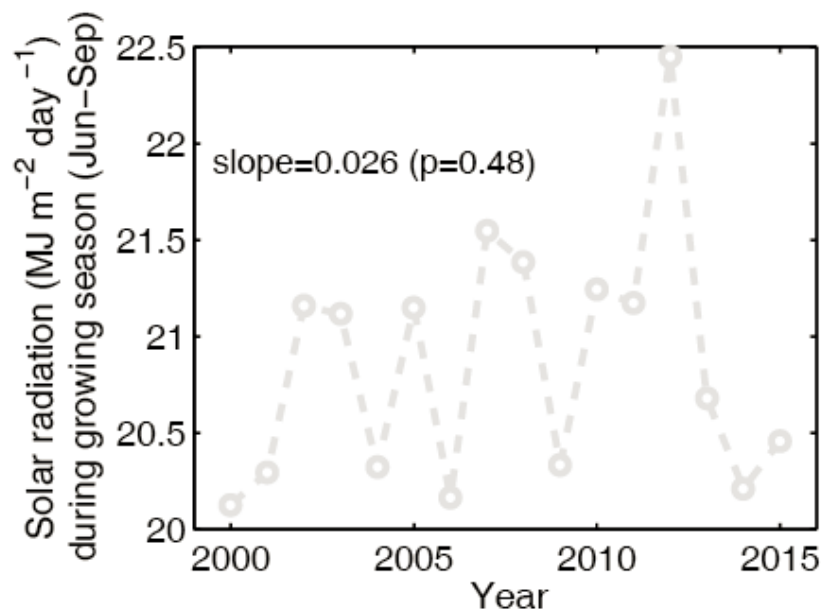
Figure A6 The solar radiation during the maize growing season, normally from June to September. To keep consistent with the previous study (1), we also used the solar radiation data from NASA Prediction of Worldwide Energy Resource (POWER).
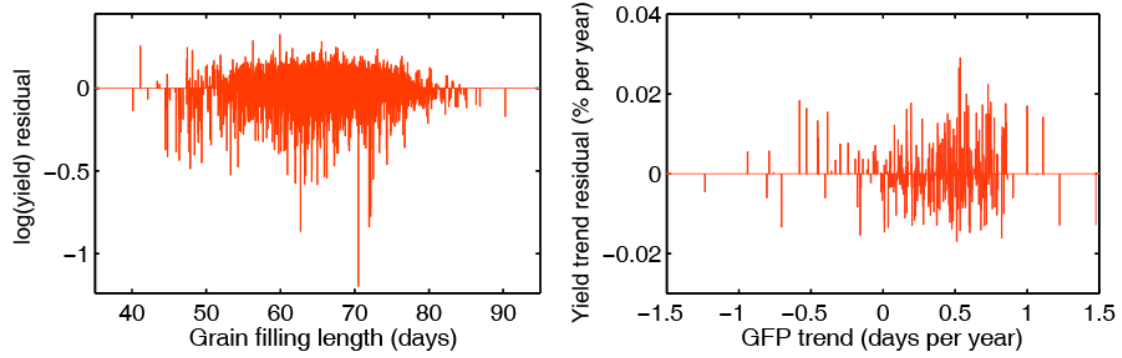
Figure A7 Residual plot of log(yield) v.s. grain filling length for each county in the equation (8) (left panel). Residual plot of yield trend v.s. GFP trend for each county in the equation (9) (right panel).
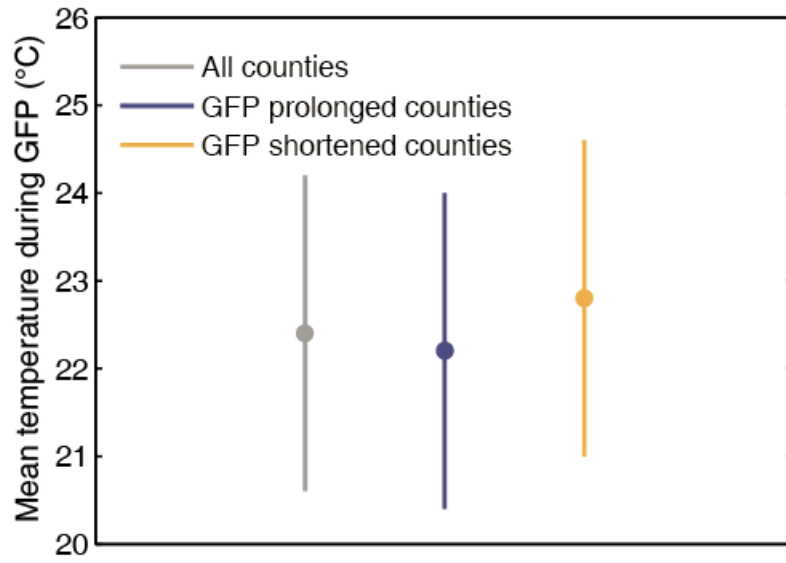
Figure A8 County level mean temperature during GFP when counties were grouped by whether their GFP has increased or not.
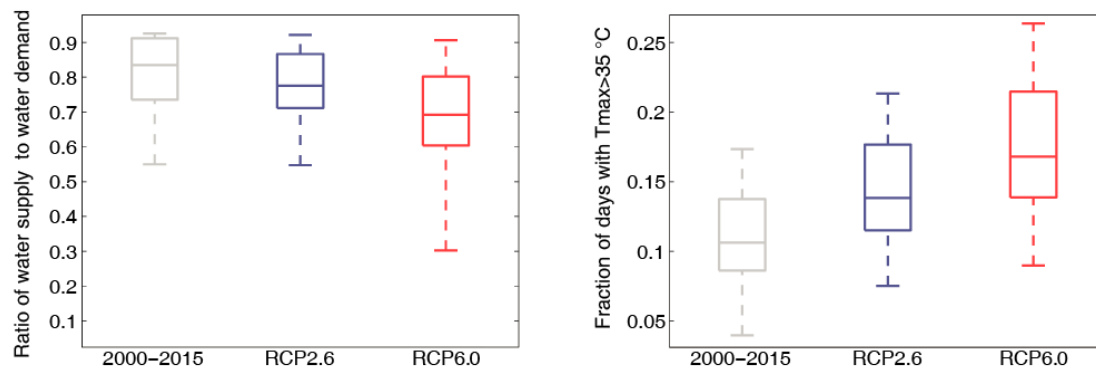
Figure A9 The water stress and heat stress during maize grain filling in three climate conditions: 2000-2015 and 2060-2070 in two RCPs. Water stress is characterized by APSIM output variables: the ratio of water supply and water demand. Heat stress is characterized by the fraction of days with its daily maximum temperature above 35°C.
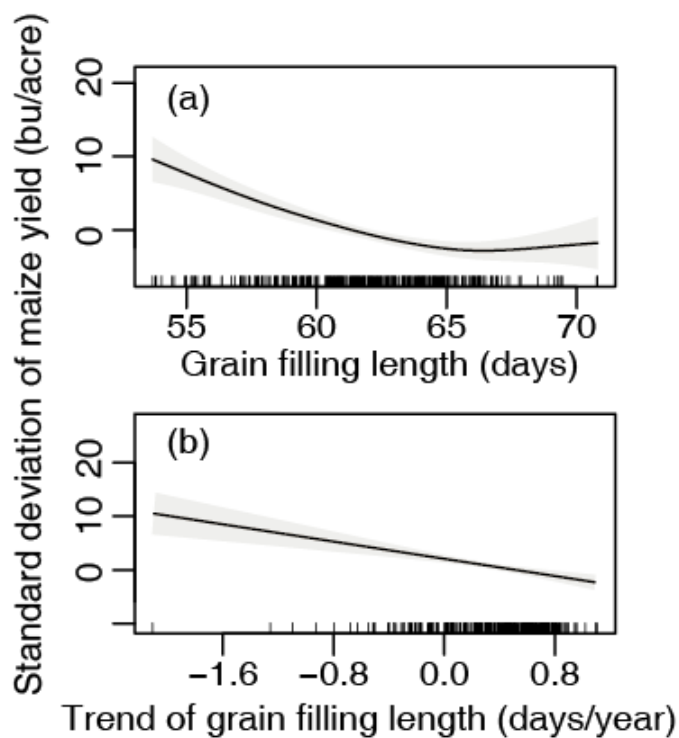
Figure A10 The effect of grain filling length on maize yield stability. Standard deviation of each county yield over time is used to represent the temporal stability of maize yield. Both longer GFP in space (a) and extended GFP over time (b) corresponds to smaller standard deviation of yield, suggesting longer GFP can be beneficial for yield stability. The shaded areas indicate the 95% confidence interval.

APPENDIX B

Table B1 Summary of temperature stress algorithm on maize photosynthesis, grain set/fillings and plants stage development.

Model	Process	Model type	References
APSIM	RUE	Piecewise linear	(Keating et al., 2003; Carberry et al., 1989)
	Grain number	Linear	
	Grain filling	Linear	
	Stage development	Piecewise linear	
CLM-crop	Enzyme kinetic	Coupled stomatal conductance and photosynthesis	Oleson et al., 2013
	Stage development	Piecewise linear	
DSSAT /DSSAT-pt	RUE	Piecewise linear	(Jones et al. 2003)
	Grain filling	Piecewise linear	
	Stage development	Piecewise linear	
GEPIC	RUE	Sinusoidal	(Sharpley & Williams 1990)
	Stage development	Piecewise linear	
LPJ-GUESS LPJml	Enzyme kinetic	Quadratic	(Lindeskog et al., 2013; Bondeau et al., 2007)
	Stage development	Coupled stomatal conductance and photosynthesis	
PEGASUS	RUE	Quadratic	Deryng et al. (2011)
	flowering	Piecewise linear	
	Stage development	Piecewise linear	
WOFOST	Assimilation rate	Piecewise linear	Supit et al. (1994)
	Stage development	Piecewise linear	
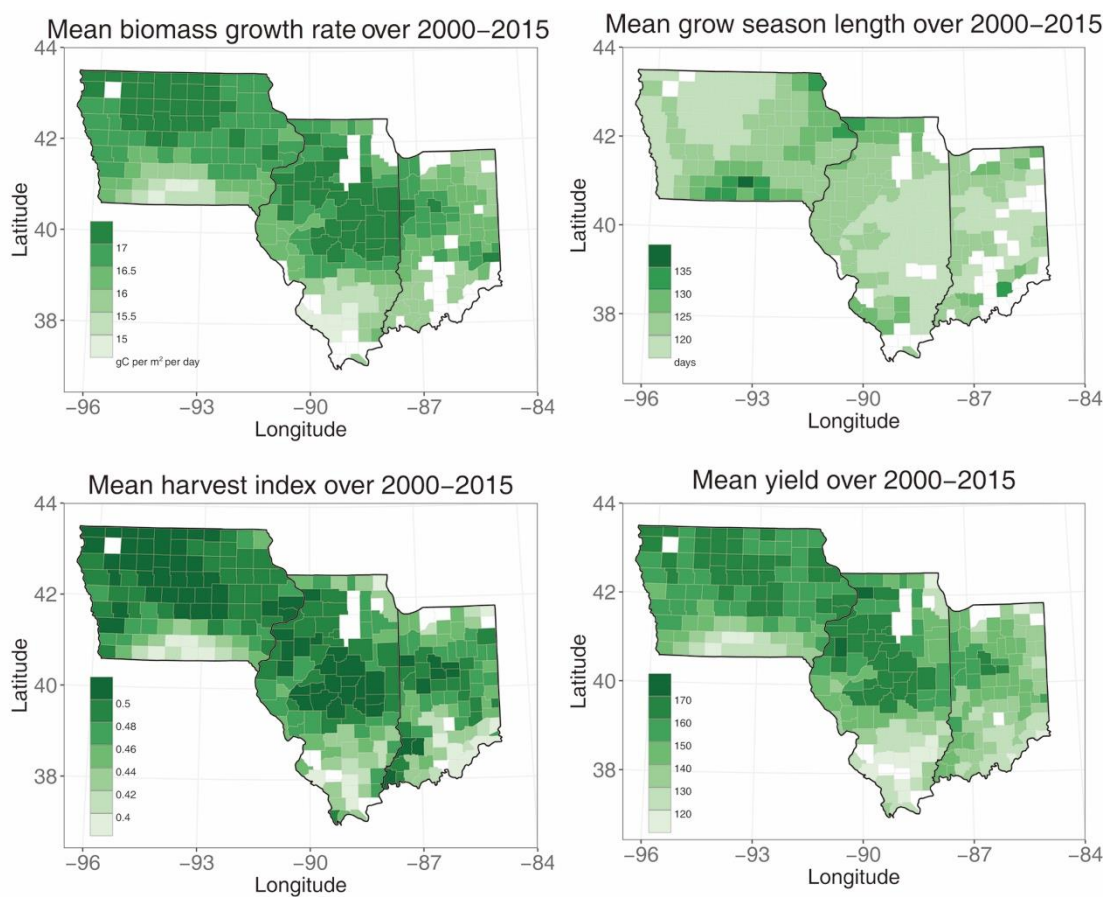
Figure B1 The spatial pattern of multi-year mean Yield, BGR, GSL and HI over the three Midwest states from observational data (county survey yield and MODIS derived GSL, BGR and HI).
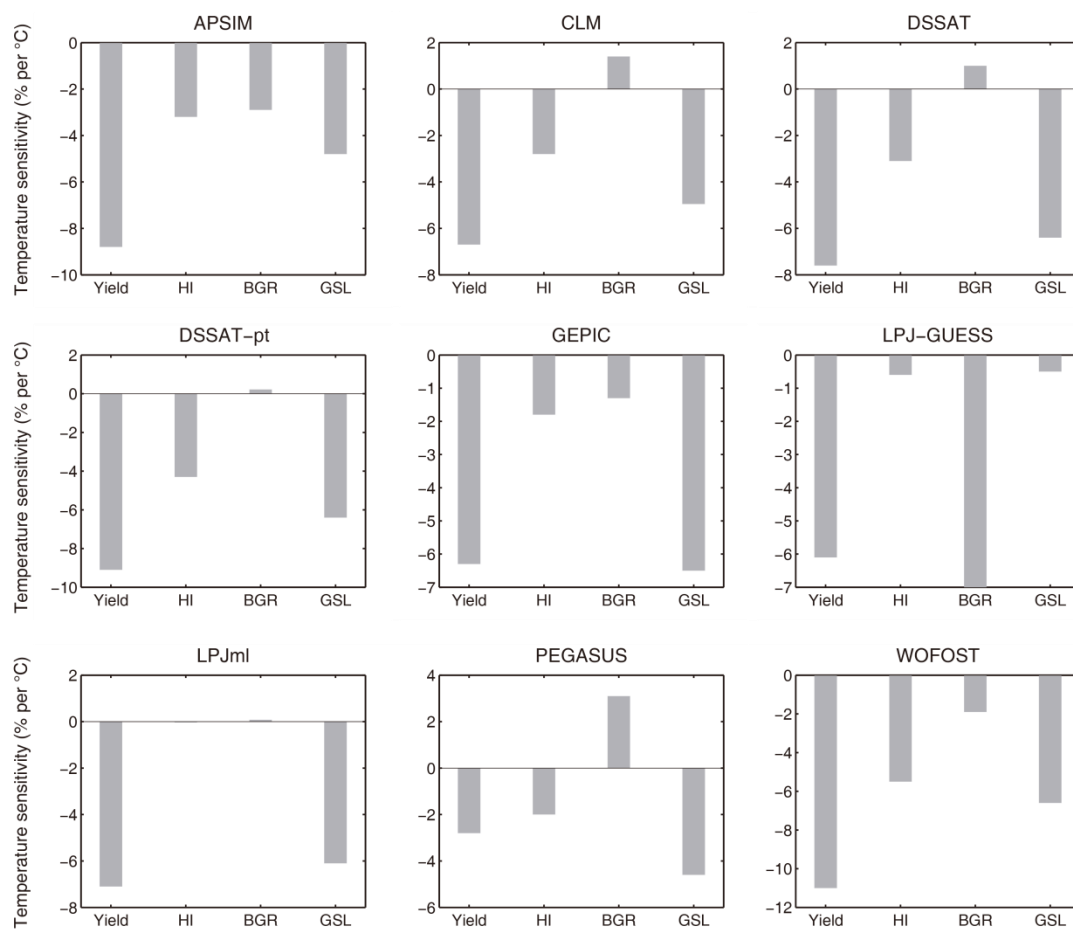
Figure B2 Temperature sensitivity of yield, HI, BGR and GSL in nine crop models.
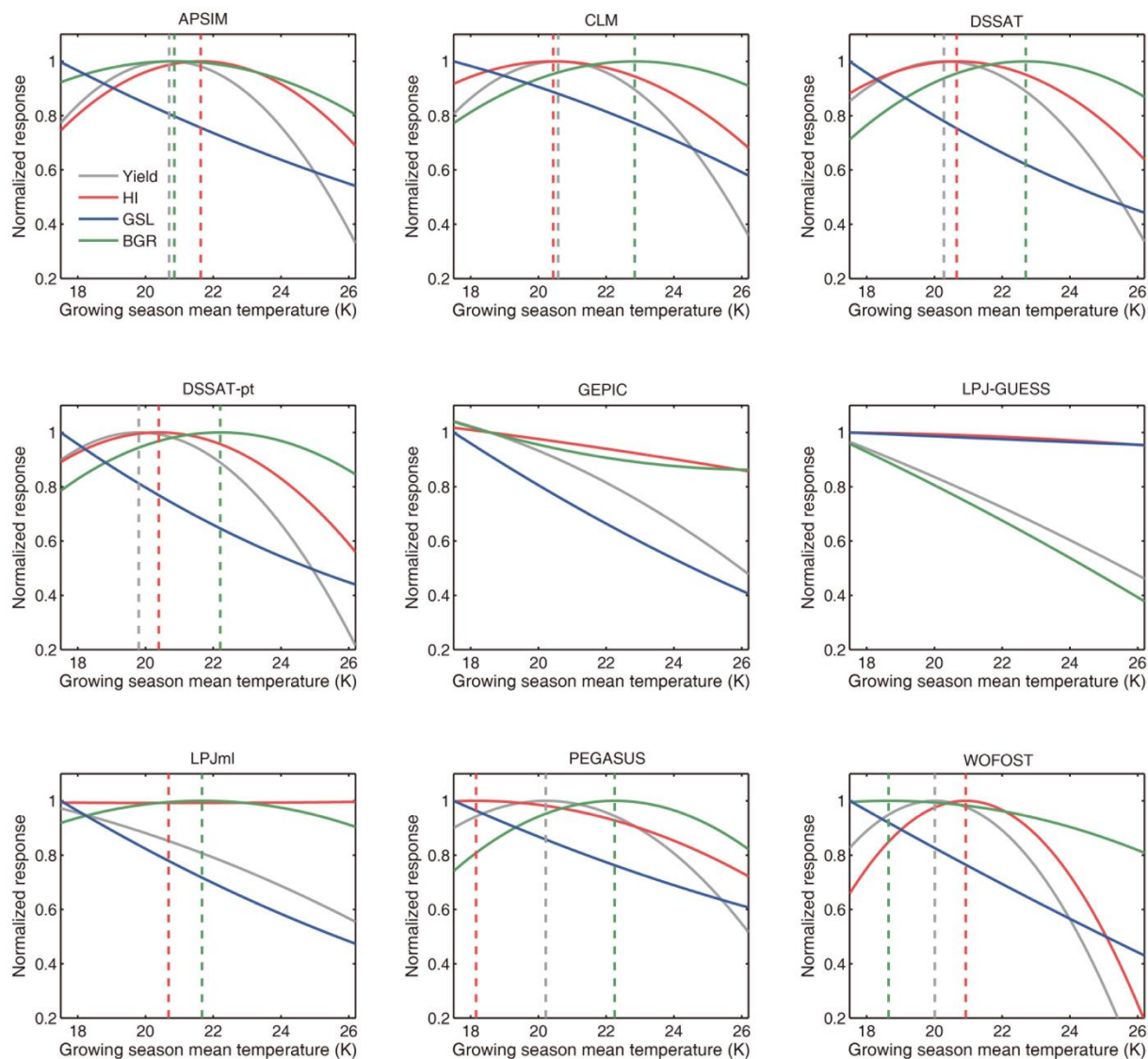
Figure B3 The response of Yield, HI, GSL and BGR to growing season mean temperature in each crop model. The vertial dashed lines indicate the optimal mean temperature where Yield, HI or BGR peaks. The response function is normalized by maximum value of each variable.
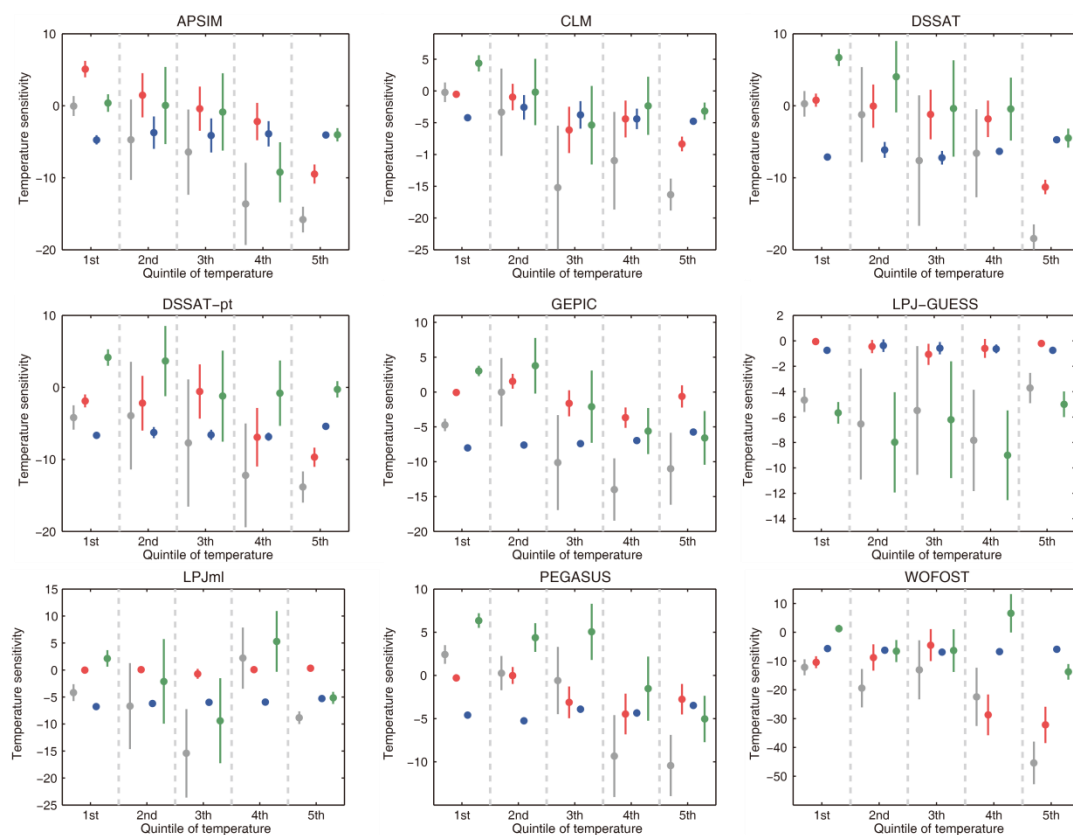
Figure B4 Temperature sensitivity of yield, HI, BGR and GSL in each crop model when the regresion data was divided by the quintile of growing season temperature. The error bars represent the 95% confidence interval of estimated sensitivity.
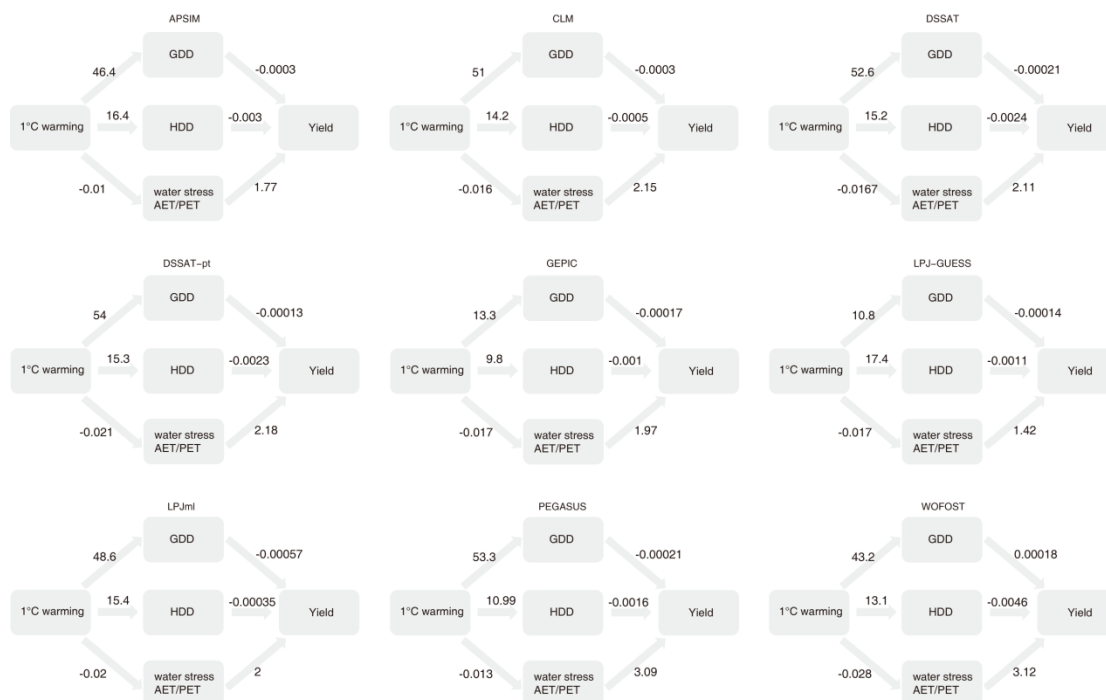
Figure B5 The direct (HDD) and indirect (WS) effect of temperature increase on maize yield in each crop model with crop model estimated yield, ET. The numbers marked on the arrows indicate the effects of 1 ℃ warming on yield through GDD, HDD and WS, corresponding to the coefficients in equation (12).
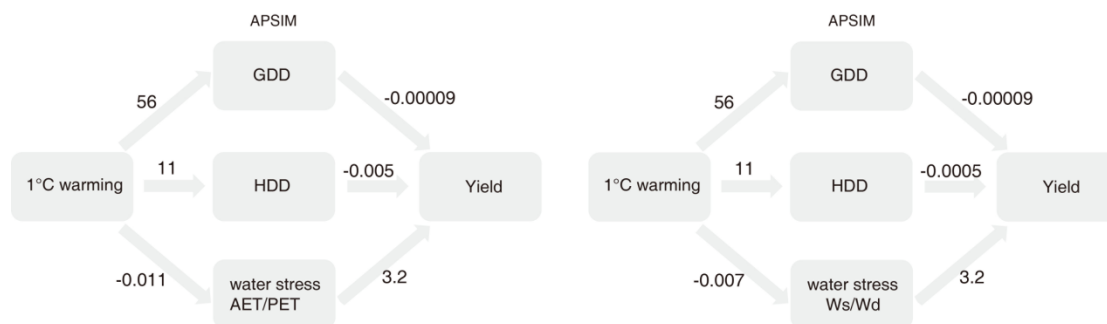
Figure B6 The direct (HDD) and indirect (WS) effect of temperature increase on maize yield in APSIM with different water stress metric: left using AET/PET as water stress and right using the ratio of water supply (Ws) to water demand (Wd) as water stress.

REFERENCES

Abatzoglou, John T. "Development of gridded surface meteorological data for ecological applications and modelling." International Journal of Climatology 33.1 (2013): 121-131.

Abraha, Michael, et al. "Evapotranspiration of annual and perennial biofuel crops in a variable climate." Gcb Bioenergy 7.6 (2015): 1344-1356.

Albanito, Fabrizio, et al. "Carbon implications of converting cropland to bioenergy crops or forest for climate mitigation: a global assessment." Gcb Bioenergy 8.1 (2016): 81-95.

Anderson-Teixeira, Kristina, et al. "Changes in soil organic carbon under biofuel crops." Gcb Bioenergy 1.1 (2009): 75-96.

Anderson, Ray G., et al. "Biophysical considerations in forestry for climate protection." Frontiers in Ecology and the Environment 9.3 (2011): 174-182.

Anderson-Teixeira, Kristina J., et al. "Climate-regulation services of natural and agricultural ecoregions of the Americas." Nature Climate Change 2.3 (2012): 177.

Anderson‑teixeira, Kristina J., and E. V. A. N. DeLucia. "The greenhouse gas value of ecosystems." Global Change Biology 17.1 (2011): 425-438.

Atkinson, Christopher J. "Establishing perennial grass energy crops in the UK: A review of current propagation options for Miscanthus." Biomass and bioenergy 33.5 (2009): 752-759.

Azzari, G., and D. B. Lobell. "Landsat-based classification in the cloud: An opportunity for a paradigm shift in land cover monitoring." Remote Sensing of Environment 202 (2017): 64-74.

Badu-Apraku, aB, R. B. Hunter, and M. Tollenaar. "Effect of temperature during grain filling on whole plant and grain yield in maize (Zea mays L.)." Canadian Journal of Plant Science 63.2 (1983): 357-363.

Beringer, T. I. M., Wolfgang Lucht, and Sibyll Schaphoff. "Bioenergy production potential of global biomass plantations under environmental and agricultural constraints." Gcb Bioenergy 3.4 (2011): 299-312.

Bhardwaj, A. K., et al. "Water and energy footprints of bioenergy crop production on marginal lands." Gcb Bioenergy 3.3 (2011): 208-222.

Bonan, Gordon B. Land surface model (LSM version 1.0) for ecological, hydrological, and atmospheric studies: Technical description and users guide. Technical note. No. PB-97-131494/XAB; NCAR/TN-417-STR. National Center for Atmospheric Research, Boulder, CO (United States). Climate and Global Dynamics Div., 1996.

Bonan, Gordon B., et al. "Improving canopy processes in the Community Land Model version 4 (CLM4) using global flux fields empirically inferred from FLUXNET data." Journal of Geophysical Research: Biogeosciences 116.G2 (2011).

Bondeau, Alberte, et al. "Modelling the role of agriculture for the 20th century global terrestrial carbon balance." Global Change Biology 13.3 (2007): 679-706.

Burney, J. A. et al. Greenhouse gas mitigation by agricultural intensification. Proc. Natl Acad. Sci. USA 107, 12052–12057 (2010)

Butler, Ethan E., and Peter Huybers. "Variations in the sensitivity of US maize yield to extreme temperatures by region and growth phase." Environmental Research Letters 10.3 (2015): 034009.

Cai, Ximing, Xiao Zhang, and Dingbao Wang. "Land availability for biofuel production." Environmental science & technology 45.1 (2010): 334-339.

Cakir, Recep. "Effect of water stress at different development stages on vegetative and reproductive growth of corn." Field Crops Research 89.1 (2004): 1-16.

Campbell, Bruce M., et al. "Reducing risks to food security from climate change." Global Food Security 11 (2016): 34-43.

Carberry, P. S., R. C. Muchow, and R. L. McCown. "Testing the CERES-Maize simulation model in a semi-arid tropical environment." Field Crops Research 20.4 (1989): 297-315.

Chamberlain, Jim F., Shelie A. Miller, and James R. Frederick. "Using DAYCENT to quantify on-farm GHG emissions and N dynamics of land use conversion to N-managed switchgrass in the Southern US." Agriculture, ecosystems & environment 141.3-4 (2011): 332-341.

Cheikh, Nordine, and Robert J. Jones. "Disruption of maize kernel growth and development by heat stress (role of cytokinin/abscisic acid balance)." Plant physiology 106.1 (1994): 45-51.

Chemura, Abel, Onisimo Mutanga, and Timothy Dube. "Separability of coffee leaf rust infection levels with machine learning methods at Sentinel-2 MSI spectral resolutions." Precision Agriculture 18.5 (2017): 859-881.

CLIFTON‑BROWN, JOHN C., Joeern Breuer, and Michael B. Jones. "Carbon mitigation by the energy crop, Miscanthus." Global Change Biology 13.11 (2007): 2296-2307.

Cohn, Avery S., et al. "Cropping frequency and area response to climate variability can exceed yield response." Nature Climate Change 6.6 (2016): 601.

Commuri, P. D., and R. J. Jones. "High temperatures during endosperm cell division in maize." Crop Science 41.4 (2001): 1122-1130.

Crafts-Brandner, Steven J., and Michael E. Salvucci. "Sensitivity of photosynthesis in a C4 plant, maize, to heat stress." Plant physiology 129.4 (2002): 1773-1780.

Crosbie, T. M., and J. J. Mock. "Changes in Physiological Traits Associated With Grain Yield Improvement in Three Maize Breeding Programs 1." Crop Science 21.2 (1981): 255-259.

Daly, Christopher, et al. "Physiographically sensitive mapping of climatological temperature and precipitation across the conterminous United States." International journal of climatology 28.15 (2008): 2031-2064.

Davis, Morgan P., et al. "Effect of nitrogen addition on Miscanthus× giganteus yield, nitrogen losses, and soil organic matter across five sites." Gcb Bioenergy 7.6 (2015): 1222-1231.

Davis, Sarah C., et al. "Impact of second‑generation biofuel agriculture on greenhouse‑gas emissions in the corn‑growing regions of the US." Frontiers in Ecology and the Environment 10.2 (2012): 69-74.

Davis, Sarah C., et al. "Management swing potential for bioenergy crops." Gcb Bioenergy 5.6 (2013): 623-638.

Deines, Jillian M., Anthony D. Kendall, and David W. Hyndman. "Annual Irrigation Dynamics in the US Northern High Plains Derived from Landsat Satellite Data." Geophysical Research Letters 44.18 (2017): 9350-9360.

Dekov, I., T. Tsonev, and I. Yordanov. "Effects of water stress and high-temperature stress on the structure and activity of photosynthetic apparatus of Zea mays and Helianthus annuus." Photosynthetica 38.3 (2000): 361-366.

Delegido, J., et al. "A red-edge spectral index for remote sensing estimation of green LAI over agroecosystems." European Journal of Agronomy 46 (2013): 42-52.

Deryng, Delphine, et al. "Simulating the effects of climate and agricultural management practices on global crop yield." Global biogeochemical cycles 25.2 (2011).

Dohleman, F. G., et al. "Does greater leaf‐level photosynthesis explain the larger solar energy conversion efficiency of Miscanthus relative to switchgrass?." Plant, cell & environment 32.11 (2009): 1525-1537.

Driedonks, Nicky, Ivo Rieu, and Wim H. Vriezen. "Breeding for plant heat tolerance at vegetative and reproductive stages." Plant reproduction 29.1-2 (2016): 67-79.

Duncan, John, Jadunandan Dash, and Peter M. Atkinson. "The potential of satellite-observed crop phenology to enhance yield gap assessments in smallholder landscapes." Frontiers in Environmental Science 3 (2015): 56.

Duvick, Donald N. "The contribution of breeding to yield advances in maize (Zea mays L.)." Advances in agronomy 86 (2005): 83-145.

Dwyer, L. M., et al. "Maize physiological traits related to grain yield and harvest moisture in mid-to short-season environments." Crop science 34.4 (1994): 985-992.

Edreira, Juan I. Rattalino, et al. "Assessing causes of yield gaps in agricultural areas with diversity in climate and soils." Agricultural and Forest Meteorology 247 (2017): 170-180.

Edreira, JI Rattalino, and Maria Elena Otegui. "Heat stress in temperate and tropical maize hybrids: A novel approach for assessing sources of kernel loss in field conditions." Field Crops Research 142 (2013): 58-67.

Edreira, Juan I. Rattalino, and María E. Otegui. "Heat stress in temperate and tropical maize hybrids: Differences in crop growth, biomass partitioning and reserves use." Field Crops Research 130 (2012): 87-98.

Edreira, Juan I. Rattalino, Luis I. Mayer, and María E. Otegui. "Heat stress in temperate and tropical maize hybrids: Kernel growth, water relations and assimilate availability for grain filling." Field Crops Research 166 (2014): 162-172.

Egli, Dennis B. Seed biology and the yield of grain crops. CAB INTERNATIONAL, 1998.

Elshout, P. M. F., et al. "Greenhouse-gas payback times for crop-based biofuels." Nature Climate Change 5.6 (2015): 604.

Estel, Stephan, et al. "Mapping cropland-use intensity across Europe using MODIS NDVI time series." Environmental Research Letters 11.2 (2016): 024015.

Fargione, Joseph, et al. "Land clearing and the biofuel carbon debt." Science 319.5867 (2008): 1235-1238.

Field, Christopher B., J. Elliott Campbell, and David B. Lobell. "Biomass energy: the scale of the potential resource." Trends in ecology & evolution 23.2 (2008): 65-72.

Fike, John H., et al. "Long-term yield potential of switchgrass-for-biofuel systems." Biomass and bioenergy 30.3 (2006): 198-206.

Gibbs, Holly K., et al. "Carbon payback times for crop-based biofuel expansion in the tropics: the effects of changing yield and technology." Environmental research letters 3.3 (2008): 034001.

Gitelson, Anatoly A. "Wide dynamic range vegetation index for remote quantification of biophysical characteristics of vegetation." Journal of plant physiology 161.2 (2004): 165-173.

Gitelson, Anatoly A., John F. Schalles, and Christine M. Hladik. "Remote chlorophyll-a retrieval in turbid, productive estuaries: Chesapeake Bay case study." Remote Sensing of Environment 109.4 (2007): 464-472.

Guindin-Garcia, Noemi, et al. "An evaluation of MODIS 8-and 16-day composite products for monitoring maize green leaf area index." Agricultural and Forest Meteorology 161 (2012): 15-25.

Foley, Jonathan A., et al. "An integrated biosphere model of land surface processes, terrestrial carbon balance, and vegetation dynamics." Global Biogeochemical Cycles 10.4 (1996): 603-628.

Gao, Feng, et al. "Toward mapping crop progress at field scales through fusion of Landsat and MODIS imagery." Remote Sensing of Environment 188 (2017): 9-25.

Gelfand, Ilya, et al. "Sustainable bioenergy production from marginal lands in the US Midwest." Nature 493.7433 (2013): 514.

Georgescu, Matei, David B. Lobell, and Christopher B. Field. "Direct climate effects of perennial bioenergy crops in the United States." Proceedings of the National Academy of Sciences 108.11 (2011): 4307-4312.

Gitelson, Anatoly A., John F. Schalles, and Christine M. Hladik. "Remote chlorophyll-a retrieval in turbid, productive estuaries: Chesapeake Bay case study." Remote Sensing of Environment 109.4 (2007): 464-472.

Gopalakrishnan, Gayathri, Cristina Negri, and William Salas. "Modeling biogeochemical impacts of bioenergy buffers with perennial grasses for a row‑crop field in Illinois." Gcb Bioenergy 4.6 (2012): 739-750.

Guan, Kaiyu, et al. "Improving the monitoring of crop productivity using spaceborne solar‑induced fluorescence." Global change biology 22.2 (2016): 716-726.

Guanter, Luis, et al. "Global and time-resolved monitoring of crop photosynthesis with chlorophyll fluorescence." Proceedings of the National Academy of Sciences 111.14 (2014): E1327-E1333.

Guindin-Garcia, Noemi, et al. "An evaluation of MODIS 8-and 16-day composite products for monitoring maize green leaf area index." Agricultural and Forest Meteorology 161 (2012): 15-25.

Hammer, Graeme L., et al. "Adapting APSIM to model the physiology and genetics of complex adaptive traits in field crops." Journal of experimental botany 61.8 (2010): 2185-2202.

Hatfield, Jerry L., and John H. Prueger. "Temperature extremes: effect on plant growth and development." Weather and climate extremes 10 (2015): 4-10.

He, Feng, et al. "Simulating global and local surface temperature changes due to Holocene anthropogenic land cover change." Geophysical Research Letters 41.2 (2014): 623-631.

Heaton, Emily, Tom Voigt, and Stephen P. Long. "A quantitative review comparing the yields of two candidate C4 perennial biomass crops in relation to nitrogen, temperature and water." Biomass and bioenergy 27.1 (2004): 21-30.

Heaton, Emily A., Frank G. Dohleman, and Stephen P. Long. "Meeting US biofuel goals with less land: the potential of Miscanthus." Global change biology 14.9 (2008): 2000-2014.

Hickman, George C., et al. "A comparison of canopy evapotranspiration for maize and two perennial grasses identified as potential bioenergy crops." Gcb Bioenergy 2.4 (2010): 157-168.

Holzworth, Dean P., et al. "APSIM–evolution towards a new generation of agricultural systems simulation." Environmental Modelling & Software 62 (2014): 327-350.

Hudiburg, Tara W., et al. "Bioenergy crop greenhouse gas mitigation potential under a range of management practices." Gcb Bioenergy 7.2 (2015): 366-374.

Huete, Alfredo, et al. "Overview of the radiometric and biophysical performance of the MODIS vegetation indices." Remote sensing of environment 83.1-2 (2002): 195-213.

IPCC Climate change: the scientific basis. Intergovernment panel on climate change Cambridge Univ. Press, Cambridge (UK) (2001)

Irmak, Suat, Dorota Z. Haman, and Ruhi Bastug. "Determination of crop water stress index for irrigation timing and yield estimation of corn." Agronomy Journal 92.6 (2000): 1221-1227.

Jin, Zhenong, et al. "Increasing drought and diminishing benefits of elevated carbon dioxide for soybean yields across the US Midwest." Global change biology 24.2 (2018).

Jones, James W., et al. "The DSSAT cropping system model." European journal of agronomy 18.3-4 (2003): 235-265.

Jones, Michael B., John Finnan, and Trevor R. Hodkinson. "Morphological and physiological traits for higher biomass production in perennial rhizomatous grasses grown on marginal land." Gcb Bioenergy 7.2 (2015): 375-385.

Keating, Brian A., et al. "An overview of APSIM, a model designed for farming systems simulation." European journal of agronomy 18.3-4 (2003): 267-288.

Keenan, Trevor F., et al. "Net carbon uptake has increased through warming-induced changes in temperate forest phenology." Nature Climate Change 4.7 (2014): 598.

Kiniry, J. R., and R. Bonhomme. "Predicting maize phenology." Predicting crop phenology 11 (1991): 5-131.

Knoke, Thomas, et al. "How can climate policy benefit from comprehensive land‐use approaches?." Frontiers in Ecology and the Environment 10.8 (2012): 438-445.

Kucharik, Christopher J., et al. "Testing the performance of a dynamic global ecosystem model: water balance, carbon balance, and vegetation structure." Global Biogeochemical Cycles 14.3 (2000): 795-825.

Lal, Rattan. "Carbon emission from farm operations." Environment international 30.7 (2004): 981-990.

Lawrence, David M., et al. "Parameterization improvements and functional and structural advances in version 4 of the Community Land Model." Journal of Advances in Modeling Earth Systems 3.1 (2011).

Lee, Juhwan, et al. "Simulating switchgrass biomass production across ecoregions using the DAYCENT model." Gcb Bioenergy 4.5 (2012): 521-533.

Lee, Xuhui, et al. "Observed increase in local cooling effect of deforestation at higher latitudes." Nature 479.7373 (2011): 384.

Levis, Samuel, M. D. Hartman, and G. B. Bonan. "The Community Land Model underestimates land-use CO 2 emissions by neglecting soil disturbance from cultivation." Geoscientific Model Development 7.2 (2014): 613-620.

Lewandowski, Iris, et al. "The development and current status of perennial rhizomatous grasses as energy crops in the US and Europe." Biomass and Bioenergy 25.4 (2003): 335-361.

Lindeskog, Mats, et al. "Implications of accounting for land use in simulations of ecosystem carbon cycling in Africa." Earth System Dynamics 4.2 (2013): 385-407.

Liska, Adam J., et al. "Biofuels from crop residue can reduce soil carbon and increase CO 2 emissions." Nature Climate Change 4.5 (2014): 398.

Loarie, Scott R., et al. "Direct impacts on local climate of sugar-cane expansion in Brazil." Nature Climate Change 1.2 (2011): 105.

Lobell, David, et al. "Regional differences in the influence of irrigation on climate." Journal of Climate 22.8 (2009): 2248-2255.

Lobell, David B., Wolfram Schlenker, and Justin Costa-Roberts. "Climate trends and global crop production since 1980." Science 333.6042 (2011): 616-620.

Lobell, David B., and Christopher B. Field. "Estimation of the carbon dioxide (CO_2) fertilization effect using growth rate anomalies of CO_2 and crop yields since 1961." Global Change Biology 14.1 (2008): 39-45.

Lobell, David B., Adam Sibley, and J. Ivan Ortiz-Monasterio. "Extreme heat effects on wheat senescence in India." Nature Climate Change 2.3 (2012): 186.

Lobell, David B., et al. "The critical role of extreme heat for maize production in the United States." Nature Climate Change 3.5 (2013): 497.

Lobell, David B., et al. "Greater sensitivity to drought accompanies maize yield increase in the US Midwest." Science 344.6183 (2014): 516-519.

Lobell, David B., Adam Sibley, and J. Ivan Ortiz-Monasterio. "Extreme heat effects on wheat senescence in India." Nature Climate Change 2.3 (2012): 186.

Loveland, Thomas R., and A. S. Belward. "The IGBP-DIS global 1km land cover data set, DISCover: first results." International Journal of Remote Sensing 18.15 (1997): 3289-3295.

Luyssaert, Sebastiaan, et al. "Land management and land-cover change have impacts of similar magnitude on surface temperature." Nature Climate Change 4.5 (2014): 389.

McMaster, G. S. "Phytomers, phyllochrons, phenology and temperate cereal development." The Journal of Agricultural Science 143.2-3 (2005): 137-150.

Meinshausen, Malte, et al. "The RCP greenhouse gas concentrations and their extensions from 1765 to 2300." Climatic change 109.1-2 (2011): 213.

Miguez, Fernando E., et al. "Modeling spatial and dynamic variation in growth, yield, and yield stability of the bioenergy crops Miscanthus× giganteus and Panicum virgatum across the conterminous United States." Gcb Bioenergy 4.5 (2012): 509-520.

Miller, Jesse N., et al. "Candidate perennial bioenergy grasses have a higher albedo than annual row crops." Gcb Bioenergy 8.4 (2016): 818-825.

Mitchell, Timothy D., and Philip D. Jones. "An improved method of constructing a database of monthly climate observations and associated high‐resolution grids." International journal of climatology 25.6 (2005): 693-712.

Mitchell, Kenneth E., et al. "The multi‐institution North American Land Data Assimilation System (NLDAS): Utilizing multiple GCIP products and partners in a continental distributed hydrological modeling system." Journal of Geophysical Research: Atmospheres 109.D7 (2004).

Mu, Qiaozhen, Maosheng Zhao, and Steven W. Running. "Improvements to a MODIS global terrestrial evapotranspiration algorithm." Remote Sensing of Environment 115.8 (2011): 1781-1800.

National Research Council. The impact of genetically engineered crops on farm sustainability in the United States. National Academies Press, 2010.

Niki èma, Paligwende, et al. "Nitrogen fertilization of switchgrass increases biomass yield and improves net greenhouse gas balance in northern Michigan, USA." Biomass and Bioenergy 35.10 (2011): 4356-4367.

Ogle, S. M., Breidt, F. J. & Paustian, K. Agricultural management impacts on soil organic carbon storage under moist and dry climatic conditions of temperate and tropical regions. Biogeochemistry 72, 87–121 (2005)

Olesen, J ørgen E., et al. "Impacts and adaptation of European crop production systems to climate change." European Journal of Agronomy 34.2 (2011): 96-112.

Oleson, K., et al., "Technical description of version 4.5 of the Community Land Model (CLM)." (2013).

Ordóñez, Raziel A., et al. "Yield response to heat stress as affected by nitrogen availability in maize." Field Crops Research 183 (2015): 184-203.

Ozdogan, Mutlu, et al. "Simulating the effects of irrigation over the United States in a land surface model based on satellite-derived agricultural data." Journal of Hydrometeorology 11.1 (2010): 171-184.

Peng, Shu-Shi, et al. "Afforestation in China cools local land surface temperature." Proceedings of the National Academy of Sciences 111.8 (2014): 2915-2919.

Ponce-Campos, Guillermo E., et al. "Ecosystem resilience despite large-scale altered hydroclimatic conditions." Nature 494.7437 (2013): 349.

Porter, John R., and Mikhail A. Semenov. "Crop responses to climatic variation." Philosophical Transactions of the Royal Society B: Biological Sciences 360.1463 (2005): 2021-2035.

Propheter, J. L., et al. "Performance of annual and perennial biofuel crops: yield during the first two years." Agronomy Journal 102.2 (2010): 806-814.

Puma, M. J., and B. I. Cook. "Effects of irrigation on global climate during the 20th century." Journal of Geophysical Research: Atmospheres 115.D16 (2010).

Qin, Zhangcai, Qianlai Zhuang, and Min Chen. "Impacts of land use change due to biofuel crops on carbon balance, bioenergy production, and agricultural yield, in the conterminous United States." Gcb Bioenergy 4.3 (2012): 277-288.

Qin, Zhangcai, Qianlai Zhuang, and Xudong Zhu. "Carbon and nitrogen dynamics in bioenergy ecosystems: 1. Model development, validation and sensitivity analysis." GCB bioenergy 6.6 (2014): 740-755.

Qin, Zhangcai, Qianlai Zhuang, and Xudong Zhu. "Carbon and nitrogen dynamics in bioenergy ecosystems: 2. Potential greenhouse gas emissions and global warming intensity in the conterminous United States." Gcb Bioenergy 7.1 (2015): 25-39.

Rahmstorf, Stefan, and Dim Coumou. "Increase of extreme events in a warming world." Proceedings of the National Academy of Sciences 108.44 (2011): 17905-17909.

Ray, Deepak K., et al. "Climate variation explains a third of global crop yield variability." Nature communications 6 (2015): 5989.

Roncucci, Neri, et al. "Influence of soil texture and crop management on the productivity of miscanthus (Miscanthus× giganteus Greef et Deu.) in the Mediterranean." Gcb Bioenergy 7.5 (2015): 998-1008.

Rosenzweig, Cynthia, et al. "The agricultural model intercomparison and improvement project (AgMIP): protocols and pilot studies." Agricultural and Forest Meteorology 170 (2013): 166-182.

Roth, Brendan, et al. "Are the benefits of yield responses to nitrogen fertilizer application in the bioenergy crop Miscanthus×giganteus offset by increased soil emissions of nitrous oxide?." Gcb Bioenergy 7.1 (2015): 145-152.

Sacks, William J., and Christopher J. Kucharik. "Crop management and phenology trends in the US Corn Belt: Impacts on yields, evapotranspiration and energy balance." Agricultural and Forest Meteorology 151.7 (2011): 882-894.

Sacks, William J., et al. "Crop planting dates: an analysis of global patterns." Global Ecology and Biogeography 19.5 (2010): 607-620.

Sakamoto, Toshihiro, et al. "A two-step filtering approach for detecting maize and soybean phenology with time-series MODIS data." Remote Sensing of Environment 114.10 (2010): 2146-2159.

Sánchez, Berta, Anton Rasmussen, and John R. Porter. "Temperatures and the growth and development of maize and rice: a review." Global change biology 20.2 (2014): 408-417.

Schlenker, Wolfram, and Michael J. Roberts. "Nonlinear temperature effects indicate severe damages to US crop yields under climate change." Proceedings of the National Academy of sciences 106.37 (2009): 15594-15598.

Sharpley, A. N., and J. R. Williams. "EPIC erosion productivity impact calculator: 2. User manual." US Department of Agriculture Technical Bulletin 1768 (1990): 127.

Siebers, Matthew H., et al. "Heat waves imposed during early pod development in soybean (Glycine max) cause significant yield loss despite a rapid recovery from oxidative stress." Global change biology 21.8 (2015): 3114-3125.

Siebers, Matthew H., et al. "Simulated heat waves during maize reproductive stages alter reproductive growth but have no lasting effect when applied during vegetative stages." Agriculture, ecosystems & environment 240 (2017): 162-170.

Smith, W. N., et al. "Crop residue removal effects on soil carbon: Measured and inter-model comparisons." Agriculture, ecosystems & environment 161 (2012): 27-38.

Smith, P. Soils and climate change. Curr. Opin. Environ. Sust. 4, 539–544 (2012)

Stewart, J., et al. "The ecology and agronomy of Miscanthus sinensis, a species important to bioenergy crop development, in its native range in Japan: a review." Gcb Bioenergy 1.2 (2009): 126-153.

Supit, I., A. A. Hooijer, and C. A. Van Diepen. "System description of the WOFOST 6.0 crop growth simulation model." Joint Research Center, Commission of the European Communities. Brussels, Luxembourg (1994).

Surendran Nair, Sujithkumar, et al. "Bioenergy crop models: descriptions, data requirements, and future challenges." Gcb Bioenergy 4.6 (2012): 620-633.

Tack, Jesse, Andrew Barkley, and Lawton Lanier Nalley. "Effect of warming temperatures on US wheat yields." Proceedings of the National Academy of Sciences 112.22 (2015): 6931-6936.

Tack, Jesse, Jane Lingenfelser, and SV Krishna Jagadish. "Disaggregating sorghum yield reductions under warming scenarios exposes narrow genetic diversity in US breeding programs." Proceedings of the National Academy of Sciences 114.35 (2017): 9296-9301.

Thomas, Amy RC, Alan J. Bond, and Kevin M. Hiscock. "A multi‐criteria based review of models that predict environmental impacts of land use‐change for perennial energy crops on water, carbon and nitrogen cycling." Gcb Bioenergy 5.3 (2013): 227-242.

Thomas, Howard, and Helen Ougham. "The stay-green trait." Journal of Experimental Botany 65.14 (2014): 3889-3900.

Tilman, David, et al. "Global food demand and the sustainable intensification of agriculture." Proceedings of the National Academy of Sciences 108.50 (2011): 20260-20264.

Tollenaar, Matthijs, et al. "The contribution of solar brightening to the US maize yield trend." Nature Climate Change 7.4 (2017): 275.

Tollenaar, M., and E. A. Lee. "Yield potential, yield stability and stress tolerance in maize." Field Crops Research 75.2-3 (2002): 161-169.

Tollenaar, M., and J. Wu. "Yield improvement in temperate maize is attributable to greater stress tolerance." Crop Science 39.6 (1999): 1597-1604.

USDA, September. "World Agricultural Supply and Demand Estimates." Internet site: http://usda. mannlib. cornell. edu/reports/waobr/wasde-bb (Accessed May 11, 2005) (2012).

Valentine, John, et al. "Food vs. fuel: the use of land for lignocellulosic 'next generation' energy crops that minimize competition with primary food production." Gcb Bioenergy 4.1 (2012): 1-19.

Vanloocke, Andy, Carl J. Bernacchi, and Tracy E. Twine. "The impacts of Miscanthus× giganteus production on the Midwest US hydrologic cycle." Gcb Bioenergy 2.4 (2010): 180-191.

VanLoocke, Andy, et al. "A regional comparison of water use efficiency for miscanthus, switchgrass and maize." Agricultural and Forest Meteorology 164 (2012): 82-95.

Vermote, E. F., and A. Vermeulen. "Atmospheric correction algorithm: spectral reflectances (MOD09)." ATBD version 4 (1999).

Viovy, N. "CRU-NCEPv4, CRUNCEP dataset." See http://dods. extra. cea. fr/data/p529viov/cruncep/readme. htm (2011).

Wang, Guilin, Manjit S. Kang, and Orlando Moreno. "Genetic analyses of grain-filling rate and duration in maize1." Field Crops Research 61.3 (1999): 211-222.

Wahid, Abdul, et al. "Heat tolerance in plants: an overview." Environmental and experimental botany 61.3 (2007): 199-223.

Warszawski, Lila, et al. "The inter-sectoral impact model intercomparison project (ISI–MIP): project framework." Proceedings of the National Academy of Sciences 111.9 (2014): 3228-3232.

Westhoff, Patrick C. The Energy Independence and Security Act of 2007: Preliminary Evaluation of Selected Provisions. No. 37820. Food and Agricultural Policy Research Institute at University of Missouri, 2008.

Wheeler, Tim, and Joachim Von Braun. "Climate change impacts on global food security." Science 341.6145 (2013): 508-513.

Wieder, William R., Jennifer Boehnert, and Gordon B. Bonan. "Evaluating soil biogeochemistry parameterizations in Earth system models with observations." Global Biogeochemical Cycles 28.3 (2014): 211-222.

Wilhelm, W. W., Johnson, J. M. F., Hatfield, J. L., Voorhees, W. B. & Linden, D. R. Crop and soil productivity response to corn residue removal: a literature review. Agron. J. 96, 1–17 (2004)

Wood, Simon. Generalized additive models: an introduction with R. CRC press, 2006.

Zeng, Linglin, et al. "A hybrid approach for detecting corn and soybean phenology with time-series MODIS data." Remote Sensing of Environment 181 (2016): 237-250.

Zeri, Marcelo, et al. "Carbon exchange by establishing biofuel crops in Central Illinois." Agriculture, ecosystems & environment 144.1 (2011): 319-329.

Zeri, Marcelo, et al. "Water use efficiency of perennial and annual bioenergy crops in central Illinois." Journal of Geophysical Research: Biogeosciences 118.2 (2013): 581-589.

Zhang, Mi, et al. "Response of surface air temperature to small-scale land clearing across latitudes." Environmental Research Letters 9.3 (2014): 034002.

Zhao, Chuang, Bing Liu, Shilong Piao, Xuhui Wang, David B. Lobell, Yao Huang, Mengtian Huang et al. "Temperature increase reduces global yields of major crops in four independent estimates." Proceedings of the National Academy of Sciences 114, no. 35 (2017): 9326-9331.

VITA

EDUCATION

Aug.14-Present	Department of Earth, Atmospheric, and Planetary Sciences, Purdue University,
Sep.11-Jun.14	Institute of Remote Sensing and Digital Earth, Chinese Academy of Sciences, M.S in Cartography and Geographic Information System,
Sep.07-Jul.11	Wuhan University, School of Remote Sensing and Information Engineering, B.S. in Remote Sensing Science and Technology

PUBLICATIONS

1. Xin QC, Mark Broich, **Peng Zhu**, Peng Gong. Modeling grassland spring onset across the Western United States using climate variables and MODIS-derived phenology metrics. Remote Sensing of Environment 161 (2015): 63-77.

2. **Zhu, P.**, Zhuang, Q., Eva, J., Bernacchi, C., Importance of biophysical effects on climate warming mitigation potential of biofuel crops over the conterminous United States. *GCB Bioenergy* 9.3 (2017): 577-590.

3. **Zhu, P.**, Q. Zhuang, P. Ciais, L. Welp, W. Li, and Q. Xin, Elevated atmospheric CO_2 negatively impacts photosynthesis through radiative forcing and physiology-mediated climate feedback, *Geophysical Research Letters* 44.4 (2017): 1956-1963

4. **Zhu, P.** Qianlai Zhuang, Lisa Welp, Philippe Ciais, Martin Heimann, Bin Peng, Wenyu Li, Carl Bernacchi, Christian Roedenbeck, Trevor Keenan, 2016. Recent warming has resulted in smaller gains in net carbon uptake in northern high latitudes. In review.

5. **Zhu, P.** Zhenong Jin, Qianlai Zhuang, Philippe Ciais, David Lobell, Carl Bernacchi, Xuhui Wang. Adapting to the future warmer climate through prolonged grain filling period in US Midwest. In review.